

# Investigation of quasifree $\eta$ -photoproduction with the BGOOD-experiment

Master-Thesis in Physics by Mel Philippe Biel

- 1. Reviewer*    Prof. Dr. Hartmut Schmieden  
                    Physikalisches Institut  
                    Rheinische Friedrich-Wilhelms-Universität Bonn
- 2. Reviewer*    Prof. Dr. Ulrike Thoma  
                    Helmholtz-Institut für Strahlen- und Kernphysik  
                    Rheinische Friedrich-Wilhelms-Universität Bonn

Submitted to the Faculty of Mathematics and Natural Sciences  
04.04.2022

I hereby declare that the work presented here was formulated by myself and that no sources or tools other than those cited were used.

04.04.2022

date

Biel

signature

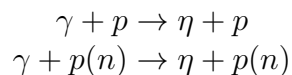
# Contents

<b>1. Introduction</b>	<b>5</b>
<b>2. Experimental Setup</b>	<b>6</b>
2.1. Electron Stretcher Accelerator (ELSA) . . . . .	6
2.2. The BGOOD experiment . . . . .	8
2.2.1. Photon tagging system . . . . .	8
2.2.2. Central detectors . . . . .	9
2.2.3. Forward spectrometer . . . . .	10
2.2.4. Flux monitoring . . . . .	11
2.3. Simulation . . . . .	12
<b>3. Calibration and Event Selection</b>	<b>13</b>
3.1. Energy calibration of the BGO crystals . . . . .	13
3.2. Energy and position reconstruction in the BGO calorimeter . . . . .	13
3.3. Momentum reconstruction . . . . .	15
3.3.1. Central detectors . . . . .	15
3.3.2. Forward detectors . . . . .	16
<b>4. Analysis of <math>\eta</math> photoproduction off the proton</b>	<b>17</b>
4.1. Initial state analysis . . . . .	18
4.1.1. General selection of the $\gamma p \rightarrow \eta p$ channel . . . . .	18
4.1.2. Cross section determination . . . . .	27
4.1.3. Tagger energy shift . . . . .	27
4.1.4. Hydrogen target . . . . .	28
4.1.5. Deuterium target . . . . .	32
4.1.6. Comparison of hydrogen and deuterium target . . . . .	34
4.2. Final state analysis . . . . .	37
4.3. Synopsis of analysing methods . . . . .	40
<b>5. Summary and Conclusion</b>	<b>42</b>
<b>List of Figures</b>	<b>44</b>
<b>List of Tables</b>	<b>48</b>
<b>A. Appendix</b>	<b>49</b>

# 1. Introduction

In physics, like in all other scientific fields, it is necessary to come up with theories and to investigate them. This pursuit of knowledge, the verification and falsification of theories is what makes the human being unique. It is the reason why a species as frail as ours, did such spectacular things as building the great pyramid of Giza and traveling to the moon.

One of these theories is one of the most influential and most investigated theory in modern particle physics, the standard model of particle physics. It describes the elementary particles, which the mass we know is composed of. The standard model includes the quarks, the leptons, the gauge bosons and a scalar boson. All everyday matter around us is composed of the lightest quarks, the up and down, and one of the leptons, the electron. Combining either two ups and one down or two downs and one up, protons or neutrons can be formed. The proton and the electron can form the simplest atom, the hydrogen atom. When adding a neutron, the deuterium can be formed. It is a heavier isotope of the hydrogen. Both liquid hydrogen and deuterium can be used as targets in modern particles experiments. They are used, for example at the BGOOD experiment, to investigate strange and non-strange meson photoproduction. In this thesis the free and quasi free photoproduction of the  $\eta$  meson is investigated. In free photoproduction the photon interacts with an unbound particle, while in quasi free photoproduction the photon interacts with a bound particle. The reactions can be seen here:



The first line shows the reaction at the hydrogen target, while the second line for the deuterium target. In the second case the proton is demanded to be the participant particle. The structure of this thesis is as follows. In chapter 2 the structure and the operating principle of the electron stretcher accelerator (ELSA) is explained, as well as the setup of the BGOOD experiment.

In chapter 3 the energy calibration of the BGO calorimeter is explained. Furthermore a more detailed look into the momentum reconstruction and particle identification of the experiment is provided.

Chapter 4 discusses the main topic of the thesis, which is free and quasi free photoproduction of the  $\eta$ . Here the  $\gamma p \rightarrow \eta p$  reaction is selected, and the  $\eta$  cross section is extracted. In chapter 5 a summary of the results is given.

## 2. Experimental Setup

The BGOOD experiment is located at the electron stretcher facility ELSA in Bonn, Germany. It focuses mainly on non-strange and strange meson photoproduction. In section 2.1 the structure and operating principle of ELSA is discussed, while in section 2.2 the BGOOD experiment and its components are described.

### 2.1. Electron Stretcher Accelerator (ELSA)

The **EL**ectron **St**retcher **A**ccelerator (ELSA) [4] is located at the Rheinische-Friedrich-Wilhelms-Universität in Bonn, Germany. Figure 2.1 shows an overview of the facility. The electrons needed for the experiments are provided by an electron gun. Inside the gun, electrons are released from the cathode material and accelerated away from the cathode by a potential difference. These electrons enter the linear accelerator (LINAC 2) and are accelerated up to an energy of 26 MeV, before entering the booster synchrotron. After accelerating the electrons up to a typical energy of 1.2 GeV, the electrons are extracted from the booster synchrotron and transferred into the stretcher ring. This process produces one bunch of electrons, and is repeated until the stretcher ring is completely filled. After that the electrons are accelerated to an energy of up to 3.2 GeV. When this energy is met, the quasi-continuous electron beam is slowly extracted and directed to either the Crystal Barrel experiment or the BGOOD experiment. This process ends when the stretcher ring is completely depleted, and then repeated from the beginning.

## 2. Experimental Setup

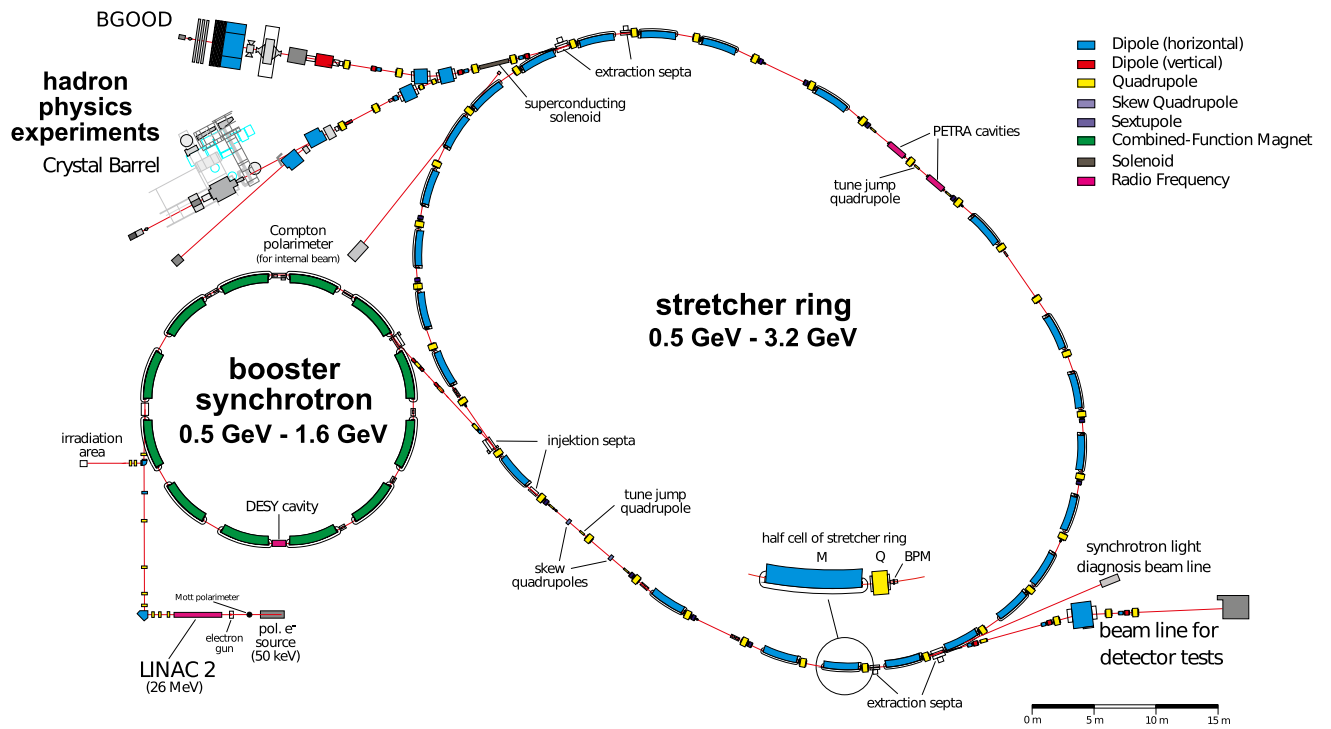


Figure 2.1.: Overview of the electron stretcher facility ELSA in Bonn [4]

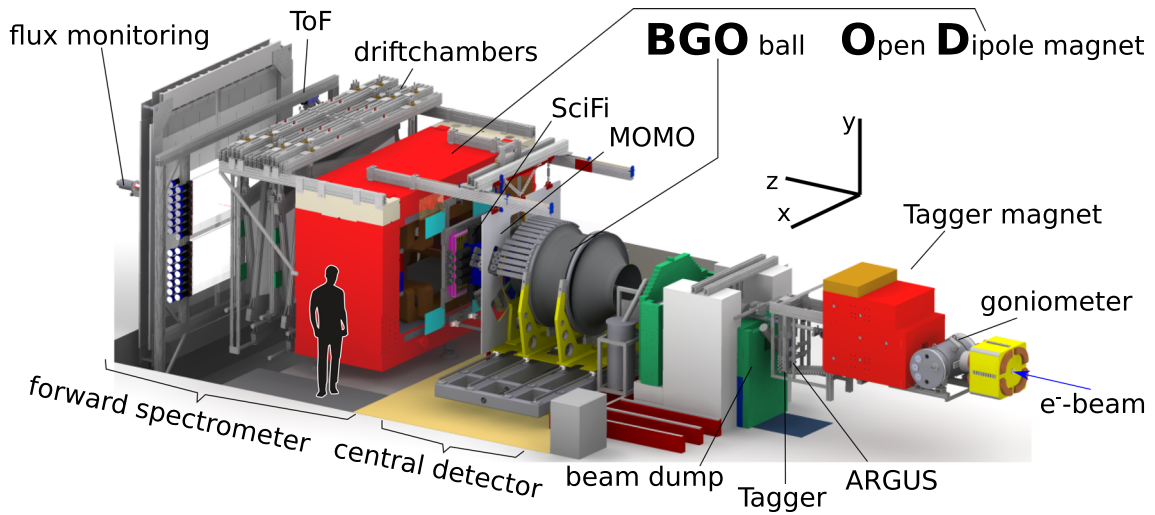


Figure 2.2.: Overview of the BGOOD experiment [3]. The electron beam, provided by ELSA, is coming from the right side as indicated by the arrow. The main components used in this thesis are described in section 2.2

## 2.2. The BGOOD experiment

The BGOOD experiment is located at ELSA, below the Physikalisches Institut building of at the University of Bonn [3]. It is best suited for the investigation of meson photo-production reactions off nucleon targets. An overview of the experiment is depicted in figure 2.2. It is composed of two main parts, the BGO Rugby Ball calorimeter and the forward spectrometer, which the open dipole magnet is part of. The BGO calorimeter and the Open Dipole magnet give the experiment its name. The BGO ball covers 90% of  $4\pi$  of solid angle, while the magnetic forward spectrometer, covers almost the rest of the solid angle in forward direction. The gap is covered by SciRi (Scintillating Ring detector).

The electron beam, coming from ELSA, hits a radiator for example a copper foil, where it produces photons via bremsstrahlung. The electrons get deflected by the magnetic field of the tagger magnet, while the photons enter the main part of the experiment. The electrons enter the tagging system, where their momentum is determined (see chapter 2.2.1). The photons impinge on a liquid hydrogen or deuterium target, which may lead to a hadronic interaction. The resulting decay products can be detected by either the central detectors (see chapter 2.2.2) or by the forward spectrometer (see chapter 2.2.3). The intermediate detector SciRi covers the gap between these two. Photons, which have not interacted with the target cell, are monitored at the end of the experiment, to analyse the photon flux (see chapter 2.2.4).

### 2.2.1. Photon tagging system

The electron beam hits a radiator and produces photons via bremsstrahlung. This process produces a photon beam with a continuous energy spectrum. The exact value of the energy of the photons is needed for further analysis, so the energy of the electrons has to be determined. This is done by the tagging system, which is depicted in figure 2.3. The electrons are deflected by the magnetic field of the tagger magnet, depending on their remaining energy. A set of plastic scintillators is used to determine the deflection angle of the electrons, which allows to calculate their momentum and thereby their energy. The wanted photon energy  $E_\gamma$  is the difference between the initial electron beam energy and the determined electron energy. Electrons which did not undergo bremsstrahlung are directed into the beam dump, while the photons, which are not affected by the magnetic field, traverse toward the target.

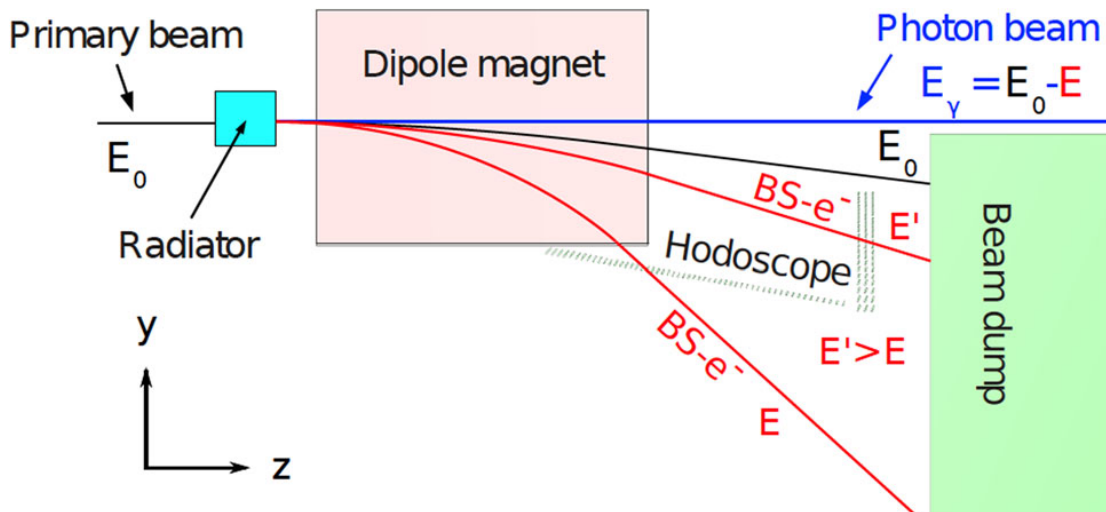


Figure 2.3.: Overview of the photon tagger [3]. The electron beam is coming from the left. Upon hitting the radiator the electron beam produces a photon beam which moves in the same direction as the electron beam. The electrons are deflected by the magnetic field of the tagger magnet and hit the scintillators of the tagger hodoscope.

### 2.2.2. Central detectors

The central detector consists of two main components, which are relevant to this thesis. The BGO Rugby Ball calorimeter, which is optimized for photon detection, and the scintillator barrel, which is used for charge identification. In figure 2.4 an overview of the different components is given.

#### BGO Rugby Ball calorimeter

The BGO calorimeter is the main part of the central detector. It consists of 480 bismuth germanate (BGO) crystals with a length of 24 cm, which corresponds to 21 radiation lengths. The crystals cover the full azimuthal angle  $\phi$ , and  $25^\circ$  to  $155^\circ$  in polar angle  $\theta$ . The individual crystals cover  $\Delta\phi = 11.25$  in azimuth and  $\Delta\theta = 6^\circ$  to  $10^\circ$  in polar angle. For the light readout photomultiplier tubes (PMTs) are used, which are connected to the individual crystals. A high energetic photon that enters a crystal produces an electromagnetic shower via pair production and bremsstrahlung. These showers can be combined into clusters, which improves the angular resolution beyond the individual crystal size. A closer look at the interaction of the photon can be seen in chapter 3. The BGO calorimeter is the only detector of the experiment which is capable of detecting photons, but is also able to measure the kinetic energy of charged particles.



## 2. Experimental Setup

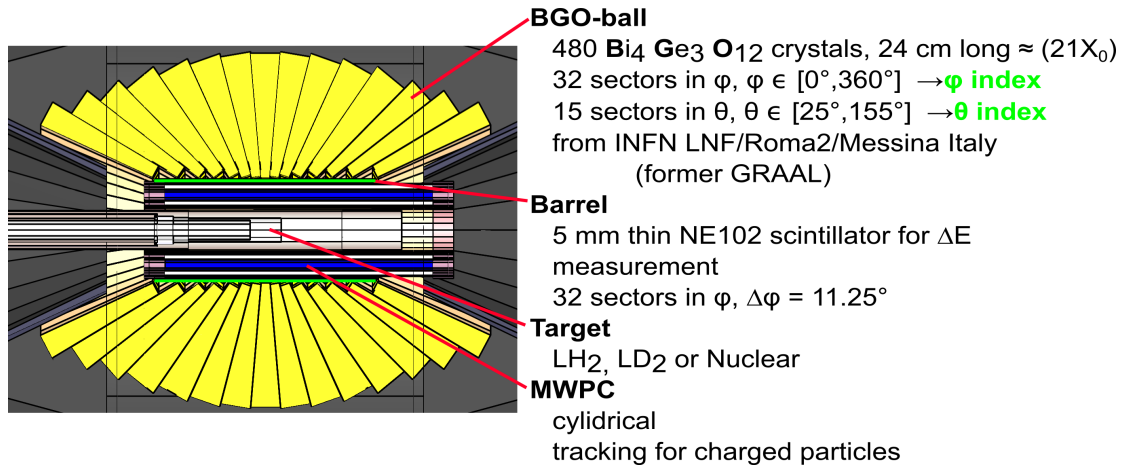


Figure 2.4.: Side view of the central detectors [1]. The photon beam is coming from the left and impinges on the target. The target is surrounded by the MWPCs which are surrounded by the scintillator barrel. Most outward the BGO calorimeter is located.

### Scintillator barrel

The scintillator barrel is composed of 32 plastic scintillators, which are cylindrically arranged. It is used to distinguish between charged and uncharged particles, and to provide an  $\Delta E/\Delta x$  energy loss measurement. One scintillator has a length of 43 cm, and covers an angle of  $11.25^\circ$  in  $\phi$ , and an angular range of  $25^\circ$  to  $155^\circ$  in  $\theta$ .

### 2.2.3. Forward spectrometer

Charged particles, which have a  $\theta$  angle smaller than  $10^\circ$ , and thereby escape the central detector, can be detected by the forward spectrometer. It is able to measure the time of flight of these particles, as well as their momentum. An overview of the spectrometer is given in figure 2.5. To determine the momentum of the charged particles, a magnetic field is used, as well as the track information before and after the deflection. The open dipole magnet provides a 0.4 T magnetic field to deflect the particles. The scintillating fibre detectors MOMO and SciFi2 measure the particle track upstream of the magnet, while eight drift chambers measure the track downstream of the magnet. To determine the time of flight three walls of plastic scintillators, each divided into individual horizontal bars, are used. On each end of these bars, a PMT is located to read out the signal. This allows to determine the horizontal hit position by taking the time difference between the two PMT signals. The vertical position is reconstructed from the bar that is hit by the particle. Combining this information, and the different response times, allows to calculate the time of flight.

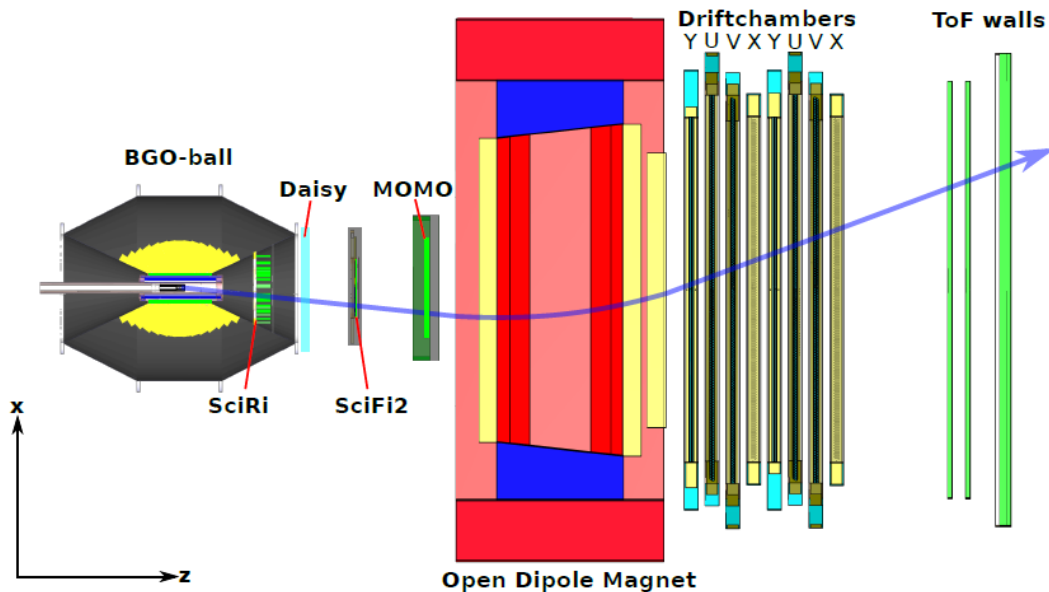


Figure 2.5.: Top view on the BGO-OD experiment [3]. The blue arrow indicates the trajectory of a charged particle. The forward spectrometer consists of SciFi2, MOMO, the open dipole magnet, the driftchambers and the ToF walls

#### 2.2.4. Flux monitoring

Knowing the photon flux is necessary to perform normalization, for example, for cross section measurements. To monitor the flux a combination of two different detectors is used, the Flux Monitor (FluMo) and the Gamma Intensity Monitor (GIM). These two detectors monitor the photons that have not interacted with the target, and therefore are placed most downstream. The GIM is a fully absorbing lead glass detector, which detects practically all incoming photons. A photon that enters the GIM produces an electromagnetic shower, which is detected by a PMT. FluMo is made of five plastic scintillators in series, which are placed in the photon beam. It can only detect the fraction of photons that undergo pair production, thus only sees a fraction of the bremsstrahlung photons GIM has seen. Since GIM is subject to radiation damage, it can only be used for low intensity photon beams and for a short period of time, while FluMo can be used for higher intensities. To determine the photon flux, FluMo and GIM are placed in a low intensity photon beam, as depicted in figure 2.6. The fraction of the photons FluMo detects can be determined, and used for higher intensity beams to determine the photon flux.

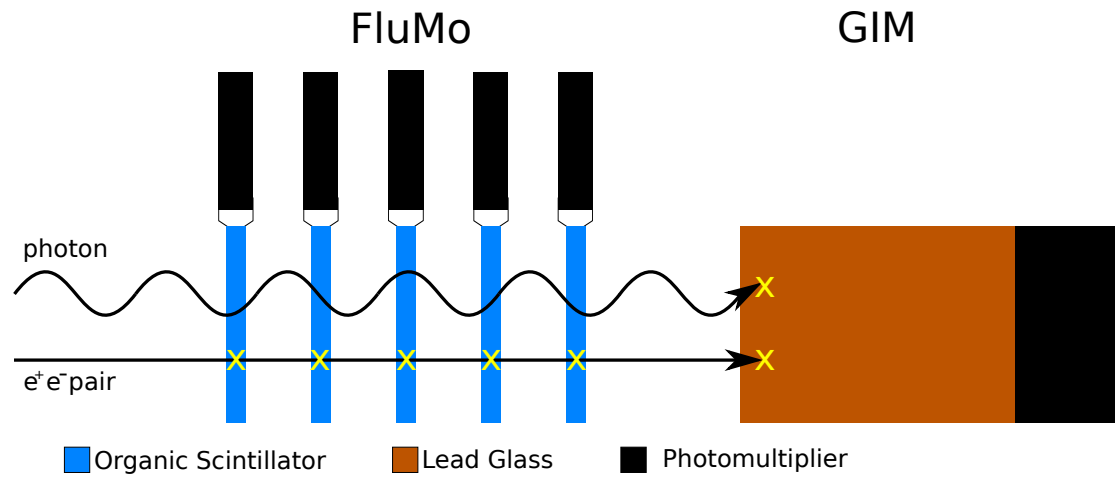


Figure 2.6.: Depiction of FluMo and GIM. The color scheme depicts the components of the detectors. The electron positron pairs can be detected by both detectors (indicated with a yellow x), while the photon is only detected by GIM.

### 2.3. Simulation

Simulation is used to understand the influence of the different components of the experiments. For this, simulated data is generated. Firstly all initial and final state particles are created by an event generator. Also a post bremsstrahlung electron is created, since it is needed for the energy of the incoming photon. After that the decay of the final state particles and their energy deposition within the detectors is simulated via Monte Carlo methods. The different parts of the detectors, including the magnetic fields of the magnets, have been implemented, and the particle interaction with them is simulated by using Geant4.

## 3. Calibration and Event Selection

In this chapter, the energy calibration of the BGO crystals (see chapter 3.1) and the interaction of particles with the crystals is explained (see chapter 3.2). Furthermore the reconstruction of the momentum of the particles (see chapter 3.3) for the different detectors, and in case of the forward detector, the particle identification is discussed.

### 3.1. Energy calibration of the BGO crystals

To understand the information given by the electronics, an absolute energy calibration of the crystals is performed [3]. To do so a  $^{22}\text{Na}$  radioactive source is inserted into the BGO calorimeter.

$^{22}\text{Na}$  decays via the emission of an  $e^+$  to  $^{22}\text{Ne}^*$ . The emitted  $e^+$  annihilates with an atomic electron to produce 511 keV photons. Another 1.275 MeV photon is emitted by the de-excitation of the  $^{22}\text{Ne}^*$  to its ground state. These photons are detected by the BGO calorimeter, and the electronic response can be seen in figure 3.1. The response can be mapped to the known energies.

The next step of the calibration is the consideration of the decay  $\pi^0 \rightarrow 2\gamma$ . This is done, since the photons of the  $^{22}\text{Na}$  decay have energies of the order 1 MeV, while the photons of the pion decay can have energies in order of 100 MeV. The scaling can not be assumed to be linear, and therefore this step is necessary. The invariant mass spectrum of the  $\pi$  is fitted, and a correction is applied to the single crystals, to ensure the correct peak position.

### 3.2. Energy and position reconstruction in the BGO calorimeter

The interaction of protons and photons with the calorimeter can be seen in figure 3.2. On the right side is the interaction of the proton with the crystals depicted. The protons, like all other heavy charged particles, lose their energy mostly via Bethe-Bloch ionization when they interact with matter. They deposit only energy in crystals which are traversed. The energy detected by the PMTs is concentrated in a single crystal, hence the position resolution is limited to the crystal size.

The photon on the other hand, produces an electromagnetic shower when it enters a

### 3. Calibration and Event Selection

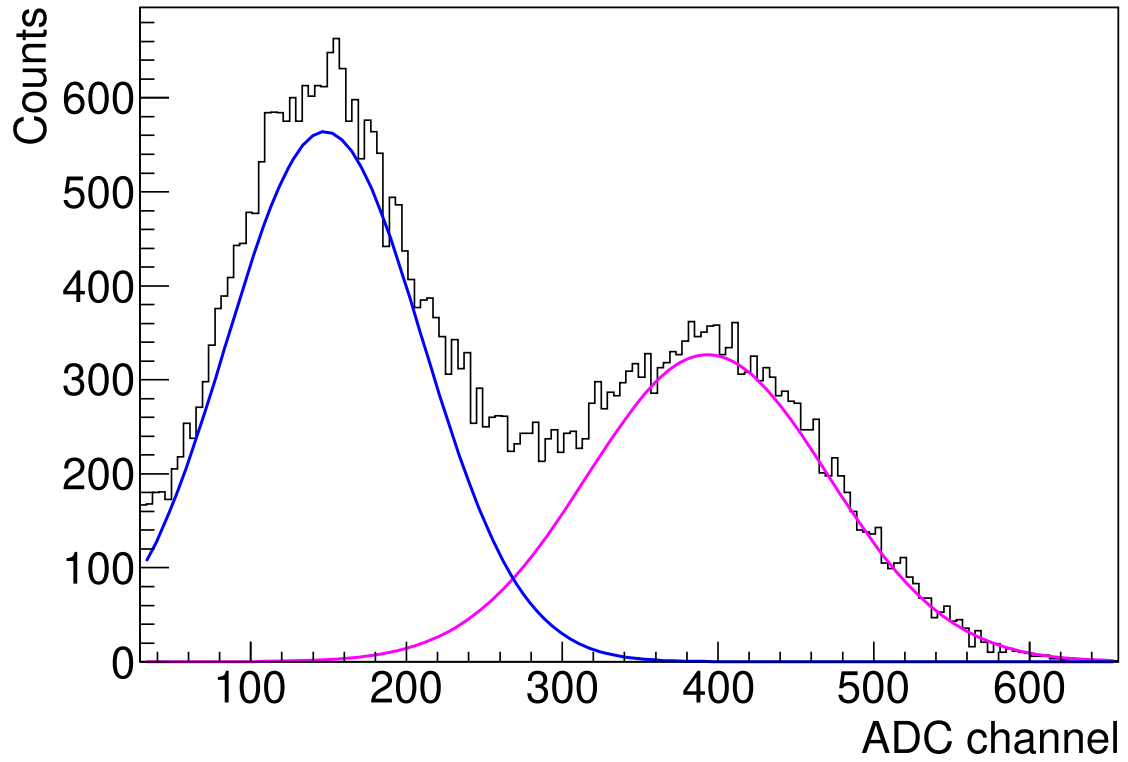


Figure 3.1.:  $^{22}\text{Na}$  energy spectrum in one BGO crystal [3]. The first peak corresponds to the 511 keV photon, while the second peak corresponds to the 1.275 MeV photon. With this spectrum, the electronic response can be mapped to the energies.

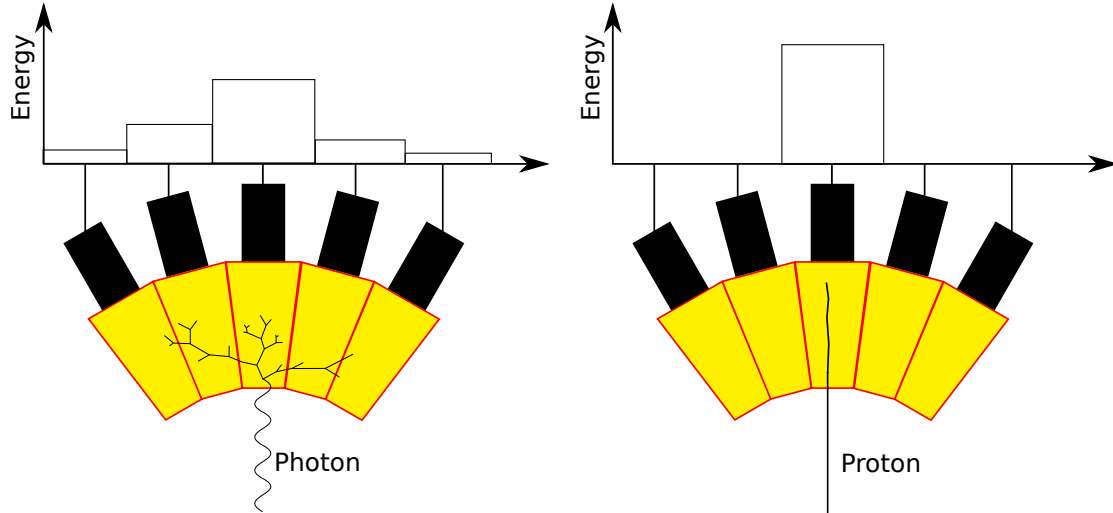


Figure 3.2.: Schematic depiction of the energy deposition mechanism in the BGO calorimeter for different particles. Exemplary photons and protons are shown. In yellow the calorimeter crystals are shown, in black the PMTs. On top the deposited energy distribution over several crystals is depicted.

crystal. This electromagnetic shower is produced via bremsstrahlung and pair production, and develops into neighboring crystals. The involvement of several crystals allows to improve the angular resolution by determining the center of the energy distribution. The position resolution of the entrance point of the photon can be improved beyond the size of a single crystal.

### 3.3. Momentum reconstruction

#### 3.3.1. Central detectors

To reconstruct the momentum of particles that enter the central detectors, only the information provided by the BGO calorimeter is needed. The BGO calorimeter, can provide the position of the entering particle and its deposited energy. However, also the mass of the particle is needed to calculate its the momentum, as can be seen here:

$$E^2 = m^2 + p^2$$

Since the mass is a quantity that the calorimeter is not able to access, a hypothesis on the mass of the detected particle has to be done. The calculation of the momentum has a few problems. On the one hand, the particle hypothesis has to be correct, or else the momentum is wrong, and on the other hand it is not guaranteed that the particle deposits all of its energy in the calorimeter. Especially for high energetic protons this is the case.

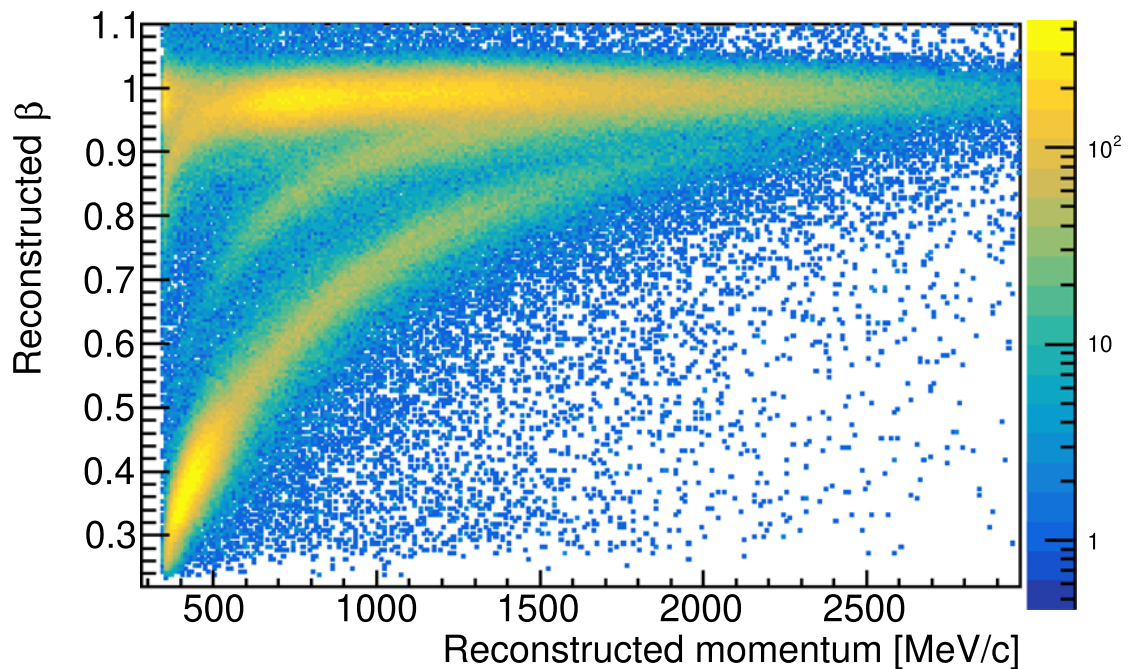


Figure 3.3.: Charged particle identification in the forward spectrometer [3]. Particle velocity  $\beta$  against momentum. Different charged particles can be identified with this plot.

### 3.3.2. Forward detectors

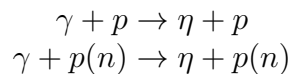
Only charged particles can be detected by the forward spectrometer. A combination of information provided by MOMO, SciFi and the drift chambers is needed, in order to reconstruct the momentum of the particle.

The scintillating fibre detectors MOMO and SciFi2 measure the particle track upstream of the magnet, while the drift chambers measure the track downstream of the magnet. The charged particle is deflected by the magnetic field. By measuring every interaction point of the particle with the detectors, the track of the particle can be reconstructed. With this, the deflection angle, and also the radius of the curvature of the particle, can be determined. The momentum can be calculated by using the radius and the magnetic field strength.

Additionally the ToF walls allow to calculate the velocity of the particles, which can be expressed as the fraction of the velocity of light  $\beta = v/c$ . When plotting this information against the reconstructed momentum, as seen in figure 3.3, each different particle type forms a distinct band, allowing for particle identification.

## 4. Analysis of $\eta$ photoproduction off the proton

In modern physics it is necessary to utilize a wide range of different targets, to investigate interesting behavior. Many reactions demand more than a simple proton target, which can be easily obtained by using a liquified hydrogen target. A free neutron target, on the other hand, is impossible to achieve, as the neutron has a lifetime of only several minutes when not bound into a nucleus. To work around this problem, the heavier isotope of the hydrogen is used as a target, the deuterium. The deuterium nucleus is composed of a proton and a neutron; it is what comes closest to a pure neutron target. The only problem with a deuterium target is that, even when the nucleus is at rest, the constituent particles are moving. This motion is called Fermi motion. Both particles have a momentum, which lies within the Fermi momentum distribution, and is unknown to the observer. When impinging a photon beam on a deuterium target, it is unknown which particle has interacted with the photon, and how much momentum it carried. This leads to two problems. The first problem is that having two target particles, produces unwanted background from the neutron target. The second problem on the other hand is that the momentum of the target particle is unknown. To circumvent the first problem, the pure hydrogen target is also being considered, while the second problem is approached by assuming the target particle at rest. When a reaction is investigated for both targets, the influence of the proton can be calculated out, leading to a quasi-free neutron target. A well known reaction channel is the photo production of the  $\eta$  meson off the proton target. In this thesis the free and the quasi-free  $\eta$  production is considered, the corresponding reactions can be seen here:



The cross section of  $\eta$  photoproduction is dominated by the  $S_{11}$  resonance, which has a steep rise directly at threshold and falls off towards higher energies. In  $\cos(\theta)$  the cross section is almost flat. The produced  $\eta$  meson decays into different decay channels (see Table 4.1), for this thesis the neutral decay channel  $\eta \rightarrow \gamma\gamma$  is considered. The proton that is also produced, can be detected in one of the two main detectors which are described in 2.2, the central detector or the forward detector. In the following it is distinguished between these two cases because these two detectors differ significantly.



## 4. Analysis of $\eta$ photoproduction off the proton

To analyze the  $\eta$  channel, the cross section needs to be determined. This is done considering both the initial state (chapter 4.1) and the final state (chapter 4.2). In the initial state analysis, hydrogen and deuterium target are considered and compared, while in the final state analysis only the deuterium target is investigated. The methods used in the initial state analysis are compared to the final state analysis in chapter 4.3.

decay modes	branching ratio / %
$\gamma\gamma$	39.4
$\pi^0\pi^0\pi^0$	32.7
$\pi^+\pi^-\pi^0$	22.9
$\pi^+\pi^-\gamma$	4.2

Table 4.1.: Dominant decay channels of the  $\eta$  meson [2]. The neutral decay channel  $\eta \rightarrow \gamma\gamma$  is chosen.

### 4.1. Initial state analysis

In the initial state analysis the reference frame is the center of mass system of the initial state. The initial state is composed of the four momentum of the incoming photon and the four momentum of the target. The photon moves in beam direction, while the target is assumed at rest. This assumption is correct for the proton in the hydrogen target. The deuterium, as a nucleus, is at rest while the proton inside the deuterium target is in motion, due to the Fermi momentum. This uncertainty in the momentum of the proton, for the deuterium target, smears out the initial state, therefore the hydrogen target is considered as a reference point.

In the following the selection cuts, that are used to identify the  $\eta$ , are described in chapter 4.1.1. To analyse the initial state the cross section has to be determined, which is discussed in chapter 4.1.2. In chapter 4.1.3 the implemented tagger energy shift is motivated. In the chapters 4.1.4 and 4.1.5, the results of the hydrogen and the deuterium analysis will be presented, while in chapter 4.1.6 the results will be compared.

#### 4.1.1. General selection of the $\gamma p \rightarrow \eta p$ channel

To determine the  $\eta p$  cross section, the  $\eta$  has to be reconstructed. To do so, different selection cuts were implemented, which will be discussed in this chapter. The considered decay channel of the  $\eta$  is the neutral decay into two photons.

##### Photon selection cut

The number of neutral particles detected in the BGO calorimeter can be seen in figure 4.1. These particles are assumed to be photons. To weaken the effect of, for example,

#### 4. Analysis of $\eta$ photoproduction off the proton

photon split-offs, two and three photons are allowed.

When a photon enters the calorimeter it produces an electromagnetic shower, which develops into neighboring crystals. When the electromagnetic shower does not deposit energy in crystal it passes through, but an crystal after that, it looks like the deposition from another photon, this is called a photon split off.

The  $\eta$  is reconstructed by adding the four momentum of two photons. In case of three detected photons, all combinations of two photons are evaluated. The case of false combination of two photons, which results in the mass of this combination not matching the mass of the  $\eta$ , will be handled by later selection cuts.

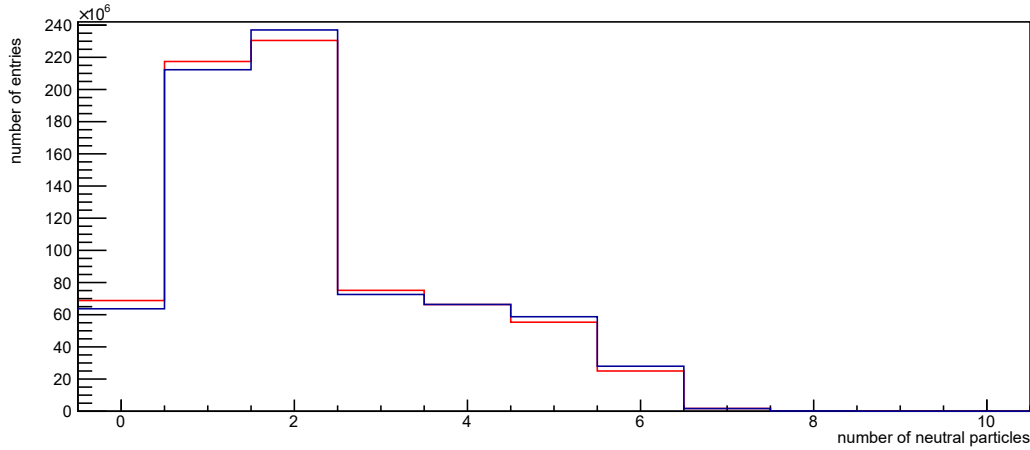


Figure 4.1.: Number of neutral particles per decay in simulation. There are no restrains on which neutral particles and how many neutral particles are allowed. The blue line indicates the hydrogen target, the red line the deuterium target. All decay channels of the  $\eta$  are included.

#### Angular selection cuts

Using the calculated invariant mass, the corresponding missing mass can be determined. The four momentum of missing mass can be accessed by subtracting the four momentum of the invariant mass from the four momentum of the initial state.

$$P_{missing} = P_{initial} - P_{invariant}$$

To satisfy momentum conservation, both the invariant mass of  $2\gamma$  and the missing mass to the  $\eta$  have to fulfill certain criteria, which will be discussed in the following.

In the center of mass frame of a two body decay, the decay products have to be emitted back to back. Therefore the angular difference in  $\phi$  between the reconstructed  $\eta$  and the detected proton has to be close to  $180^\circ$ .

#### 4. Analysis of $\eta$ photoproduction off the proton

$$\Delta\phi = |\phi_{CMS,invariant} - \phi_{CMS,p}|$$

This difference is depicted in figure 4.2 for the hydrogen target and in figure 4.3 for the deuterium target. To enhance the signal to noise ratio, the data is compared to a simulation of the signal channel. This allows to determine an allowed angular range in which the signal channel is the dominant part in the data sample. The derived difference in  $\phi$  is in the range of  $[160^\circ, 200^\circ]$  in the case that the proton is detected in the central detector. In the case where the proton is detected in the forward detector no restrictions are set. This is because the angular difference in the simulation is significantly broader than in the data sample, hence finding a reasonable selection cut is not possible. A possible reason behind this is that the angular resolution of  $\phi$  is not correctly described in the simulation.

To assure that the missing mass to the  $\eta$ , and therefor the invariant mass of the  $2\gamma$ , match the real reaction, the difference in the  $\theta$  angle between the missing mass and the detected proton has to be considered.

$$\Delta\theta = |\theta_{CMS,missing} - \theta_{CMS,p}|$$

This difference can be seen in figure 4.4 for the hydrogen target, while in figure 4.5 the deuterium target is depicted. The allowed angular difference in  $\theta$  is  $[0^\circ, 20^\circ]$  in case the proton is detected in the central detector. All differences are allowed for the forward case.

#### **Influences of the selection cuts on the missing mass and the invariant mass**

The influences on both the invariant mass and the missing mass, caused by the implemented selection cuts, can be seen in figure 4.6 for the hydrogen target, and in figure 4.7 for the deuterium target. Comparing the missing mass for the case that the proton is detected in the central detector with the case that the proton is detected in the forward detector, it becomes clear that not implementing cuts in the forward case has an impact on the missing mass distribution. To now select the  $\eta$ , a mass cut is implemented on the missing and the invariant mass. The fit ranges of the missing mass and the invariant mass are restricted by  $[400 \text{ MeV}, 700 \text{ MeV}]$  and  $[0 \text{ MeV}, 1900 \text{ MeV}]$  respectively.

#### 4. Analysis of $\eta$ photoproduction off the proton

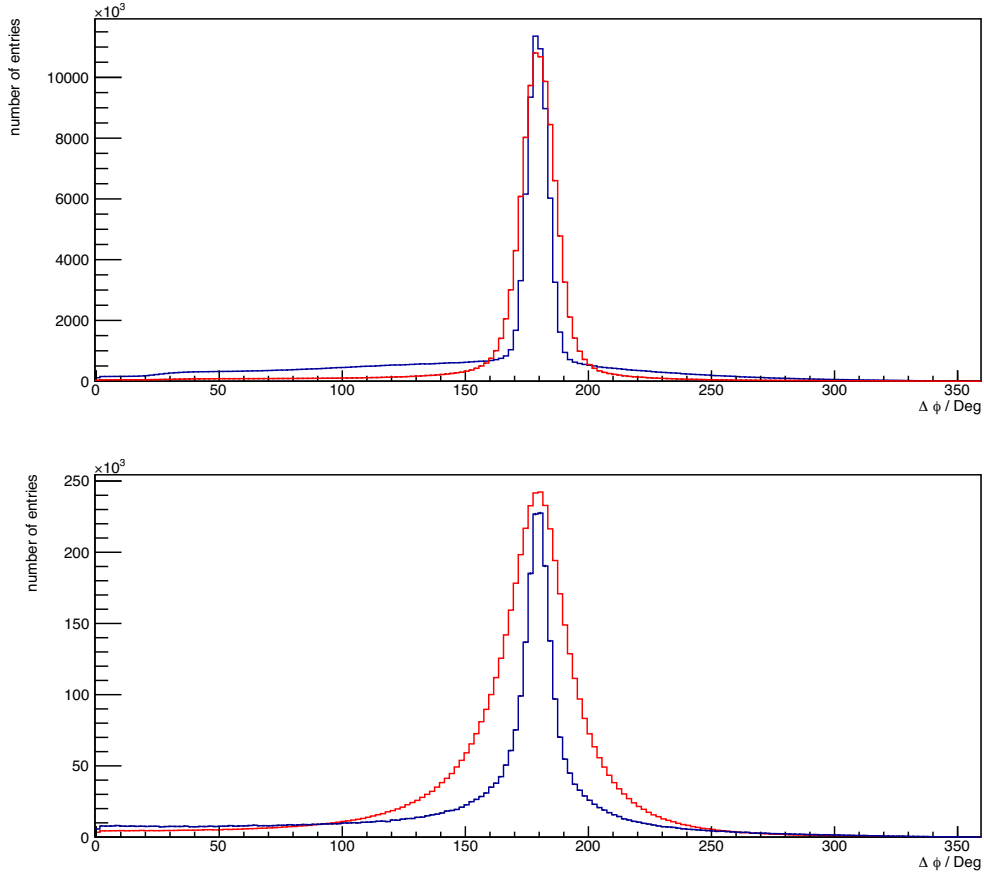


Figure 4.2.: Absolute angular difference in  $\phi$  between the invariant mass and the detected proton for the hydrogen target. The proton is detected in the central detector in the top image, and in the forward detector in the lower image. In blue the real data is shown, while in red the simulated data. In the case of the proton being detected in the central detector, an angular difference of  $[160^\circ, 200^\circ]$  is allowed, while all differences are allowed for the forward case.

#### 4. Analysis of $\eta$ photoproduction off the proton

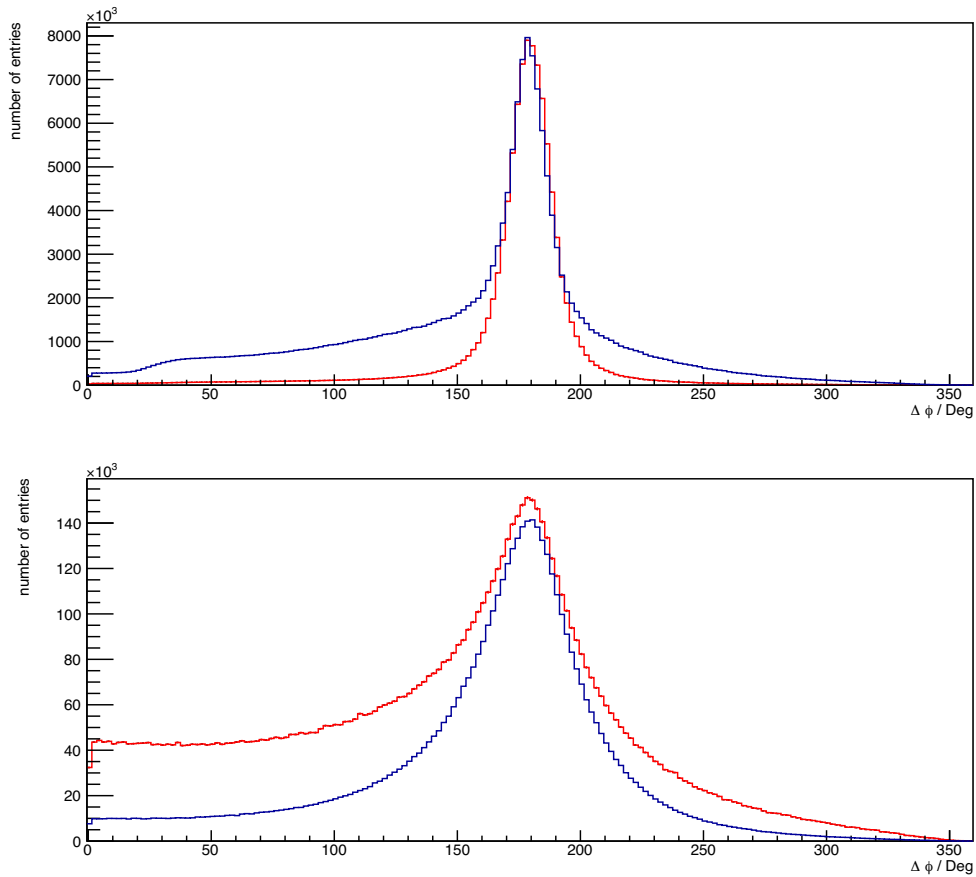


Figure 4.3.: Absolute angular difference in  $\phi$  between the invariant mass and the detected proton for the deuterium target. The proton is detected in the central detector in the top image, and in the forward detector in the lower image. In blue the real data is shown, while in red the simulated data. In the case of the proton being detected in the central detector, an angular difference of  $[160^\circ, 200^\circ]$  is allowed, while all differences are allowed for the forward case.

#### 4. Analysis of $\eta$ photoproduction off the proton

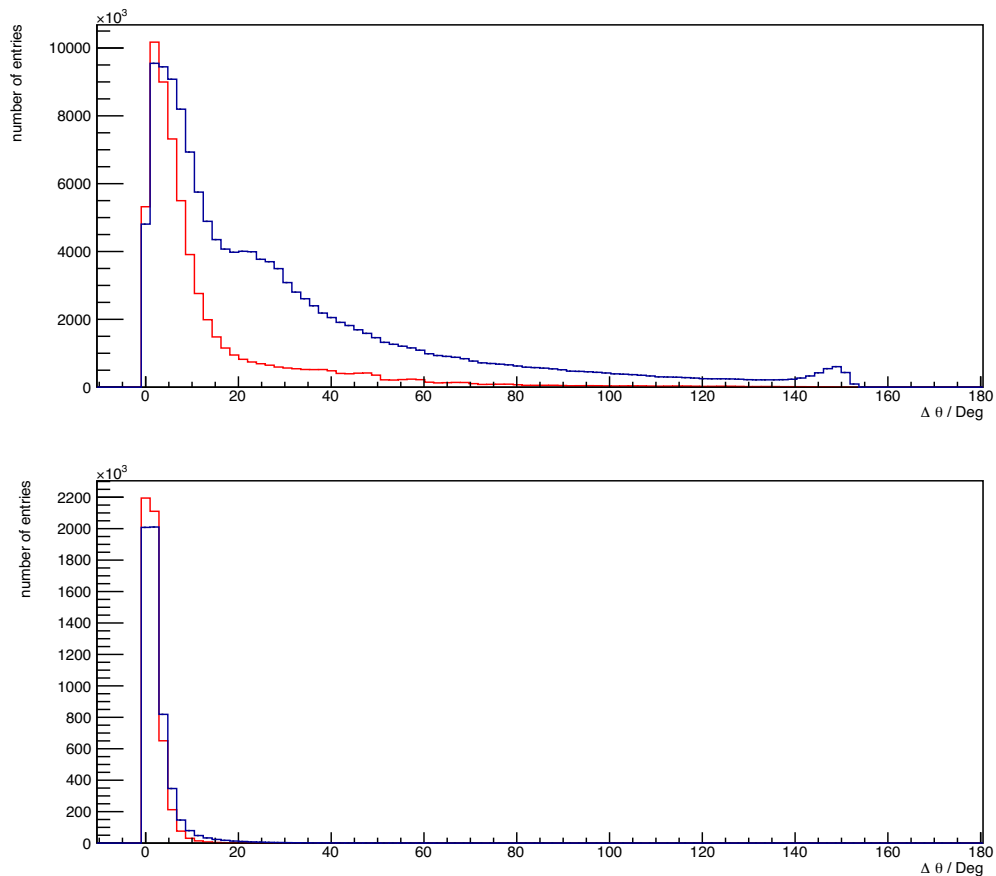


Figure 4.4.: Absolute angular difference in  $\theta$  between the missing mass and the detected proton for the hydrogen target. The proton is detected in the central detector in the top image, and in the forward detector in the lower image. In blue the real data is shown, while in red the simulated data. In the case of the proton being detected in the central detector, an angular difference of  $[0^\circ, 20^\circ]$  is allowed, while all differences are allowed for the forward case.

#### 4. Analysis of $\eta$ photoproduction off the proton

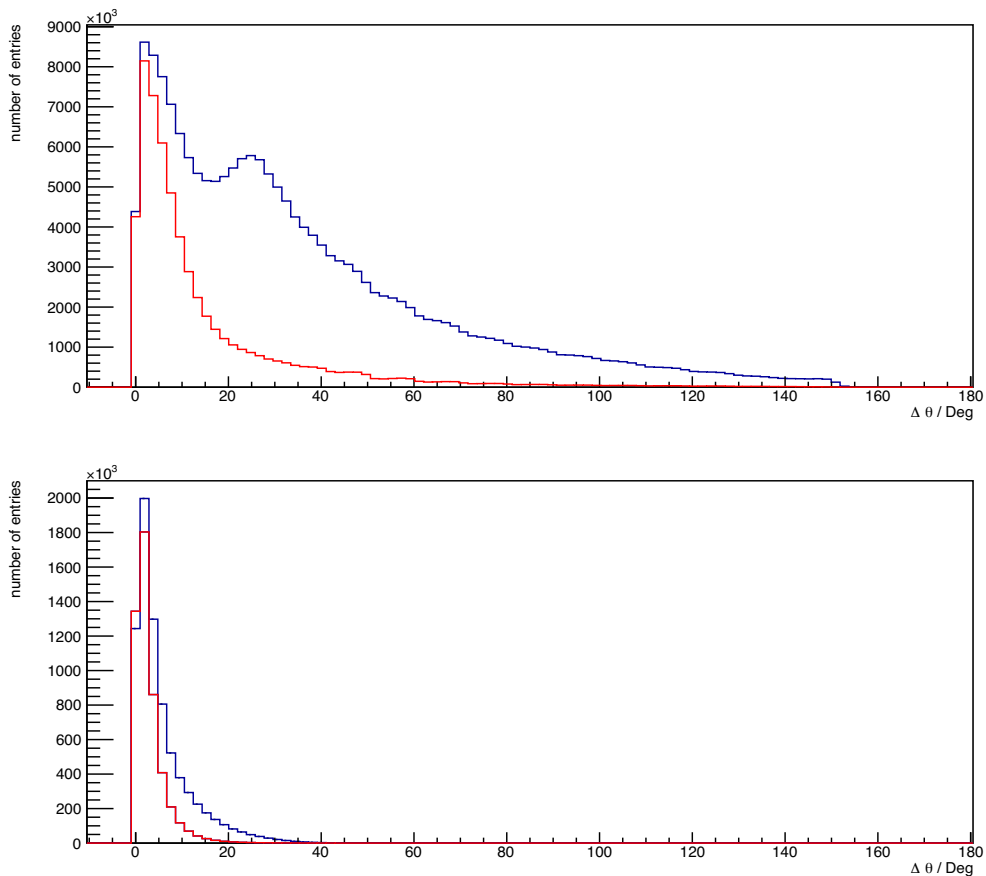


Figure 4.5.: Absolute angular difference in  $\theta$  between the missing mass and the detected proton for the deuterium target. The proton is detected in the central detector in the top image, and in the forward detector in the lower image. In blue the real data is shown, while in red the simulated data. In the case of the proton being detected in the central detector, an angular difference of  $[0^\circ, 20^\circ]$  is allowed, while all differences are allowed for the forward case.

#### 4. Analysis of $\eta$ photoproduction off the proton

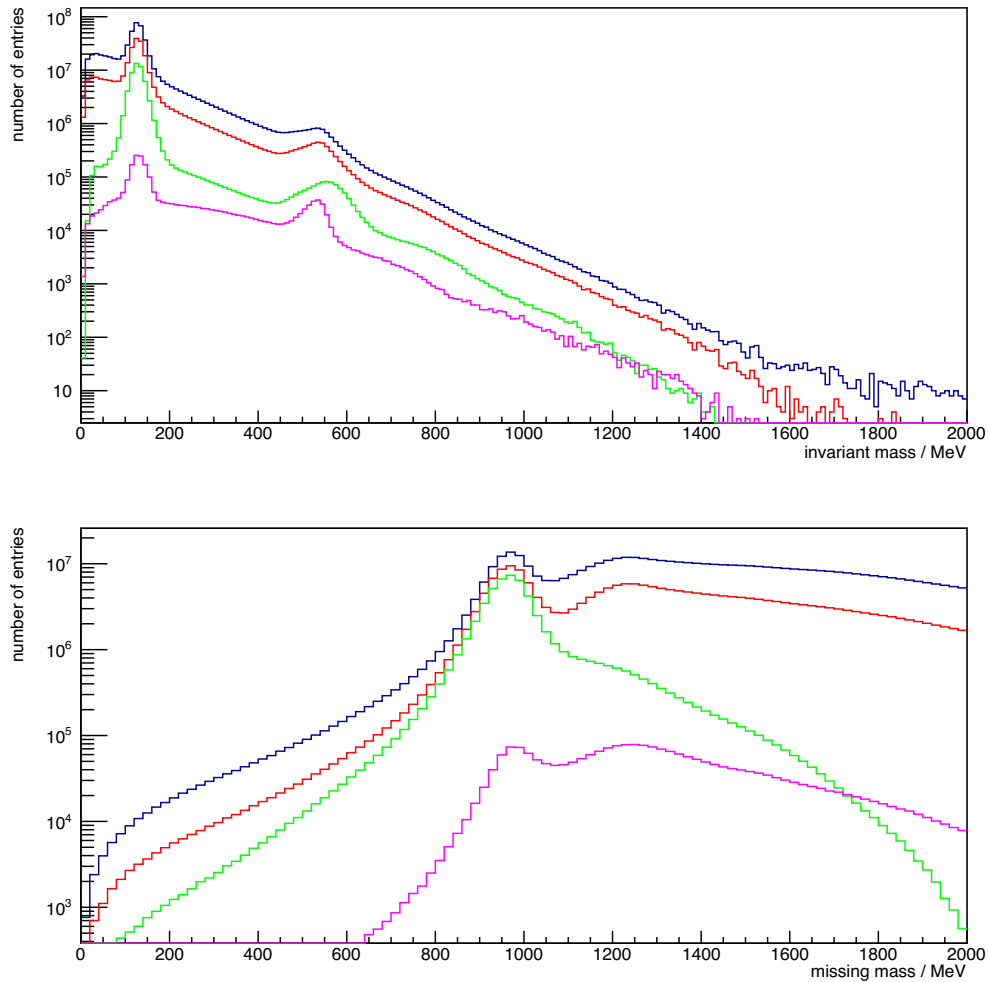


Figure 4.6.: Invariant mass (top) and missing mass (bottom) after the different implemented cuts for the hydrogen target. The blue line describes the data after the photon selection cut. The red line is after demanding one charged hit. The green line after demanding the proton in the central detector, while the magenta line is after demanding the proton in the forward detector.



#### 4. Analysis of $\eta$ photoproduction off the proton

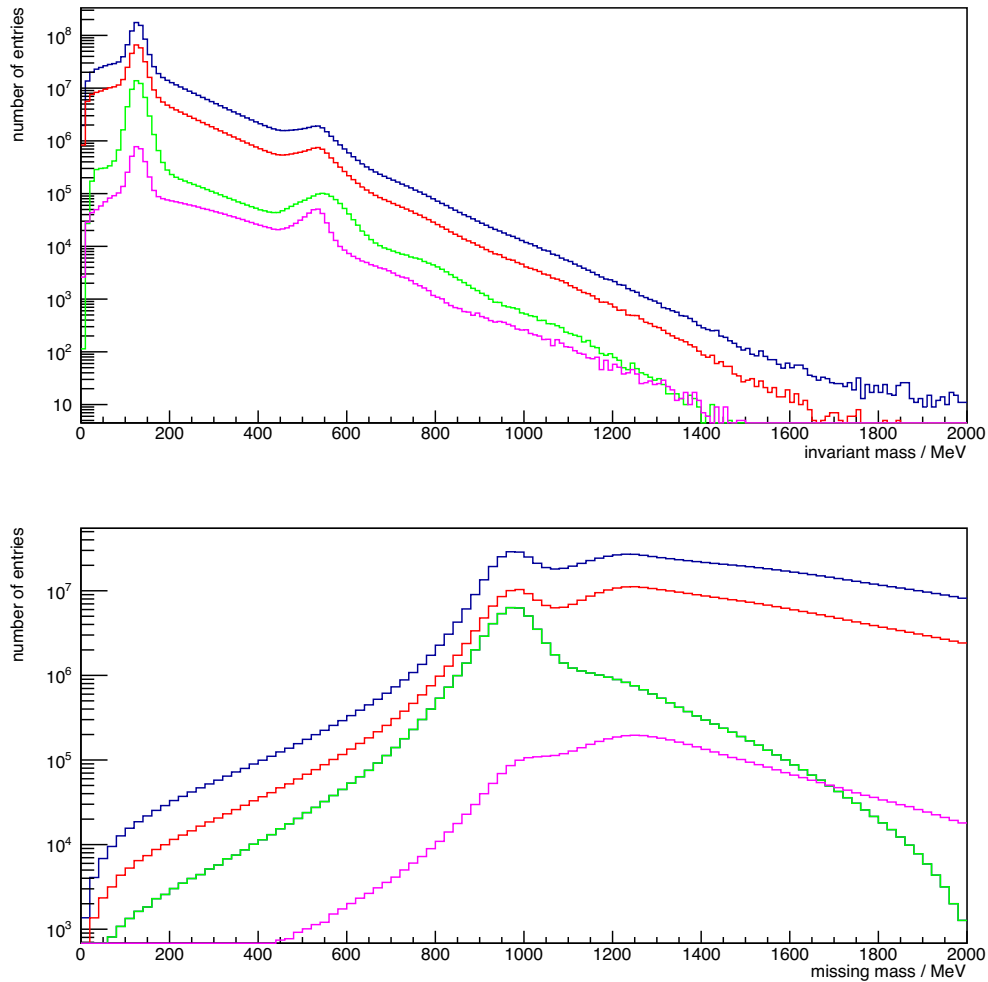


Figure 4.7.: Invariant mass (top) and missing mass (bottom) after the different implemented cuts for the deuterium target. The blue line describes the data after the photon selection cut. The red line is after demanding one charged hit. The green line after demanding the proton in the central detector, while the magenta line is after demanding the proton in the forward detector.

### 4.1.2. Cross section determination

The cross section is the probability of a reaction to occur. The differential cross section  $d\sigma/d\Omega$ , is the cross section measured in certain energy and angle ranges, and can be written as [1]:

$$\frac{d\sigma}{d\Omega}(E, \theta) = \frac{1}{2\pi \cdot \rho_{target} \cdot z} \cdot \frac{N}{F(E_\gamma) \cdot \eta_{reco}} \cdot \frac{1}{\cos(\theta_{CMS}^B) - \cos(\theta_{CMS}^A)}$$

Here  $\rho_{target}$  is the target density. The target density for hydrogen is  $\rho_{hydrogen} = 4.237 \times 10^{-8} 1/(\mu\text{barn} \cdot \text{cm})$ , while it is  $\rho_{deuterium} = 5.053 \times 10^{-8} 1/(\mu\text{barn} \cdot \text{cm})$  for the deuterium [1]. The target length  $z$  is 10 cm for both used targets, while  $F$  is the photon flux which is measured by the FluMo.

The reconstruction efficiency  $\eta_{reco}$  is the ratio between the amount of the reconstructed simulated  $\eta$  over amount of generated  $\eta$ , while  $N$  is the amount of detected  $\eta$  in real data; the data yield. The width of the investigated angular range is given by  $\cos(\theta_{CMS}^B) - \cos(\theta_{CMS}^A)$ .

To reduce influences of the background on the differential cross section, the signal channel and all relevant background channels are simulated and fitted using `rooFit`. This separates the signal from the background.

### 4.1.3. Tagger energy shift

In figure 4.8 the extracted differential cross sections for both the hydrogen and the deuterium target can be seen. It is distinguished between two cases: the proton being detected in the central detector, and the proton being detected in the forward detector. The extracted differential cross sections are shown for an exemplary  $\cos(\theta_{CMS,\eta})$  bin, with the corresponding Bonn Gatchina (BG) model [5]. The BG model is a parametrization of the cross section done by the Bonn Gatchina group. It is visible that the extracted differential cross sections do not match the BG model. In the central case, the extracted cross sections are significantly lower compared to the BG model. An energy offset between the extracted cross sections and the BG model can be seen in the forward case. This could have two different reasons.

The first possible reason is that in simulation, the transition region between the central and the forward detector, is not well implemented. In simulation, the protons can be assigned to the wrong detector or even completely disregarded, which influences the reconstruction efficiency and thereby the extracted differential cross section.

The other possible reason is the tagger calibration. If the electron beam is not at the intended vertical position, the electrons get deflected differently in the tagger magnet, and hence a false energy is assigned. The calculated energy of the proton, the difference of the energy of the electron beam and the energy of the tagged electron, is hereby also

#### 4. Analysis of $\eta$ photoproduction off the proton

wrong. This changes the four momentum of the initial state in the data, but not in the simulation, therefore simulation and data do not match. This would influence the differential cross section. This possible problem is approached in this thesis, by changing the simulated photon energy by a freely chosen energy value, a so called tagger energy shift.

The discussion of the different used values of energy, that are added onto the photon energy, can be found in chapter 1.1.4 for the hydrogen and in chapter 1.1.5 for the deuterium target.

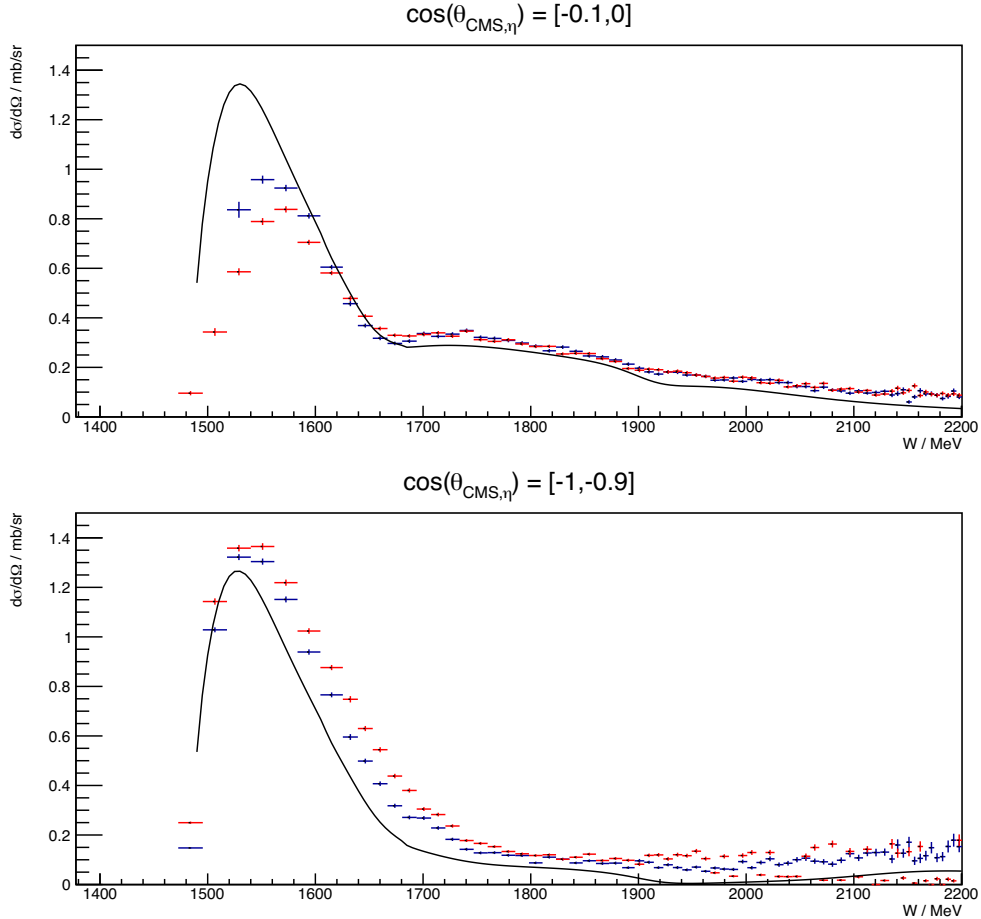


Figure 4.8.: Extracted differential cross sections for the proton in the central detector (top) and in the forward detector (bottom). In blue is the extracted differential cross section for the hydrogen target, in red for the deuterium target and in black is the BG model for the corresponding angular bins.

#### 4.1.4. Hydrogen target

As seen in the previous chapter, the extracted differential cross section does not match the BG model. This difference is corrected by adding an energy value on the energy of the

#### 4. Analysis of $\eta$ photoproduction off the proton

simulated initial state photons. In figure 4.9 examples of the extracted differential cross section in different angular bins can be seen. For the hydrogen target, energy shifts of 5 MeV and 10 MeV are tested. With these values, the extracted differential cross section comes closest to the BG model. The difficulty in determining the optimal value needed, is that for lower energies the extracted differential cross section is not within the range of the model; there is no extracted differential cross section close to the production threshold of the  $\eta$ . The reason is that at production threshold it is kinematically nearly impossible to detect the proton in the central detector. There is no energy left for the needed transverse momentum, so the decay products fly mostly towards the forward detector. There are no protons to be detected in the central detector, therefore there is no extracted differential cross section near production threshold. Furthermore, there is still the problem that in the forward case, the extracted differential cross section seems to have an energy offset of around 20 MeV. Combining the information of the central and the forward case, a 10 MeV tagger energy shift is considered to be a acceptable value. All extracted differential cross section values with a 10 MeV energy shift, for the hydrogen target, can be seen in the appendix A.

#### 4. Analysis of $\eta$ photoproduction off the proton

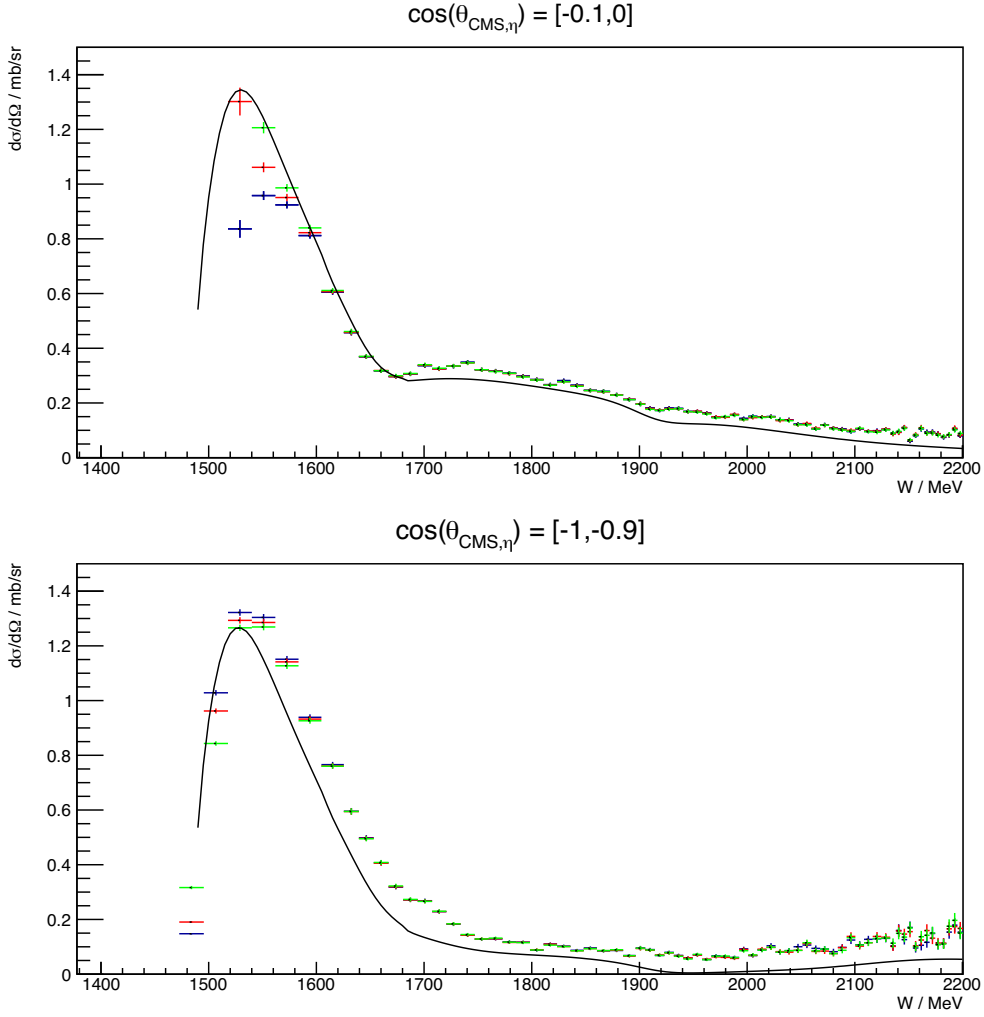


Figure 4.9.: Extracted differential cross sections for the proton in the central detector (top) and in the forward detector (bottom). In blue is the extracted differential cross section with a shifted tagger energy by 0 MeV, in red by 5 MeV and in green by 10 MeV. In black is the BG model for the corresponding angular bins.

An alternative approach is to consider the differential cross section for a fixed energy bin with variable angles. The whole angular range is examined, central and forward detector are both combined to cover the angular range. This combination can be seen in figure 4.10.

The extracted differential cross section for the central case, does agree well with the model, within the acceptance of the BGO calorimeter. In the forward case however, the data does not agree. Using the circumstance that the the extracted differential cross section has an energy offset toward the BG model, a higher energy bin can be used to investigate the difference. The combination of the cross sections can be seen in figure

#### 4. Analysis of $\eta$ photoproduction off the proton

4.11. In this case both extracted differential cross sections match the model, in the given acceptance of the detectors. This shows that there is another problem, which could not be resolved within the timescale of this thesis.

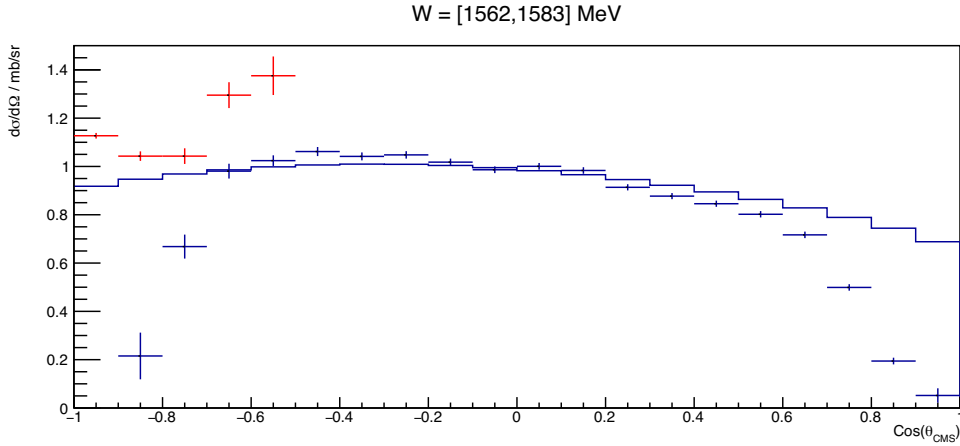


Figure 4.10.: Extracted differential cross section in the energy range of [1562,1583] MeV for variable angles. In blue is the extracted differential cross section for the central case, while in red the forward case is depicted. In black is the BG model for this energy range. Both extracted differential cross sections are taken from the same energy range.

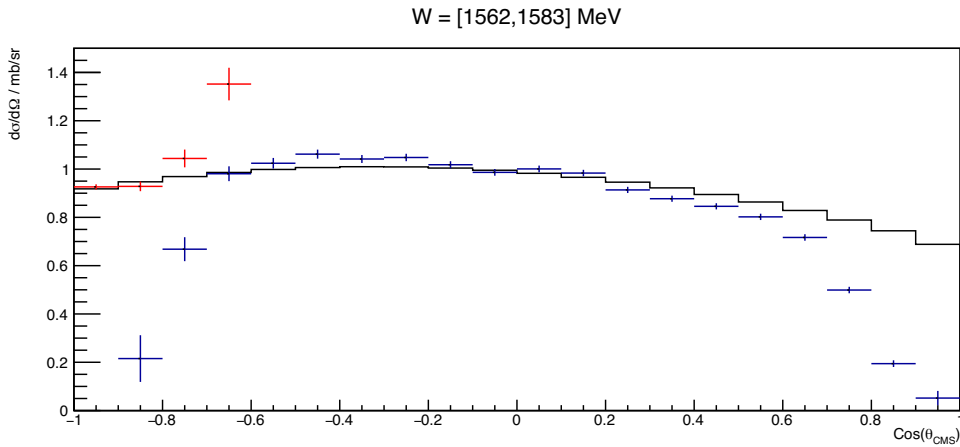


Figure 4.11.: Extracted differential cross section in the energy range of [1562,1583] MeV for variable angles. In blue is the extracted cross section for the central case, while in red the forward case is depicted. In black is the BG model for this energy range. Blue is taken from the given energy range, while red is from an higher energy bin [1583,1604] MeV.

#### 4.1.5. Deuterium target

The approach for the deuterium target is the same as for the hydrogen target. Since the deuterium target is a different data sample, the photon energy shift value could be different to the hydrogen target. The cross sections for different tagger energy shifts can be seen in figure 4.12. For the deuterium target, energy shifts of 35 MeV and 40 MeV are used. In case of the central detector it is clearly visible that the problem for energies close to the production threshold does not exist for the deuterium target. Due to the Fermi motion it is possible for the decay products to have a transverse momentum, which allows them to be detected inside the central detector. Combining the information of the central and the forward case, a 40 MeV tagger energy shift is considered to be a good value. All differential cross section values with a 40 MeV energy shift, for the deuterium target, can be seen in the appendix A.

#### 4. Analysis of $\eta$ photoproduction off the proton

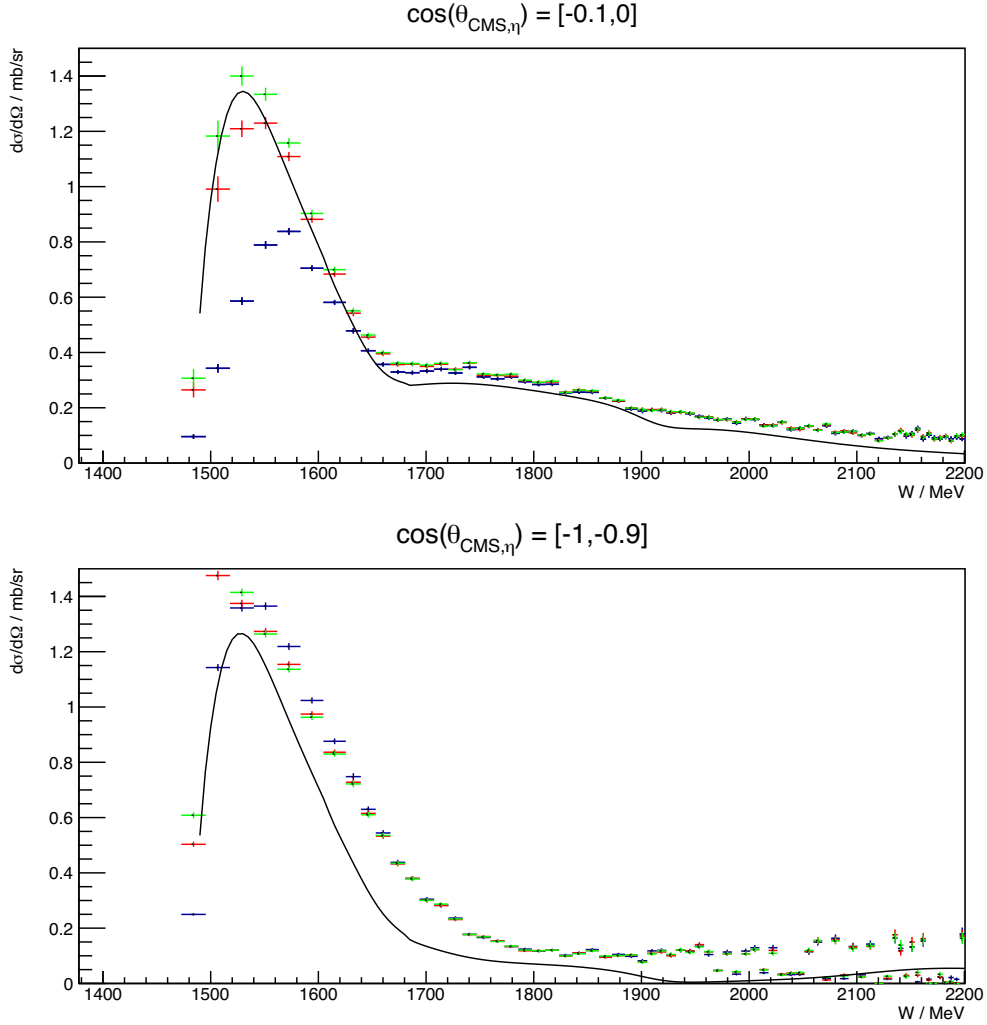


Figure 4.12.: Extracted differential cross sections for the proton in the central detector (top) and in the forward detector (bottom). In blue is the extracted differential cross section with a shifted tagger energy by 0 MeV, in red by 35 MeV and in green by 40 MeV. In black is the BG model for the corresponding angular bins.

In figure 4.13 the differential cross section is depicted with a fixed energy bin and a variable angle bin. It is clearly visible that the cross section does not match over the whole angular range. For low angles the cross section is too low, for high angles it is too high. The reason for this could not be resolved within this thesis. In figure 4.14 the extracted cross section for one higher energy bin is shown.



#### 4. Analysis of $\eta$ photoproduction off the proton

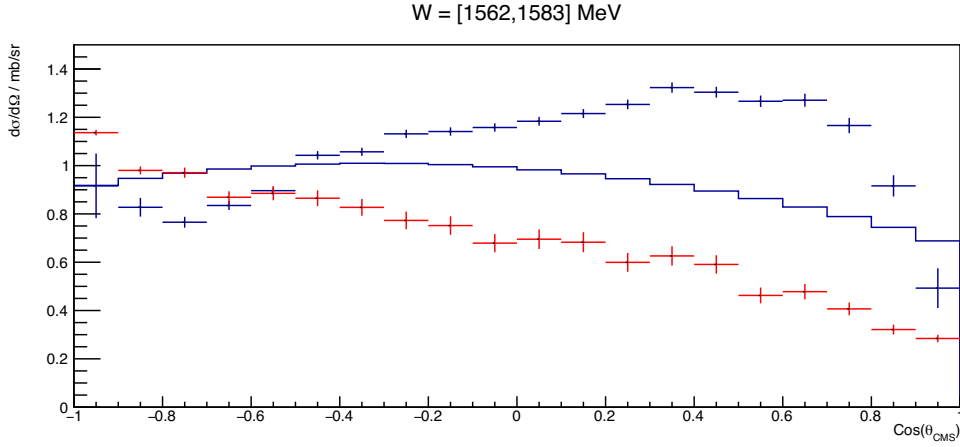


Figure 4.13.: Extracted differential cross section in the energy range of [1562,1583] MeV for variable angles. In blue is the extracted cross section for the central case, while in red the forward case is depicted. The black line shows the BG model for this energy range.

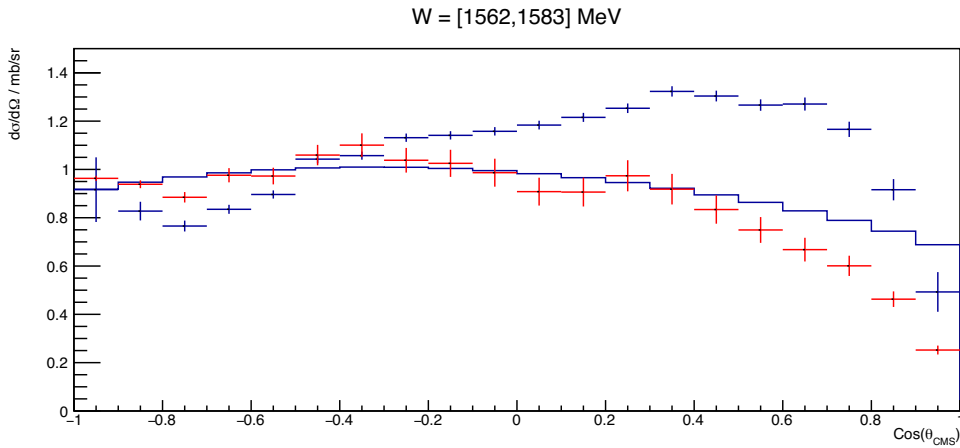


Figure 4.14.: Extracted differential cross section in the energy range of [1562,1583] MeV for variable angles. In blue is the extracted cross section for the central case, while in red the forward case is depicted. The black line shows the BG model for this energy range. Blue is taken from the given energy range, while red is from an higher energy bin [1583,1604] MeV.

#### 4.1.6. Comparison of hydrogen and deuterium target

In this chapter the results for the hydrogen and deuterium targets are compared. This is done for the reconstruction efficiency and for the differential cross section. The compared results include the concluded photon energy shift of 10 MeV for the hydrogen target and 40 MeV for the deuterium target.

### Reconstruction efficiency

The reconstruction efficiencies for hydrogen and deuterium target can be seen in figure 4.15. In case of the central detector, the reconstruction efficiencies for both targets do not match perfectly. This could be, because the selection cuts on the angular difference are optimized for the hydrogen target, as seen in chapter 4.1.1. This allows less  $\eta$ 's to be reconstructed, hence a lower reconstruction efficiency is expected.

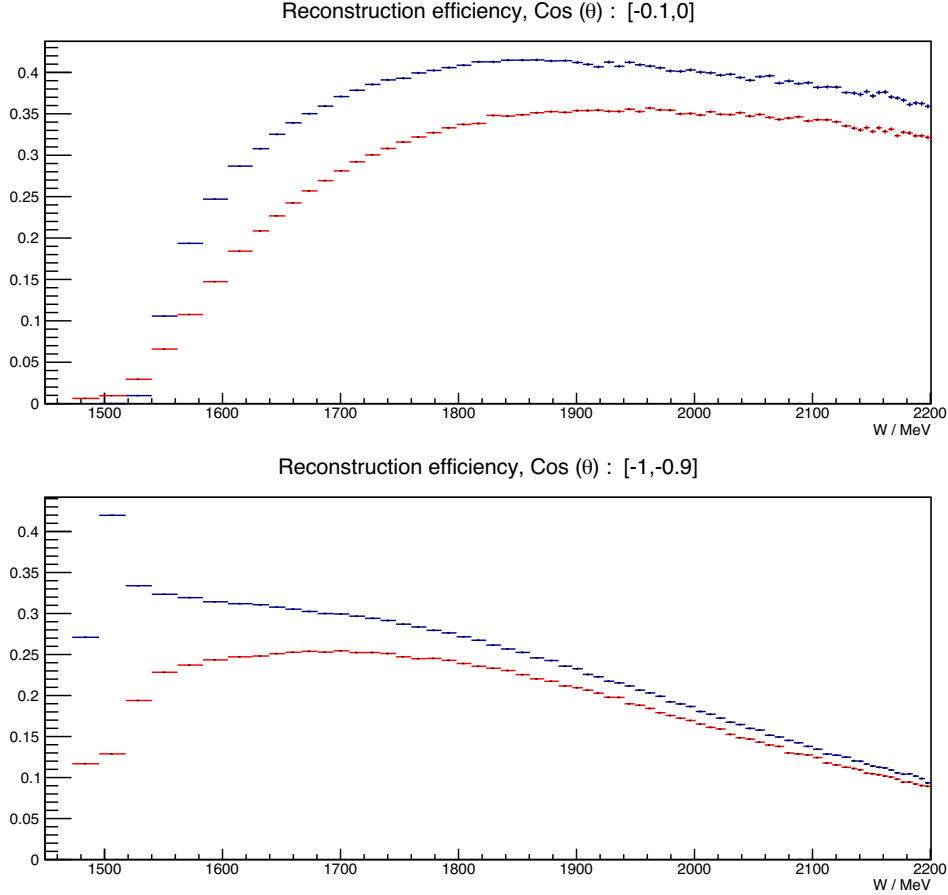


Figure 4.15.: Reconstruction efficiency for the central detector (top) and the forward detector (bottom). In blue is the hydrogen target and in red is the deuterium target.

### Cross section

In figure 4.16 the extracted differential cross section for the hydrogen and the deuterium target can be seen, both for the central and the forward case. Firstly comparing the extracted differential cross section for the hydrogen and the deuterium target in the central detector. For the hydrogen target, it is visible that the energy range, in the

#### 4. Analysis of $\eta$ photoproduction off the proton

vicinity of the production threshold, is kinematically not accessible. Therefore, only the right tail of the  $S_{11}$  resonance was considered in matching the model.

In case of the deuterium target however, these kinematic restrictions do not apply. The whole structure can be modulated according to the model. At around 1680 MeV, a clear difference is visible between the two targets. The dip that the data of the hydrogen target describes, is smeared out by the Fermi motion for the deuterium target.

In case of the forward detector, the same problems can be seen in both targets. Both differential cross sections have an energy offset with respect to the model, with the deuterium target having a higher offset than the hydrogen target. Other than the central case, the hydrogen data matches the shape of the model, while the deuterium data does not. A possible reason for this behavior is that in forward direction no selection cuts are applied, hence the  $\eta$  is less well reconstructed.

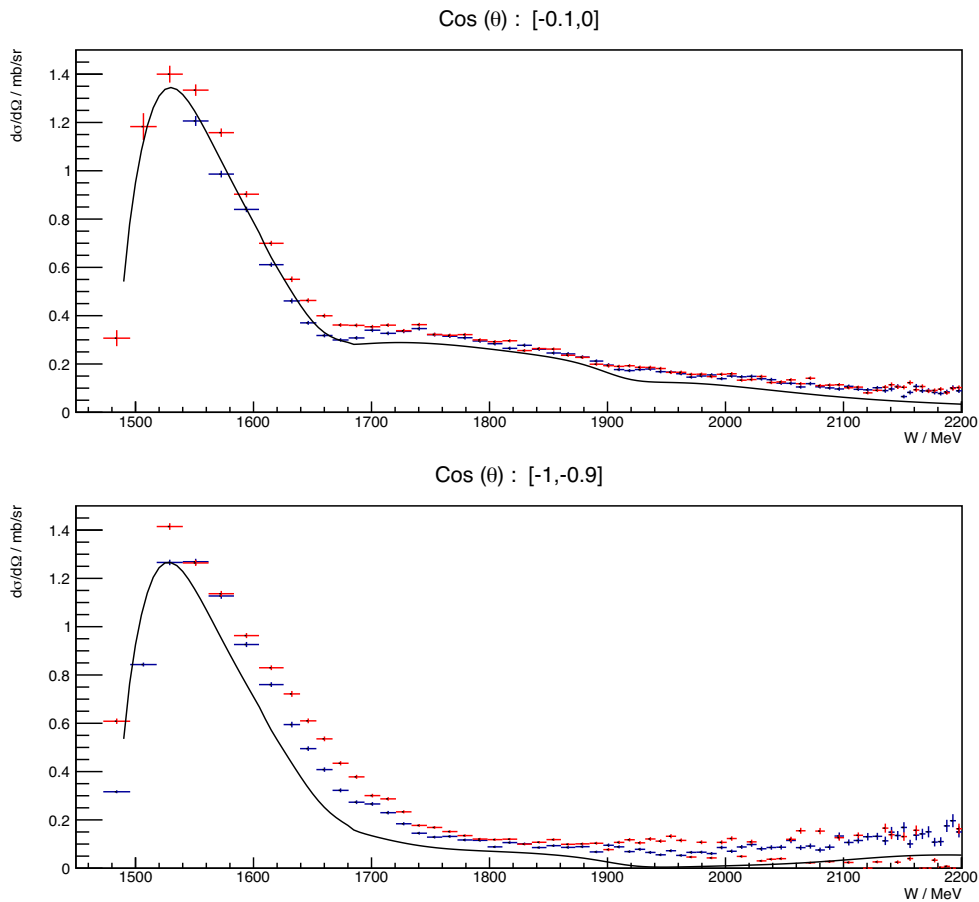


Figure 4.16.: Extracted differential cross section for the central detector (top) and the forward detector (bottom). In blue is the hydrogen target in red is the deuterium target while in black is the BG model.

## 4.2. Final state analysis

Due to Fermi motion the momentum of both proton and neutron inside the deuterium target is unknown; the target particle is not at rest. The four momentum of the initial state, calculated by adding the four momentum of the incoming bremsstrahlung photon and the target proton, is thereby not completely certain.

$$P_{initial} = P_{\gamma} + P_{target}$$

This problem is approached by assuming the proton target at rest, with the consequence that the center of mass energy  $W$ , calculated from the initial state, is smeared out. An alternative approach would be the consideration of the final state, instead of the initial state. In the final state all particles can be reconstructed, hence there are no unknown quantities. The only limiting factor in the resolution of the four momenta of the particles is the resolution of the detectors, while for the final state the energy resolution of the tagger and the Fermi motion play a role.

To analyze the suitability of the final state approach, the resolution of  $W$  in the initial and final state for central and forward detector must be determined. A way of doing so is to use an artificial cross section, which is inserted in the simulation. Using the cross section seen in figure 4.17 allows to extract the detector resolution from the smearing of the delta functions.

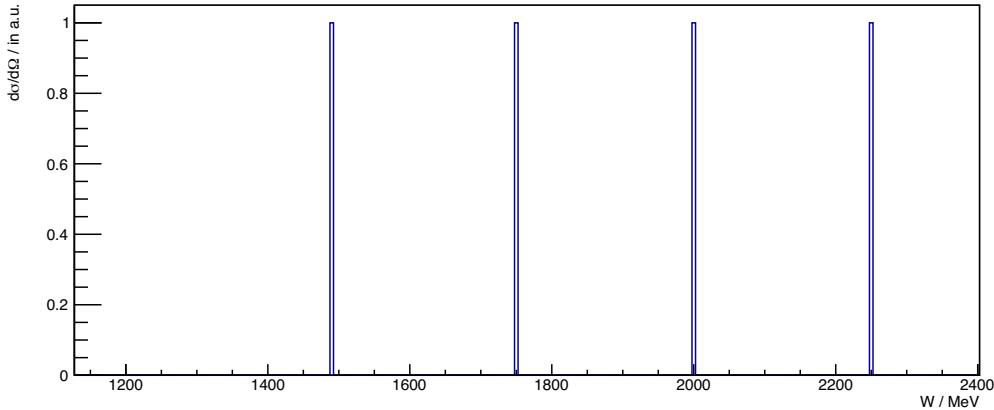


Figure 4.17.: Used artificial cross section. The structure is made of four delta functions with the same distance in energy, while being constant over all angle bins.

In the following, the first case is evaluated, which is the case of a proton detected in the central detector. As seen in figure 4.18, the inserted pattern of the cross section is no longer recognizable in the final state, while it is in the initial state. The second case, proton is detected in the forward detector, can be seen in figure 4.19. The original pattern can be seen in both the initial and the final state.

#### 4. Analysis of $\eta$ photoproduction off the proton

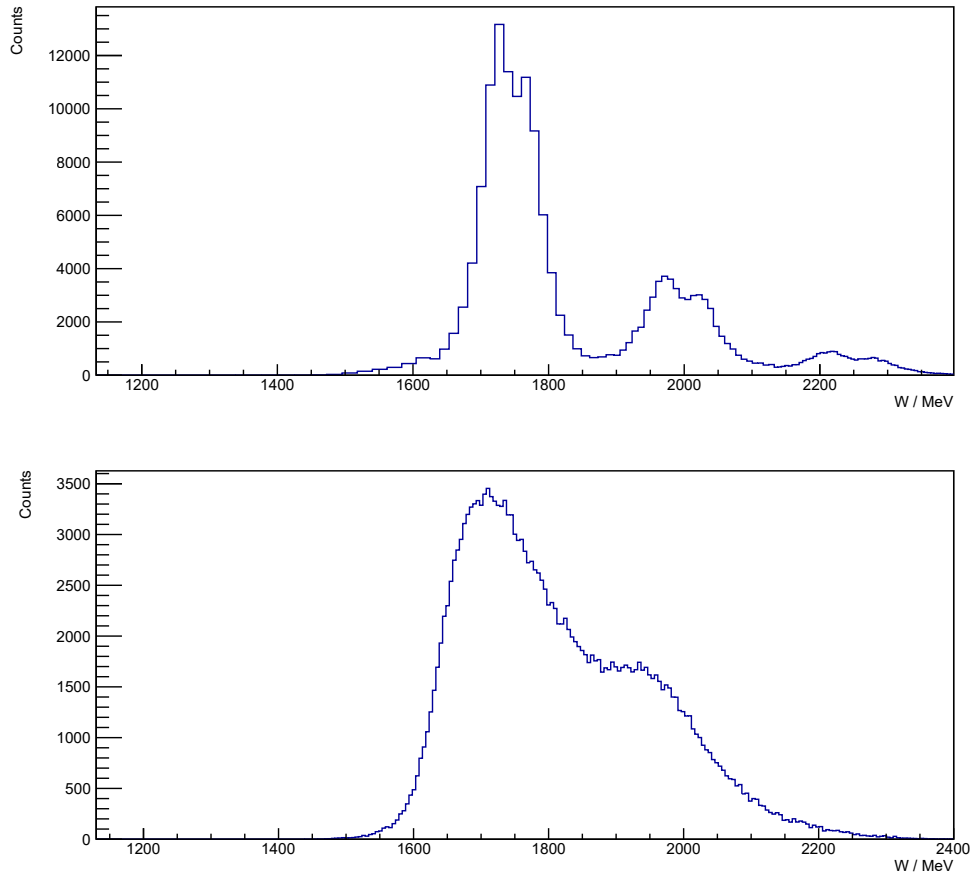


Figure 4.18.: Extracted differential cross section, for the proton being detected in the central detector. In the upper row is the initial state, in the lower row is the the final state.

#### 4. Analysis of $\eta$ photoproduction off the proton

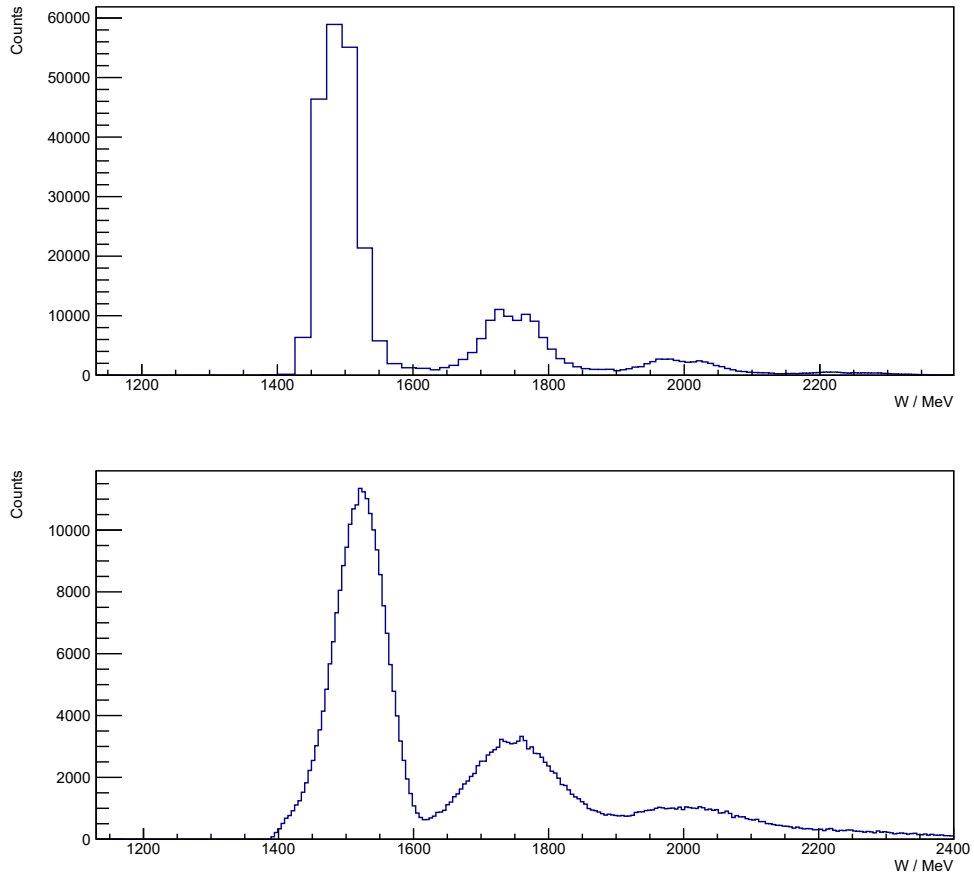


Figure 4.19.: Extracted differential cross section, for the proton being detected in the forward detector. In the upper row is the initial state, in the lower row is the the final state.

#### 4. Analysis of $\eta$ photoproduction off the proton

To acquire the resolution of  $W$  for the initial and the final state, a Gaussian distribution is fitted on every broadened line. The resolution is defined as one sigma of the Gaussian distribution.

Plotting the one sigma values against the corresponding mean value of the Gaussian distributions, as seen in figure 4.20, indicates in which energy regions the final state has a higher resolution and where the initial state. It is quite obvious that the resolution of  $W$  calculated using the final state is worse in the considered energy range than that of the initial state. The last question to be answered is, whether the experiment can be improved, so that the resolution using the final state is better than that of the initial state. To answer this question parameters from the reconstructed simulated particles, get replaced by their real value. This can only be done in simulation, hence the real value is also generated. For this analysis the following parameters get replaced by their generated real value: the energy of both photons, the angle of both photon, or the complete four momentum of the proton. By using this method the detectors gain perfect resolution in one of the parameters, giving a hint on what is to be improved in the experiment. As seen in figure 4.20 the improvement of a single resolution does not provide the needed change to get the resolution of  $W$  calculated from the final state in the vicinity of the resolution of the initial state. All results considered, the final state approach, as of now, is not reliable enough to circumvent the uncertainties of the Fermi motion in the initial state. The resolution of the final state, only dependent on the resolution of the detectors, is not better than the resolution of the Fermi smeared initial state. Furthermore it needs to be noted, that the used decay channel of the eta meson contains the least amount of particles. If a decay with more particles is considered, more particles get detected in the central detector, which worsens the resolution of the final state even more.

### 4.3. Synopsis of analysing methods

The analysis of the initial state shows that the cross section from both tested targets, does not agree with the consulted model without a shift on the energy of the incoming photons. After a correction, which has to be done for the two targets separately, especially the hydrogen target produces a good agreement of the differential cross section of the Bonn Gatchina model. The deuterium target, on the other hand, reveals an unexpected behavior in the differential cross section. It shows an angular dependence, changing from being lower than the model for low  $\cos(\theta)$ , to being higher than the model for high  $\cos(\theta)$ . The exact reason behind this problem could not be found within the scope of this thesis, it needs to be further investigated. Furthermore the adaption of the differential cross section of the deuterium target onto the BG model is not completely advisable, as this model is based on data taken with a hydrogen target.

The analysis of the final state is only done far enough to verify the validity of this approach. It is done to circumvent the smearing of the initial state through the Fermi

#### 4. Analysis of $\eta$ photoproduction off the proton

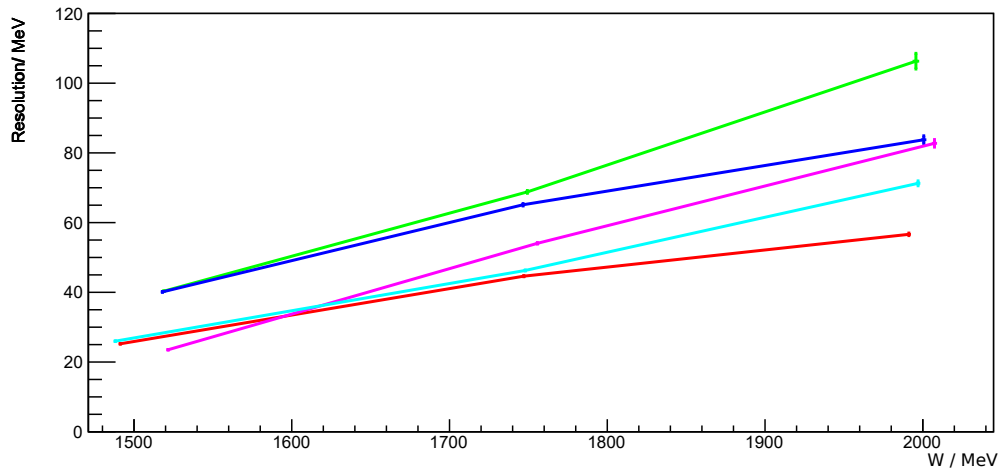


Figure 4.20.: Resolution of the center of mass energy for the final and initial state approach over a range of energy. In red is the resolution in the initial state, and green for the final state. In blue the resolution the four momentum of the final state proton is perfect, while in magenta the photon energy resolution is perfected. The cyan line indicates perfected resolution in the angle of the photon.

motion, and even more neglecting the need of the tagger energy shift. It demonstrates that the initial state has always a better resolution than the final state, and hence is not a viable approach.



## 5. Summary and Conclusion

The initial task of this thesis, was the investigation of the quasi free  $\eta$  photoproduction. For this, the free and quasi free photoproduction was considered; in both cases the proton was the desired participant particle.

The main problem of the deuterium target is that the constituent particles of the deuterium, the proton and the neutron, both have an unknown momentum, the Fermi momentum. To circumvent this problem, the first solution that could be considered, is to do the analysis of the quasi free photoproduction of the  $\eta$  in the center of mass system calculated from the final state.

All final state particles are detected, and hence, the Fermi motion of the target is no longer a problem, since the target is a particle in the initial state. As seen in chapter 4.2 however, the resolution of the center of mass energy is worse in the final state approach, than it is in the initial state approach. The combined resolution of the detectors, which plays a role in the final state, has a bigger influence on the resolution, than the combined effects of the Fermi motion and the energy resolution of the tagger. Thereby the initial state approach is chosen to investigate the quasi free  $\eta$  photoproduction.

In the initial state approach, it shows that the extracted differential cross section of the  $\eta$  does not match the parametrization of the Bonn Gatchina model. In case that the proton is detected in the central detector, the extracted differential cross sections are significantly lower than the model, for both targets. For the case that the proton is detected in the forward detector, the determined differential cross section has an energy offset toward the model. This could have two different reasons.

The first possible reason is that in simulation, the transition region between the central and the forward detector, is not well implemented. In simulation, the protons can be assigned to the wrong detector or even completely disregarded, which influences the reconstruction efficiency and thereby the extracted differential cross section.

The other possible reason is in the tagger calibration. If the electron beam is not at the intended position, the electrons get deflected differently in the tagger magnet, and hence get a false energy assigned. The calculated energy of the proton, the difference of the energy of the electron beam and the energy of the tagged electron, is hereby also wrong. This leads to a change of the center of mass energy, which influences the extracted differential cross section. This possible problem is approached in this thesis, by changing the simulated photon energy by a freely chosen energy value. This solves the problem of the extracted differential cross section not matching with the BG model not entirely. In the case that the proton is detected in the central detector, the determined cross sections match the model well, while in the forward case, the described energy offset still exists.

# Bibliography

- [1] G. Scheluchin. ‘ $\Lambda(1405)$  photoproduction with the BGO-OD experiment’. PhD thesis. 2019.
- [2] P.A. Zyla et al. (Particle Data Group). *The Review of Particle Physics (2021)*. 083C01. 2020.
- [3] S. Alef et al. ‘The BGOOD experimental setup at ELSA’. In: *Eur. Phys. J. A* (2020).
- [4] *Electron Stretcher Accelerator (ELSA) Homepage*. URL: [http://www-elsa.physik.uni-bonn.de/index\\_en.html](http://www-elsa.physik.uni-bonn.de/index_en.html).
- [5] *Single meson photoproduction observables off proton*. URL: [https://pwa.hiskp.uni-bonn.de/BG2011\\_02\\_obs\\_int.htm](https://pwa.hiskp.uni-bonn.de/BG2011_02_obs_int.htm).

# List of Figures

2.1.	Overview of the electron stretcher facility ELSA in Bonn [4] . . . . .	7
2.2.	Overview of the BGOOD experiment [3]. The electron beam, provided by ELSA, is coming from the right side as indicated by the arrow. The main components used in this thesis are described in section 2.2 . . . . .	7
2.3.	Overview of the photon tagger [3]. The electron beam is coming from the left. Upon hitting the radiator the electron beam produces a photon beam which moves in the same direction as the electron beam. The electrons are deflected by the magnetic field of the tagger magnet and hit the scintillators of the tagger hodoscope. . . . .	9
2.4.	Side view of the central detectors [1]. The photon beam is coming from the left and impinges on the target. The target is surrounded by the MWPCs which are surrounded by the scintillator barrel. Most outward the BGO calorimeter is located. . . . .	10
2.5.	Top view on the BGO-OD experiment [3]. The blue arrow indicates the trajectory of a charged particle. The forward spectrometer consists of SciFi2, MOMO, the open dipole magnet, the driftchambers and the ToF walls . . . . .	11
2.6.	Depiction of FluMo and GIM. The color scheme depicts the components of the detectors. The electron positron pairs can be detected by both detectors (indicated with a yellow x), while the photon is only detected by GIM. . . . .	12
3.1.	$^{22}\text{Na}$ energy spectrum in one BGO crystal [3]. The first peak corresponds to the 511 keV photon, while the second peak corresponds to the 1.275 MeV photon. With this spectrum, the electronic response can be mapped to the energies. . . . .	14
3.2.	Schematic depiction of the energy deposition mechanism in the BGO calorimeter for different particles. Exemplary photons and protons are shown. In yellow the calorimeter crystals are shown, in black the PMTs. On top the deposited energy distribution over several crystals is depicted. . . . .	15
3.3.	Charged particle identification in the forward spectrometer [3]. Particle velocity $\beta$ against momentum. Different charged particles can be identified with this plot. . . . .	16

*List of Figures*

4.1.	Number of neutral particles per decay in simulation. There are no restraints on which neutral particles and how many neutral particles are allowed. The blue line indicates the hydrogen target, the red line the deuterium target. All decay channels of the $\eta$ are included. . . . .	19
4.2.	Absolute angular difference in $\phi$ between the invariant mass and the detected proton for the hydrogen target. The proton is detected in the central detector in the top image, and in the forward detector in the lower image. In blue the real data is shown, while in red the simulated data. In the case of the proton being detected in the central detector, an angular difference of $[160^\circ, 200^\circ]$ is allowed, while all differences are allowed for the forward case. . . . .	21
4.3.	Absolute angular difference in $\phi$ between the invariant mass and the detected proton for the deuterium target. The proton is detected in the central detector in the top image, and in the forward detector in the lower image. In blue the real data is shown, while in red the simulated data. In the case of the proton being detected in the central detector, an angular difference of $[160^\circ, 200^\circ]$ is allowed, while all differences are allowed for the forward case. . . . .	22
4.4.	Absolute angular difference in $\theta$ between the missing mass and the detected proton for the hydrogen target. The proton is detected in the central detector in the top image, and in the forward detector in the lower image. In blue the real data is shown, while in red the simulated data. In the case of the proton being detected in the central detector, an angular difference of $[0^\circ, 20^\circ]$ is allowed, while all differences are allowed for the forward case. . . . .	23
4.5.	Absolute angular difference in $\theta$ between the missing mass and the detected proton for the deuterium target. The proton is detected in the central detector in the top image, and in the forward detector in the lower image. In blue the real data is shown, while in red the simulated data. In the case of the proton being detected in the central detector, an angular difference of $[0^\circ, 20^\circ]$ is allowed, while all differences are allowed for the forward case. . . . .	24
4.6.	Invariant mass (top) and missing mass (bottom) after the different implemented cuts for the hydrogen target. The blue line describes the data after the photon selection cut. The red line is after demanding one charged hit. The green line after demanding the proton in the central detector, while the magenta line is after demanding the proton in the forward detector. . . . .	25
4.7.	Invariant mass (top) and missing mass (bottom) after the different implemented cuts for the deuterium target. The blue line describes the data after the photon selection cut. The red line is after demanding one charged hit. The green line after demanding the proton in the central detector, while the magenta line is after demanding the proton in the forward detector. . . . .	26

*List of Figures*

4.8. Extracted differential cross sections for the proton in the central detector (top) and in the forward detector (bottom). In blue is the extracted differential cross section for the hydrogen target, in red for the deuterium target and in black is the BG model for the corresponding angular bins.	28
4.9. Extracted differential cross sections for the proton in the central detector (top) and in the forward detector (bottom). In blue is the extracted differential cross section with a shifted tagger energy by 0 MeV, in red by 5 MeV and in green by 10 MeV. In black is the BG model for the corresponding angular bins. . . . .	30
4.10. Extracted differential cross section in the energy range of [1562,1583] MeV for variable angles. In blue is the extracted differential cross section for the central case, while in red the forward case is depicted. In black is the BG model for this energy range. Both extracted differential cross sections are taken from the same energy range. . . . .	31
4.11. Extracted differential cross section in the energy range of [1562,1583] MeV for variable angles. In blue is the extracted cross section for the central case, while in red the forward case is depicted. In black is the BG model for this energy range. Blue is taken from the given energy range, while red is from an higher energy bin [1583,1604] MeV. . . . .	31
4.12. Extracted differential cross sections for the proton in the central detector (top) and in the forward detector (bottom). In blue is the extracted differential cross section with a shifted tagger energy by 0 MeV, in red by 35 MeV and in green by 40 MeV. In black is the BG model for the corresponding angular bins. . . . .	33
4.13. Extracted differential cross section in the energy range of [1562,1583] MeV for variable angles. In blue is the extracted cross section for the central case, while in red the forward case is depicted. The black line shows the BG model for this energy range. . . . .	34
4.14. Extracted differential cross section in the energy range of [1562,1583] MeV for variable angles. In blue is the extracted cross section for the central case, while in red the forward case is depicted. The black line shows the BG model for this energy range. Blue is taken from the given energy range, while red is from an higher energy bin [1583,1604] MeV. . . . .	34
4.15. Reconstruction efficiency for the central detector (top) and the forward detector (bottom). In blue is the hydrogen target and in red is the deuterium target. . . . .	35
4.16. Extracted differential cross section for the central detector (top) and the forward detector (bottom). In blue is the hydrogen target in red is the deuterium target while in black is the BG model. . . . .	36
4.17. Used artificial cross section. The structure is made of four delta functions with the same distance in energy, while being constant over all angle bins.	37
4.18. Extracted differential cross section, for the proton being detected in the central detector. In the upper row is the initial state, in the lower row is the the final state. . . . .	38

*List of Figures*

4.19. Extracted differential cross section, for the proton being detected in the forward detector. In the upper row is the initial state, in the lower row is the the final state. . . . . 39

4.20. Resolution of the center of mass energy for the final and initial state approach over a range of energy. In red is the resolution in the initial state, ind green for the final state. In blue the resolution the four momentum of the final state proton is perfect, while in magenta the photon energy resolution is perfected. The cyan line indicates perfected resolution in the angle of the photon. . . . . 41

# List of Tables

4.1. Dominant decay channels of the $\eta$ meson [2]. The neutral decay channel $\eta \rightarrow \gamma\gamma$ is chosen. . . . .	18
--	----

# A. Appendix

Hydrogen target:  $\cos(\theta_{CMS}) = [-0.8,-0.7]$

W / MeV		$d\sigma/d\Omega$ / mb/sr		W / MeV		$d\sigma/d\Omega$ / mb/sr	
lower bound	upper bound	value	stat. error	lower bound	upper bound	value	stat. error
1472	1495	0.0000	0.0000	1923	1931	0.0809	0.0247
1495	1517	0.8551	0.3917	1931	1940	0.1172	0.0331
1517	1540	0.5454	0.1113	1940	1949	0.0559	0.0221
1540	1561	0.7034	0.0680	1949	1958	0.0782	0.0252
1561	1583	0.6682	0.0496	1958	1966	0.1152	0.0317
1583	1604	0.5410	0.0383	1966	1975	0.1173	0.0320
1604	1625	0.5524	0.0361	1975	1984	0.0962	0.0311
1625	1639	0.4774	0.0429	1984	1992	0.0505	0.0245
1639	1653	0.4216	0.0348	1992	2001	0.0606	0.0262
1653	1666	0.3545	0.0329	2001	2009	0.1286	0.0419
1666	1680	0.2895	0.0298	2009	2017	0.1061	0.0390
1680	1694	0.3407	0.0326	2017	2026	0.0518	0.0293
1694	1707	0.2268	0.0267	2026	2034	0.0758	0.0372
1707	1720	0.2553	0.0282	2034	2043	0.0676	0.0372
1720	1733	0.2805	0.0299	2043	2051	0.0733	0.0405
1733	1746	0.2206	0.0268	2051	2059	0.0244	0.0238
1746	1759	0.2297	0.0279	2059	2067	0.0575	0.0391
1759	1772	0.2270	0.0277	2067	2076	0.0931	0.0491
1772	1785	0.2082	0.0277	2076	2084	0.0395	0.0354
1785	1798	0.1855	0.0265	2084	2092	0.0662	0.0453
1798	1810	0.1654	0.0256	2092	2100	0.0000	0.0001
1810	1823	0.2195	0.0295	2100	2108	0.0411	0.0387
1823	1835	0.1363	0.0240	2108	2116	0.0738	0.0482
1835	1848	0.1771	0.0275	2116	2124	0.0000	0.0000
1848	1860	0.1551	0.0268	2124	2132	0.1490	0.0805
1860	1872	0.0026	0.0038	2132	2138	0.0000	0.0001
1872	1884	0.0002	0.0012	2138	2143	0.0000	0.0004
1884	1896	0.1068	0.0259				
1896	1905	0.1338	0.0351				
1905	1914	0.1297	0.0300				
1914	1923	0.0715	0.0232				



A. Appendix

Hydrogen target:  $\cos(\theta_{CMS}) = [-0.7,-0.6]$

W / MeV		$d\sigma/d\Omega$ / mb/sr		W / MeV		$d\sigma/d\Omega$ / mb/sr	
lower bound	upper bound	value	stat. error	lower bound	upper bound	value	stat. error
1472	1495	0.0000	0.0000	1975	1984	0.1078	0.0129
1495	1517	5.5525	1.0980	1984	1992	0.1192	0.0143
1517	1540	1.4821	0.1154	1992	2001	0.1031	0.0130
1540	1561	1.1534	0.0450	2001	2009	0.1247	0.0144
1561	1583	0.9806	0.0307	2001	2009	0.0834	0.0125
1583	1604	0.8131	0.0239	2009	2017	0.0966	0.0133
1604	1625	0.6100	0.0193	2017	2026	0.1102	0.0156
1625	1639	0.5374	0.0232	2026	2034	0.1044	0.0159
1639	1653	0.4163	0.0175	2034	2043	0.1109	0.0169
1653	1666	0.3369	0.0162	2043	2051	0.0932	0.0159
1666	1680	0.3175	0.0155	2051	2059	0.0714	0.0144
1680	1694	0.3213	0.0158	2059	2067	0.0875	0.0164
1694	1707	0.2986	0.0153	2067	2076	0.0820	0.0161
1707	1720	0.3326	0.0159	2076	2084	0.0703	0.0155
1720	1733	0.2797	0.0147	2084	2092	0.0753	0.0162
1733	1746	0.2501	0.0137	2092	2100	0.0890	0.0192
1746	1759	0.2464	0.0139	2100	2108	0.0815	0.0175
1759	1772	0.2293	0.0132	2108	2116	0.0903	0.0170
1772	1785	0.2324	0.0139	2116	2124	0.0448	0.0144
1785	1798	0.2077	0.0130	2124	2132	0.0605	0.0158
1798	1810	0.1843	0.0125	2132	2138	0.0836	0.0242
1810	1823	0.1905	0.0125	2138	2143	0.0625	0.0229
1823	1835	0.2012	0.0133	2143	2148	0.0411	0.0164
1835	1848	0.1956	0.0129	2148	2153	0.0447	0.0180
1848	1860	0.1749	0.0125	2153	2159	0.0392	0.0172
1860	1872	0.1740	0.0139	2159	2164	0.0190	0.0129
1872	1884	0.1797	0.0144	2164	2169	0.0435	0.0192
1884	1896	0.1413	0.0128	2169	2174	0.0299	0.0164
1896	1905	0.1462	0.0156	2174	2179	0.0576	0.0214
1905	1914	0.1350	0.0126	2179	2184	0.0417	0.0183
1914	1923	0.1341	0.0129	2184	2190	0.0496	0.0219
1923	1931	0.1041	0.0117	2190	2195	0.0205	0.0143
1931	1940	0.1107	0.0130				
1940	1949	0.0909	0.0114				
1949	1958	0.1105	0.0123				
1958	1966	0.1063	0.0121				
1966	1975	0.1280	0.0136				

A. Appendix

Hydrogen target:  $\cos(\theta_{CMS}) = [-0.7,-0.6]$

W / MeV		$d\sigma/d\Omega$ / mb/sr	
lower bound	upper bound	value	stat. error
2195	2200	0.0284	0.0161
2200	2205	0.1019	0.0300
2205	2210	0.0000	0.0000
2210	2215	0.0561	0.0238
2215	2220	0.0448	0.0220
2220	2225	0.0110	0.0107
2225	2230	0.0414	0.0222
2230	2235	0.0578	0.0254
2235	2241	0.0134	0.0131
2241	2246	0.0119	0.0117
2246	2251	0.0448	0.0248

A. Appendix

Hydrogen target:  $\cos(\theta_{CMS}) = [-0.6,-0.5]$

W / MeV		$d\sigma/d\Omega$ / mb/sr		W / MeV		$d\sigma/d\Omega$ / mb/sr	
lower bound	upper bound	value	stat. error	lower bound	upper bound	value	stat. err
1472	1495	338.0843	341.3962	1975	1984	0.1163	0.0090
1495	1517	6.9822	1.0958	1984	1992	0.1106	0.0093
1517	1540	1.9734	0.0995	1992	2001	0.1004	0.0087
1540	1561	1.2484	0.0319	2001	2009	0.1301	0.0105
1561	1583	1.0240	0.0220	2009	2017	0.1089	0.0095
1583	1604	0.8461	0.0176	2017	2026	0.1105	0.0104
1604	1625	0.6352	0.0142	2026	2034	0.0938	0.0099
1625	1639	0.5313	0.0166	2034	2043	0.1091	0.0110
1639	1653	0.4078	0.0125	2043	2051	0.1073	0.0112
1653	1666	0.3479	0.0120	2051	2059	0.0935	0.0106
1666	1680	0.3166	0.0113	2059	2067	0.0942	0.0109
1680	1694	0.3052	0.0111	2067	2076	0.1035	0.0116
1694	1707	0.3087	0.0113	2076	2084	0.0957	0.0116
1707	1720	0.2941	0.0108	2084	2092	0.0902	0.0114
1720	1733	0.2748	0.0104	2092	2100	0.1029	0.0129
1733	1746	0.2765	0.0104	2100	2108	0.0826	0.0110
1746	1759	0.2409	0.0099	2108	2116	0.0673	0.0092
1759	1772	0.2373	0.0096	2116	2124	0.0650	0.0108
1772	1785	0.2404	0.0101	2124	2132	0.0682	0.0102
1785	1798	0.2330	0.0098	2132	2138	0.0457	0.0108
1798	1810	0.2186	0.0096	2138	2143	0.0446	0.0115
1810	1823	0.2191	0.0096	2143	2148	0.0602	0.0120
1823	1835	0.2119	0.0096	2148	2153	0.0619	0.0125
1835	1848	0.2082	0.0094	2153	2159	0.0715	0.0138
1848	1860	0.1995	0.0094	2159	2164	0.0480	0.0121
1860	1872	0.1925	0.0103	2164	2169	0.0484	0.0120
1872	1884	0.1543	0.0093	2169	2174	0.0729	0.0153
1884	1896	0.1744	0.0100	2174	2179	0.0403	0.0103
1896	1905	0.1527	0.0110	2179	2184	0.0447	0.0110
1905	1914	0.1464	0.0091	2184	2190	0.0532	0.0131
1914	1923	0.1335	0.0089	2190	2195	0.0461	0.0123
1923	1931	0.1275	0.0089	2195	2200	0.0302	0.0093
1931	1940	0.1288	0.0097	2200	2205	0.0468	0.0115
1940	1949	0.1324	0.0095	2205	2210	0.0683	0.0148
1949	1958	0.1294	0.0091	2210	2215	0.0501	0.0126
1958	1966	0.1334	0.0093	2215	2220	0.0329	0.0105
1966	1975	0.1277	0.0091	2220	2225	0.0426	0.0116
				2225	2230	0.0321	0.0105
				2230	2235	0.0339	0.0106

A. Appendix

Hydrogen target:  $\cos(\theta_{CMS}) = [-0.6,-0.5]$

W / MeV		$d\sigma/d\Omega$ / mb/sr	
lower bound	upper bound	value	stat. error
2235	2241	0.0446	0.0124
2241	2246	0.0259	0.0095
2246	2251	0.0449	0.0130
2251	2256	0.0369	0.0114
2256	2261	0.0150	0.0079
2261	2266	0.0204	0.0088
2266	2270	0.0354	0.0124
2270	2275	0.0446	0.0136
2275	2280	0.0451	0.0140
2280	2285	0.0378	0.0122
2285	2290	0.0198	0.0094
2290	2295	0.0378	0.0130
2295	2300	0.0289	0.0116
2300	2305	0.0381	0.0130
2305	2310	0.0150	0.0084
2310	2315	0.0610	0.0168
2315	2320	0.0483	0.0156
2320	2324	0.0448	0.0147
2324	2329	0.0279	0.0122
2329	2334	0.0120	0.0079
2334	2339	0.0283	0.0124
2339	2344	0.0408	0.0141
2344	2349	0.0127	0.0083
2349	2353	0.0316	0.0132
2353	2358	0.0195	0.0106
2358	2363	0.0127	0.0085
2363	2368	0.0186	0.0105
2368	2372	0.0145	0.0100
2372	2377	0.0300	0.0145
2377	2382	0.0350	0.0143
2382	2387	0.0271	0.0133
2387	2391	0.0326	0.0148

A. Appendix

Hydrogen target:  $\cos(\theta_{CMS}) = [-0.5,-0.4]$

W / MeV		$d\sigma/d\Omega$ / mb/sr		W / MeV		$d\sigma/d\Omega$ / mb/sr	
lower bound	upper bound	value	stat. error	lower bound	upper bound	value	stat. err
1472	1495	411.7643	415.1915	1975	1984	0.1257	0.0079
1495	1517	9.6029	1.4777	1984	1992	0.1327	0.0086
1517	1540	2.2521	0.0916	1992	2001	0.1276	0.0083
1540	1561	1.2937	0.0270	2001	2009	0.1199	0.0085
1561	1583	1.0617	0.0188	2009	2017	0.1287	0.0087
1583	1604	0.9106	0.0154	2017	2026	0.1307	0.0095
1604	1625	0.6680	0.0124	2026	2034	0.1058	0.0088
1625	1639	0.5338	0.0142	2034	2043	0.1264	0.0099
1639	1653	0.4493	0.0114	2043	2051	0.1179	0.0098
1653	1666	0.3533	0.0104	2051	2059	0.1015	0.0093
1666	1680	0.3286	0.0099	2059	2067	0.1146	0.0100
1680	1694	0.3176	0.0098	2067	2076	0.1031	0.0096
1694	1707	0.3263	0.0100	2076	2084	0.1007	0.0098
1707	1720	0.3243	0.0098	2084	2092	0.1030	0.0100
1720	1733	0.3156	0.0096	2092	2100	0.0900	0.0100
1733	1746	0.2979	0.0093	2100	2108	0.0917	0.0095
1746	1759	0.2797	0.0091	2108	2116	0.0784	0.0080
1759	1772	0.2769	0.0090	2116	2124	0.0878	0.0102
1772	1785	0.2598	0.0090	2124	2132	0.0835	0.0092
1785	1798	0.2547	0.0089	2132	2138	0.0658	0.0105
1798	1810	0.2482	0.0088	2138	2143	0.0921	0.0135
1810	1823	0.2367	0.0085	2143	2148	0.0726	0.0107
1823	1835	0.2058	0.0080	2148	2153	0.0623	0.0103
1835	1848	0.2302	0.0085	2153	2159	0.0804	0.0118
1848	1860	0.1995	0.0080	2159	2164	0.0819	0.0127
1860	1872	0.2096	0.0091	2164	2169	0.0821	0.0126
1872	1884	0.1969	0.0090	2169	2174	0.0633	0.0114
1884	1896	0.1934	0.0089	2174	2179	0.0666	0.0106
1896	1905	0.1582	0.0095	2179	2184	0.0732	0.0112
1905	1914	0.1604	0.0081	2184	2190	0.0593	0.0110
1914	1923	0.1643	0.0084	2190	2195	0.0516	0.0104
1923	1931	0.1271	0.0076	2195	2200	0.0517	0.0096
1931	1940	0.1385	0.0086	2200	2205	0.0608	0.0106
1940	1949	0.1397	0.0083	2205	2210	0.0594	0.0110
1949	1958	0.1287	0.0077	2210	2215	0.0438	0.0094
1958	1966	0.1347	0.0079	2215	2220	0.0536	0.0105
1966	1975	0.1251	0.0077	2220	2225	0.0552	0.0105
				2225	2230	0.0369	0.0090
				2230	2235	0.0469	0.0097

A. Appendix

Hydrogen target:  $\cos(\theta_{CMS}) = [-0.5,-0.4]$

W / MeV		$d\sigma/d\Omega$ / mb/sr	
lower bound	upper bound	value	stat. error
2235	2241	0.0712	0.0126
2241	2246	0.0419	0.0094
2246	2251	0.0501	0.0108
2251	2256	0.0300	0.0080
2256	2261	0.0495	0.0111
2261	2266	0.0426	0.0098
2266	2270	0.0442	0.0106
2270	2275	0.0378	0.0098
2275	2280	0.0308	0.0086
2280	2285	0.0451	0.0104
2285	2290	0.0383	0.0100
2290	2295	0.0419	0.0104
2295	2300	0.0281	0.0087
2300	2305	0.0380	0.0098
2305	2310	0.0411	0.0106
2310	2315	0.0337	0.0095
2315	2320	0.0388	0.0104
2320	2324	0.0348	0.0098
2324	2329	0.0303	0.0096
2329	2334	0.0335	0.0098
2334	2339	0.0330	0.0098
2339	2344	0.0406	0.0104
2344	2349	0.0231	0.0084
2349	2353	0.0291	0.0092
2353	2358	0.0404	0.0111
2358	2363	0.0513	0.0125
2363	2368	0.0240	0.0088
2368	2372	0.0345	0.0111
2372	2377	0.0162	0.0077
2377	2382	0.0383	0.0107
2382	2387	0.0361	0.0108
2387	2391	0.0150	0.0071

A. Appendix

Hydrogen target:  $\cos(\theta_{CMS}) = [-0.4,-0.3]$

W / MeV		$d\sigma/d\Omega$ / mb/sr		W / MeV		$d\sigma/d\Omega$ / mb/sr	
lower bound	upper bound	value	stat. error	lower bound	upper bound	value	stat. error
1472	1495	0.0000	0.0000	1975	1984	0.1276	0.0069
1495	1517	8.3061	1.2903	1984	1992	0.1381	0.0076
1517	1540	2.1877	0.0831	1992	2001	0.1173	0.0069
1540	1561	1.2634	0.0234	2001	2009	0.1394	0.0080
1561	1583	1.0416	0.0164	2009	2017	0.1135	0.0071
1583	1604	0.8657	0.0133	2017	2026	0.1130	0.0077
1604	1625	0.6311	0.0108	2026	2034	0.1252	0.0084
1625	1639	0.5006	0.0123	2034	2043	0.1309	0.0088
1639	1653	0.4132	0.0097	2043	2051	0.1068	0.0081
1653	1666	0.3398	0.0092	2051	2059	0.0856	0.0074
1666	1680	0.3043	0.0085	2059	2067	0.1163	0.0087
1680	1694	0.3002	0.0085	2067	2076	0.1040	0.0084
1694	1707	0.3105	0.0087	2076	2084	0.1019	0.0086
1707	1720	0.3243	0.0088	2084	2092	0.1141	0.0091
1720	1733	0.3057	0.0085	2092	2100	0.0873	0.0085
1733	1746	0.3060	0.0085	2100	2108	0.0924	0.0084
1746	1759	0.2731	0.0081	2108	2116	0.0741	0.0068
1759	1772	0.2586	0.0077	2116	2124	0.0804	0.0085
1772	1785	0.2715	0.0082	2124	2132	0.0714	0.0074
1785	1798	0.2554	0.0079	2132	2138	0.0656	0.0090
1798	1810	0.2390	0.0077	2138	2143	0.0678	0.0099
1810	1823	0.2315	0.0074	2143	2148	0.0772	0.0094
1823	1835	0.2337	0.0076	2148	2153	0.0596	0.0085
1835	1848	0.2191	0.0073	2153	2159	0.0728	0.0097
1848	1860	0.2230	0.0075	2159	2164	0.0707	0.0102
1860	1872	0.2209	0.0082	2164	2169	0.0824	0.0108
1872	1884	0.2163	0.0083	2169	2174	0.0641	0.0098
1884	1896	0.2031	0.0080	2174	2179	0.0863	0.0104
1896	1905	0.1604	0.0085	2179	2184	0.0620	0.0088
1905	1914	0.1674	0.0073	2184	2190	0.0708	0.0103
1914	1923	0.1426	0.0069	2190	2195	0.0800	0.0109
1923	1931	0.1374	0.0069	2195	2200	0.0662	0.0093
1931	1940	0.1478	0.0077	2200	2205	0.0531	0.0085
1940	1949	0.1438	0.0073	2205	2210	0.0546	0.0088
1949	1958	0.1417	0.0071	2210	2215	0.0812	0.0107
1958	1966	0.1469	0.0072	2215	2220	0.0433	0.0080
1966	1975	0.1360	0.0070	2220	2225	0.0591	0.0092
				2225	2230	0.0430	0.0082
				2230	2235	0.0524	0.0088

A. Appendix

Hydrogen target:  $\cos(\theta_{CMS}) = [-0.4,-0.3]$

W / MeV		$d\sigma/d\Omega$ / mb/sr	
lower bound	upper bound	value	stat. error
2235	2241	0.0615	0.0099
2241	2246	0.0587	0.0093
2246	2251	0.0543	0.0093
2251	2256	0.0476	0.0085
2256	2261	0.0390	0.0082
2261	2266	0.0516	0.0089
2266	2270	0.0447	0.0089
2270	2275	0.0632	0.0105
2275	2280	0.0412	0.0084
2280	2285	0.0321	0.0072
2285	2290	0.0454	0.0089
2290	2295	0.0548	0.0098
2295	2300	0.0569	0.0102
2300	2305	0.0453	0.0088
2305	2310	0.0426	0.0089
2310	2315	0.0546	0.0098
2315	2320	0.0467	0.0094
2320	2324	0.0333	0.0077
2324	2329	0.0406	0.0091
2329	2334	0.0418	0.0089
2334	2339	0.0321	0.0079
2339	2344	0.0318	0.0074
2344	2349	0.0555	0.0105
2349	2353	0.0511	0.0100
2353	2358	0.0344	0.0083
2358	2363	0.0354	0.0084
2363	2368	0.0252	0.0072
2368	2372	0.0436	0.0100
2372	2377	0.0186	0.0065
2377	2382	0.0410	0.0090
2382	2387	0.0511	0.0103
2387	2391	0.0354	0.0087



A. Appendix

Hydrogen target:  $\cos(\theta_{CMS}) = [-0.3,-0.2]$

W / MeV		$d\sigma/d\Omega$ / mb/sr		W / MeV		$d\sigma/d\Omega$ / mb/sr	
lower bound	upper bound	value	stat. error	lower bound	upper bound	value	stat. error
1472	1495	0.0000	0.0000	1984	1992	0.1412	0.0072
1495	1517	17.6179	2.6332	1992	2001	0.1395	0.0070
1517	1540	2.3384	0.0846	2001	2009	0.1425	0.0074
1540	1561	1.2393	0.0217	2009	2017	0.1226	0.0068
1561	1583	1.0479	0.0154	2017	2026	0.1364	0.0078
1583	1604	0.8701	0.0125	2026	2034	0.1331	0.0079
1604	1625	0.6411	0.0102	2034	2043	0.1165	0.0076
1625	1639	0.4961	0.0115	2043	2051	0.1227	0.0080
1639	1653	0.4015	0.0090	2051	2059	0.1163	0.0079
1653	1666	0.3359	0.0085	2059	2067	0.1005	0.0074
1666	1680	0.3116	0.0081	2067	2076	0.1163	0.0081
1680	1694	0.2971	0.0079	2076	2084	0.1187	0.0085
1694	1707	0.3109	0.0082	2084	2092	0.0820	0.0071
1707	1720	0.3187	0.0081	2092	2100	0.1092	0.0087
1720	1733	0.3119	0.0080	2100	2108	0.0799	0.0070
1733	1746	0.2991	0.0079	2108	2116	0.0858	0.0067
1746	1759	0.2852	0.0078	2116	2124	0.0873	0.0080
1759	1772	0.2801	0.0075	2124	2132	0.0840	0.0073
1772	1785	0.2578	0.0075	2132	2138	0.0867	0.0095
1785	1798	0.2640	0.0075	2138	2143	0.0758	0.0096
1798	1810	0.2699	0.0077	2143	2148	0.0851	0.0089
1810	1823	0.2426	0.0071	2148	2153	0.0867	0.0094
1823	1835	0.2371	0.0072	2153	2159	0.0702	0.0087
1835	1848	0.2461	0.0072	2159	2164	0.0688	0.0091
1848	1860	0.2222	0.0070	2164	2169	0.0726	0.0091
1860	1872	0.2260	0.0078	2169	2174	0.0701	0.0093
1872	1884	0.1939	0.0073	2174	2179	0.0634	0.0081
1884	1896	0.1954	0.0073	2179	2184	0.0777	0.0089
1896	1905	0.1614	0.0079	2184	2190	0.0778	0.0098
1905	1914	0.1691	0.0068	2190	2195	0.0687	0.0091
1914	1923	0.1672	0.0069	2195	2200	0.0488	0.0072
1923	1931	0.1445	0.0066	2200	2205	0.0603	0.0081
1931	1940	0.1561	0.0074	2205	2210	0.0669	0.0089
1940	1949	0.1489	0.0069	2210	2215	0.0628	0.0085
1949	1958	0.1598	0.0070	2215	2220	0.0562	0.0082
1958	1966	0.1498	0.0067	2220	2225	0.0427	0.0070
1966	1975	0.1300	0.0063	2225	2230	0.0436	0.0074
1975	1984	0.1451	0.0068	2230	2235	0.0544	0.0080

A. Appendix

Hydrogen target:  $\cos(\theta_{CMS}) = [-0.3,-0.2]$

W / MeV		$d\sigma/d\Omega$ / mb/sr	
lower bound	upper bound	value	stat. error
2235	2241	0.0454	0.0076
2241	2246	0.0580	0.0083
2246	2251	0.0519	0.0083
2251	2256	0.0495	0.0077
2256	2261	0.0434	0.0078
2261	2266	0.0732	0.0096
2266	2270	0.0392	0.0075
2270	2275	0.0544	0.0087
2275	2280	0.0477	0.0081
2280	2285	0.0544	0.0084
2285	2290	0.0453	0.0079
2290	2295	0.0501	0.0084
2295	2300	0.0398	0.0076
2300	2305	0.0626	0.0093
2305	2310	0.0468	0.0083
2310	2315	0.0315	0.0067
2315	2320	0.0367	0.0074
2320	2324	0.0346	0.0070
2324	2329	0.0433	0.0083
2329	2334	0.0463	0.0083
2334	2339	0.0407	0.0078
2339	2344	0.0432	0.0076
2344	2349	0.0257	0.0064
2349	2353	0.0441	0.0081
2353	2358	0.0239	0.0061
2358	2363	0.0309	0.0069
2363	2368	0.0403	0.0079
2368	2372	0.0345	0.0079
2372	2377	0.0385	0.0083
2377	2382	0.0293	0.0066
2382	2387	0.0398	0.0080
2387	2391	0.0407	0.0082

A. Appendix

Hydrogen target:  $\cos(\theta_{CMS}) = [-0.2,-0.1]$

W / MeV		$d\sigma/d\Omega$ / mb/sr		W / MeV		$d\sigma/d\Omega$ / mb/sr	
lower bound	upper bound	value	stat. error	lower bound	upper bound	value	stat. error
1472	1495	0.0000	0.0000	1984	1992	0.1434	0.0069
1495	1517	23.2982	3.5209	1992	2001	0.1469	0.0068
1517	1540	2.2454	0.0862	2001	2009	0.1445	0.0072
1540	1561	1.2164	0.0208	2009	2017	0.1442	0.0071
1561	1583	1.0179	0.0146	2017	2026	0.1303	0.0072
1583	1604	0.8452	0.0118	2026	2034	0.1158	0.0070
1604	1625	0.6390	0.0097	2034	2043	0.1220	0.0075
1625	1639	0.4846	0.0109	2043	2051	0.1115	0.0072
1639	1653	0.3836	0.0084	2051	2059	0.1179	0.0076
1653	1666	0.3209	0.0080	2059	2067	0.1129	0.0076
1666	1680	0.3005	0.0077	2067	2076	0.0970	0.0071
1680	1694	0.3040	0.0077	2076	2084	0.1117	0.0079
1694	1707	0.3275	0.0081	2084	2092	0.1076	0.0078
1707	1720	0.3176	0.0078	2092	2100	0.1008	0.0080
1720	1733	0.3230	0.0078	2100	2108	0.0958	0.0074
1733	1746	0.3307	0.0079	2108	2116	0.0875	0.0064
1746	1759	0.3088	0.0077	2116	2124	0.0873	0.0076
1759	1772	0.3098	0.0076	2124	2132	0.0916	0.0073
1772	1785	0.2816	0.0075	2132	2138	0.0858	0.0090
1785	1798	0.2955	0.0077	2138	2143	0.0873	0.0098
1798	1810	0.2756	0.0074	2143	2148	0.0849	0.0086
1810	1823	0.2524	0.0070	2148	2153	0.0874	0.0090
1823	1835	0.2547	0.0072	2153	2159	0.0909	0.0094
1835	1848	0.2535	0.0070	2159	2164	0.0710	0.0088
1848	1860	0.2544	0.0072	2164	2169	0.1030	0.0103
1860	1872	0.2318	0.0076	2169	2174	0.0846	0.0097
1872	1884	0.2247	0.0076	2174	2179	0.0609	0.0075
1884	1896	0.1974	0.0071	2179	2184	0.0830	0.0088
1896	1905	0.1767	0.0079	2184	2190	0.0666	0.0086
1905	1914	0.1892	0.0069	2190	2195	0.0834	0.0096
1914	1923	0.1676	0.0067	2195	2200	0.0742	0.0085
1923	1931	0.1664	0.0068	2200	2205	0.0646	0.0079
1931	1940	0.1515	0.0070	2205	2210	0.0583	0.0078
1940	1949	0.1698	0.0071	2210	2215	0.0723	0.0086
1949	1958	0.1593	0.0066	2215	2220	0.0758	0.0090
1958	1966	0.1595	0.0066	2220	2225	0.0659	0.0082
1966	1975	0.1465	0.0064	2225	2230	0.0574	0.0080
1975	1984	0.1558	0.0068	2230	2235	0.0620	0.0080

A. Appendix

Hydrogen target:  $\cos(\theta_{CMS}) = [-0.2,-0.1]$

W / MeV		$d\sigma/d\Omega$ / mb/sr	
lower bound	upper bound	value	stat. error
2235	2241	0.0717	0.0089
2241	2246	0.0530	0.0074
2246	2251	0.0637	0.0085
2251	2256	0.0658	0.0083
2256	2261	0.0721	0.0094
2261	2266	0.0627	0.0083
2266	2270	0.0699	0.0093
2270	2275	0.0691	0.0092
2275	2280	0.0415	0.0070
2280	2285	0.0578	0.0081
2285	2290	0.0493	0.0078
2290	2295	0.0495	0.0077
2295	2300	0.0608	0.0087
2300	2305	0.0516	0.0078
2305	2310	0.0468	0.0077
2310	2315	0.0592	0.0085
2315	2320	0.0606	0.0088
2320	2324	0.0474	0.0075
2324	2329	0.0469	0.0080
2329	2334	0.0445	0.0075
2334	2339	0.0458	0.0077
2339	2344	0.0458	0.0073
2344	2349	0.0567	0.0087
2349	2353	0.0509	0.0081
2353	2358	0.0486	0.0080
2358	2363	0.0373	0.0070
2363	2368	0.0339	0.0067
2368	2372	0.0421	0.0080
2372	2377	0.0534	0.0091
2377	2382	0.0441	0.0075
2382	2387	0.0554	0.0087
2387	2391	0.0356	0.0071

A. Appendix

Hydrogen target:  $\cos(\theta_{CMS}) = [-0.1, 0]$

W / MeV		$d\sigma/d\Omega$ / mb/sr		W / MeV		$d\sigma/d\Omega$ / mb/sr	
lower bound	upper bound	value	stat. error	lower bound	upper bound	value	stat. error
1472	1495	0.0000	0.0000	1984	1992	0.1548	0.0069
1495	1517	21.7464	3.4226	1992	2001	0.1392	0.0064
1517	1540	2.3009	0.0926	2001	2009	0.1500	0.0070
1540	1561	1.2062	0.0206	2009	2017	0.1470	0.0069
1561	1583	0.9863	0.0139	2017	2026	0.1488	0.0075
1583	1604	0.8400	0.0114	2026	2034	0.1389	0.0075
1604	1625	0.6112	0.0092	2034	2043	0.1350	0.0076
1625	1639	0.4611	0.0103	2043	2051	0.1207	0.0073
1639	1653	0.3703	0.0080	2051	2059	0.1199	0.0074
1653	1666	0.3179	0.0077	2059	2067	0.1049	0.0070
1666	1680	0.2994	0.0074	2067	2076	0.1186	0.0075
1680	1694	0.3078	0.0076	2076	2084	0.1055	0.0073
1694	1707	0.3399	0.0080	2084	2092	0.1009	0.0072
1707	1720	0.3269	0.0077	2092	2100	0.0966	0.0075
1720	1733	0.3351	0.0078	2100	2108	0.1074	0.0075
1733	1746	0.3466	0.0079	2108	2116	0.0951	0.0064
1746	1759	0.3215	0.0077	2116	2124	0.0930	0.0075
1759	1772	0.3149	0.0075	2124	2132	0.1017	0.0073
1772	1785	0.3087	0.0077	2132	2138	0.0896	0.0088
1785	1798	0.2952	0.0074	2138	2143	0.0965	0.0099
1798	1810	0.2840	0.0073	2143	2148	0.1070	0.0092
1810	1823	0.2648	0.0070	2148	2153	0.0651	0.0074
1823	1835	0.2774	0.0073	2153	2159	0.0823	0.0085
1835	1848	0.2611	0.0069	2159	2164	0.1071	0.0103
1848	1860	0.2455	0.0069	2164	2169	0.0889	0.0092
1860	1872	0.2417	0.0075	2169	2174	0.0901	0.0095
1872	1884	0.2287	0.0074	2174	2179	0.0821	0.0083
1884	1896	0.2120	0.0071	2179	2184	0.0778	0.0082
1896	1905	0.1954	0.0081	2184	2190	0.0846	0.0093
1905	1914	0.1768	0.0065	2190	2195	0.1017	0.0101
1914	1923	0.1727	0.0066	2195	2200	0.0889	0.0089
1923	1931	0.1770	0.0068	2200	2205	0.0796	0.0084
1931	1940	0.1792	0.0074	2205	2210	0.0796	0.0087
1940	1949	0.1682	0.0068	2210	2215	0.0954	0.0095
1949	1958	0.1665	0.0066	2215	2220	0.0521	0.0071
1958	1966	0.1596	0.0065	2220	2225	0.0741	0.0083
1966	1975	0.1454	0.0062	2225	2230	0.0652	0.0082
1975	1984	0.1503	0.0065	2230	2235	0.0636	0.0079

A. Appendix

Hydrogen target:  $\cos(\theta_{CMS}) = [-0.1,0]$

W / MeV		$d\sigma/d\Omega$ / mb/sr	
lower bound	upper bound	value	stat. error
2235	2241	0.0584	0.0078
2241	2246	0.0686	0.0082
2246	2251	0.0652	0.0084
2251	2256	0.0659	0.0080
2256	2261	0.0583	0.0081
2261	2266	0.0825	0.0091
2266	2270	0.0623	0.0085
2270	2275	0.0617	0.0083
2275	2280	0.0750	0.0091
2280	2285	0.0559	0.0077
2285	2290	0.0595	0.0082
2290	2295	0.0685	0.0087
2295	2300	0.0618	0.0084
2300	2305	0.0478	0.0073
2305	2310	0.0505	0.0077
2310	2315	0.0563	0.0079
2315	2320	0.0430	0.0071
2320	2324	0.0414	0.0069
2324	2329	0.0568	0.0084
2329	2334	0.0542	0.0079
2334	2339	0.0653	0.0089
2339	2344	0.0583	0.0079
2344	2349	0.0629	0.0087
2349	2353	0.0407	0.0070
2353	2358	0.0550	0.0082
2358	2363	0.0385	0.0068
2363	2368	0.0594	0.0086
2368	2372	0.0533	0.0086
2372	2377	0.0490	0.0083
2377	2382	0.0458	0.0073
2382	2387	0.0575	0.0084
2387	2391	0.0412	0.0073

A. Appendix

Hydrogen target:  $\cos(\theta_{CMS}) = [0,0.1]$

W / MeV		$d\sigma/d\Omega$ / mb/sr		W / MeV		$d\sigma/d\Omega$ / mb/sr	
lower bound	upper bound	value	stat. error	lower bound	upper bound	value	stat. error
1472	1495	0.0000	0.0000	1984	1992	0.1533	0.0069
1495	1517	29.8064	4.8823	1992	2001	0.1683	0.0070
1517	1540	2.3489	0.1032	2001	2009	0.1587	0.0072
1540	1561	1.2136	0.0211	2009	2017	0.1526	0.0070
1561	1583	1.0006	0.0138	2017	2026	0.1324	0.0070
1583	1604	0.8152	0.0110	2026	2034	0.1292	0.0072
1604	1625	0.6305	0.0092	2034	2043	0.1331	0.0074
1625	1639	0.4760	0.0104	2043	2051	0.1321	0.0076
1639	1653	0.3958	0.0082	2051	2059	0.1237	0.0074
1653	1666	0.3312	0.0078	2059	2067	0.1169	0.0073
1666	1680	0.2957	0.0073	2067	2076	0.1245	0.0077
1680	1694	0.3140	0.0076	2076	2084	0.1251	0.0080
1694	1707	0.3462	0.0080	2084	2092	0.1001	0.0071
1707	1720	0.3735	0.0082	2092	2100	0.1129	0.0081
1720	1733	0.3616	0.0081	2100	2108	0.0996	0.0072
1733	1746	0.3549	0.0080	2108	2116	0.1108	0.0069
1746	1759	0.3477	0.0080	2116	2124	0.0870	0.0073
1759	1772	0.3207	0.0075	2124	2132	0.1059	0.0075
1772	1785	0.3281	0.0079	2132	2138	0.1112	0.0098
1785	1798	0.3193	0.0077	2138	2143	0.0969	0.0099
1798	1810	0.3020	0.0076	2143	2148	0.1044	0.0091
1810	1823	0.3042	0.0075	2148	2153	0.1117	0.0098
1823	1835	0.2797	0.0073	2153	2159	0.1078	0.0098
1835	1848	0.2839	0.0072	2159	2164	0.0832	0.0092
1848	1860	0.2678	0.0072	2164	2169	0.0898	0.0093
1860	1872	0.2703	0.0080	2169	2174	0.0920	0.0097
1872	1884	0.2446	0.0076	2174	2179	0.0828	0.0084
1884	1896	0.2263	0.0073	2179	2184	0.0883	0.0088
1896	1905	0.2113	0.0084	2184	2190	0.0879	0.0095
1905	1914	0.1991	0.0069	2190	2195	0.1007	0.0101
1914	1923	0.1821	0.0067	2195	2200	0.0818	0.0085
1923	1931	0.1773	0.0067	2200	2205	0.0961	0.0092
1931	1940	0.1790	0.0073	2205	2210	0.0837	0.0089
1940	1949	0.1873	0.0072	2210	2215	0.0865	0.0090
1949	1958	0.1999	0.0072	2215	2220	0.1039	0.0102
1958	1966	0.1638	0.0065	2220	2225	0.0627	0.0077
1966	1975	0.1603	0.0065	2225	2230	0.0736	0.0088
1975	1984	0.1666	0.0067	2230	2235	0.0792	0.0088

A. Appendix

Hydrogen target:  $\cos(\theta_{CMS}) = [0,0.1]$

W / MeV		$d\sigma/d\Omega$ / mb/sr	
lower bound	upper bound	value	stat. error
2235	2241	0.0775	0.0090
2241	2246	0.0752	0.0086
2246	2251	0.0625	0.0082
2251	2256	0.0691	0.0083
2256	2261	0.0860	0.0099
2261	2266	0.0752	0.0087
2266	2270	0.0903	0.0102
2270	2275	0.0770	0.0093
2275	2280	0.0860	0.0097
2280	2285	0.0855	0.0094
2285	2290	0.0837	0.0097
2290	2295	0.0823	0.0095
2295	2300	0.0693	0.0089
2300	2305	0.0670	0.0085
2305	2310	0.0738	0.0092
2310	2315	0.0789	0.0094
2315	2320	0.0620	0.0085
2320	2324	0.0607	0.0082
2324	2329	0.0618	0.0088
2329	2334	0.0751	0.0093
2334	2339	0.0750	0.0095
2339	2344	0.0634	0.0082
2344	2349	0.0504	0.0078
2349	2353	0.0717	0.0091
2353	2358	0.0626	0.0087
2358	2363	0.0673	0.0090
2363	2368	0.0588	0.0084
2368	2372	0.0404	0.0074
2372	2377	0.0534	0.0086
2377	2382	0.0699	0.0089
2382	2387	0.0440	0.0073
2387	2391	0.0591	0.0086



A. Appendix

Hydrogen target:  $\cos(\theta_{CMS}) = [0.1, 0.2]$

W / MeV		$d\sigma/d\Omega$ / mb/sr		W / MeV		$d\sigma/d\Omega$ / mb/sr	
lower bound	upper bound	value	stat. error	lower bound	upper bound	value	stat. error
1472	1495	0.0000	0.0000	1984	1992	0.1691	0.0072
1495	1517	28.7942	5.1462	1992	2001	0.1732	0.0072
1517	1540	2.8060	0.1294	2001	2009	0.1644	0.0074
1540	1561	1.1928	0.0218	2009	2017	0.1649	0.0073
1561	1583	0.9833	0.0135	2017	2026	0.1531	0.0077
1583	1604	0.8138	0.0107	2026	2034	0.1452	0.0077
1604	1625	0.5987	0.0087	2034	2043	0.1299	0.0075
1625	1639	0.4422	0.0097	2043	2051	0.1317	0.0077
1639	1653	0.3672	0.0077	2051	2059	0.1463	0.0083
1653	1666	0.3127	0.0075	2059	2067	0.1371	0.0081
1666	1680	0.2956	0.0072	2067	2076	0.1196	0.0076
1680	1694	0.3180	0.0075	2076	2084	0.1208	0.0080
1694	1707	0.3392	0.0078	2084	2092	0.1203	0.0079
1707	1720	0.3884	0.0083	2092	2100	0.1233	0.0086
1720	1733	0.3830	0.0082	2100	2108	0.1072	0.0076
1733	1746	0.3771	0.0081	2108	2116	0.1140	0.0071
1746	1759	0.3523	0.0080	2116	2124	0.1073	0.0083
1759	1772	0.3494	0.0078	2124	2132	0.1043	0.0075
1772	1785	0.3468	0.0080	2132	2138	0.1362	0.0111
1785	1798	0.3306	0.0078	2138	2143	0.1140	0.0109
1798	1810	0.3158	0.0077	2143	2148	0.0946	0.0087
1810	1823	0.3212	0.0076	2148	2153	0.1052	0.0095
1823	1835	0.2932	0.0075	2153	2159	0.1225	0.0105
1835	1848	0.3064	0.0075	2159	2164	0.1134	0.0108
1848	1860	0.3043	0.0076	2164	2169	0.1014	0.0100
1860	1872	0.2803	0.0081	2169	2174	0.0999	0.0102
1872	1884	0.2660	0.0079	2174	2179	0.1137	0.0100
1884	1896	0.2477	0.0077	2179	2184	0.1103	0.0098
1896	1905	0.2156	0.0085	2184	2190	0.1206	0.0111
1905	1914	0.2114	0.0071	2190	2195	0.0968	0.0100
1914	1923	0.1980	0.0070	2195	2200	0.1176	0.0103
1923	1931	0.1964	0.0071	2200	2205	0.1074	0.0099
1931	1940	0.1994	0.0077	2205	2210	0.1075	0.0103
1940	1949	0.1903	0.0073	2210	2215	0.1100	0.0103
1949	1958	0.1941	0.0071	2215	2220	0.1075	0.0105
1958	1966	0.1773	0.0068	2220	2225	0.1045	0.0101
1966	1975	0.1758	0.0068	2225	2230	0.1015	0.0104
1975	1984	0.1838	0.0071	2230	2235	0.0998	0.0100

A. Appendix

Hydrogen target:  $\cos(\theta_{CMS}) = [0.1, 0.2]$

W / MeV		$d\sigma/d\Omega$ / mb/sr	
lower bound	upper bound	value	stat. error
2235	2241	0.0983	0.0103
2241	2246	0.0990	0.0099
2246	2251	0.0951	0.0102
2251	2256	0.1008	0.0100
2256	2261	0.0998	0.0108
2261	2266	0.0813	0.0092
2266	2270	0.0762	0.0095
2270	2275	0.0884	0.0101
2275	2280	0.0913	0.0101
2280	2285	0.0712	0.0088
2285	2290	0.0988	0.0108
2290	2295	0.0902	0.0101
2295	2300	0.0892	0.0102
2300	2305	0.0882	0.0099
2305	2310	0.0867	0.0103
2310	2315	0.0818	0.0099
2315	2320	0.0922	0.0106
2320	2324	0.0801	0.0097
2324	2329	0.0746	0.0097
2329	2334	0.0713	0.0092
2334	2339	0.0781	0.0099
2339	2344	0.0663	0.0087
2344	2349	0.0916	0.0107
2349	2353	0.0654	0.0089
2353	2358	0.0720	0.0095
2358	2363	0.0709	0.0095
2363	2368	0.0599	0.0087
2368	2372	0.0820	0.0109
2372	2377	0.0568	0.0092
2377	2382	0.0532	0.0080
2382	2387	0.0752	0.0099
2387	2391	0.0789	0.0103

## A. Appendix

Hydrogen target:  $\cos(\theta_{CMS}) = [0.2, 0.3]$

A. Appendix

W / MeV		$d\sigma/d\Omega$ / mb/sr		W / MeV		$d\sigma/d\Omega$ / mb/sr	
lower bound	upper bound	value	stat. error	lower bound	upper bound	value	stat. error
1472	1495	0.0000	0.0000	1984	1992	0.1967	0.0082
1495	1517	33.9074	5.3245	1992	2001	0.1798	0.0077
1517	1540	2.7990	0.1523	2001	2009	0.1891	0.0083
1540	1561	1.2227	0.0233	2009	2017	0.1820	0.0081
1561	1583	0.9136	0.0128	2017	2026	0.1736	0.0086
1583	1604	0.7845	0.0103	2026	2034	0.1716	0.0088
1604	1625	0.6090	0.0087	2034	2043	0.1517	0.0085
1625	1639	0.4648	0.0099	2043	2051	0.1725	0.0092
1639	1653	0.3573	0.0075	2051	2059	0.1620	0.0091
1653	1666	0.3039	0.0072	2059	2067	0.1568	0.0091
1666	1680	0.2914	0.0070	2067	2076	0.1225	0.0081
1680	1694	0.3377	0.0077	2076	2084	0.1453	0.0092
1694	1707	0.3517	0.0079	2084	2092	0.1313	0.0087
1707	1720	0.3831	0.0082	2092	2100	0.1581	0.0102
1720	1733	0.4001	0.0084	2100	2108	0.1294	0.0087
1733	1746	0.3951	0.0084	2108	2116	0.1319	0.0081
1746	1759	0.3731	0.0083	2116	2124	0.1327	0.0097
1759	1772	0.3724	0.0082	2124	2132	0.1186	0.0085
1772	1785	0.3707	0.0084	2132	2138	0.1294	0.0113
1785	1798	0.3625	0.0083	2138	2143	0.1147	0.0116
1798	1810	0.3355	0.0081	2143	2148	0.1160	0.0103
1810	1823	0.3318	0.0079	2148	2153	0.1237	0.0110
1823	1835	0.3428	0.0082	2153	2159	0.1356	0.0118
1835	1848	0.3211	0.0079	2159	2164	0.1288	0.0123
1848	1860	0.3188	0.0080	2164	2169	0.1403	0.0125
1860	1872	0.3024	0.0087	2169	2174	0.1287	0.0124
1872	1884	0.3013	0.0088	2174	2179	0.1331	0.0115
1884	1896	0.2777	0.0084	2179	2184	0.1448	0.0121
1896	1905	0.2470	0.0094	2184	2190	0.1240	0.0121
1905	1914	0.2248	0.0076	2190	2195	0.1362	0.0128
1914	1923	0.2246	0.0078	2195	2200	0.1111	0.0107
1923	1931	0.2239	0.0080	2200	2205	0.1317	0.0119
1931	1940	0.2184	0.0085	2205	2210	0.1085	0.0112
1940	1949	0.2273	0.0083	2210	2215	0.1099	0.0111
1949	1958	0.2324	0.0082	2215	2220	0.1414	0.0130
1958	1966	0.1942	0.0075	2220	2225	0.1294	0.0120
1966	1975	0.2082	0.0078	2225	2230	0.1274	0.0125
1975	1984	0.2109	0.0081	2230	2235	0.1115	0.0113
				2235	2241	0.1079	0.0116
				2241	2246	0.1160	0.0117

A. Appendix

Hydrogen target:  $\cos(\theta_{CMS}) = [0.2, 0.3]$

W / MeV		$d\sigma/d\Omega$ / mb/sr	
lower bound	upper bound	value	stat. error
2246	2251	0.1111	0.0120
2251	2256	0.1277	0.0123
2256	2261	0.1261	0.0131
2261	2266	0.1023	0.0112
2266	2270	0.0994	0.0118
2270	2275	0.0942	0.0112
2275	2280	0.1061	0.0118
2280	2285	0.0961	0.0111
2285	2290	0.0940	0.0114
2290	2295	0.1149	0.0124
2295	2300	0.1206	0.0130
2300	2305	0.1151	0.0124
2305	2310	0.0967	0.0117
2310	2315	0.1042	0.0119
2315	2320	0.0927	0.0115
2320	2324	0.1129	0.0124
2324	2329	0.0910	0.0117
2329	2334	0.1017	0.0120
2334	2339	0.1355	0.0142
2339	2344	0.0814	0.0103
2344	2349	0.0995	0.0122
2349	2353	0.1099	0.0126
2353	2358	0.0829	0.0112
2358	2363	0.0811	0.0110
2363	2368	0.1049	0.0125
2368	2372	0.1003	0.0130
2372	2377	0.0710	0.0111
2377	2382	0.0978	0.0118
2382	2387	0.0850	0.0113
2387	2391	0.0862	0.0116

A. Appendix

Hydrogen target:  $\cos(\theta_{CMS}) = [0.3, 0.4]$

W / MeV		$d\sigma/d\Omega$ / mb/sr		W / MeV		$d\sigma/d\Omega$ / mb/sr	
lower bound	upper bound	value	stat. error	lower bound	upper bound	value	stat. error
1472	1495	0.0000	0.0000	1984	1992	0.2123	0.0093
1495	1517	41.0881	7.2869	1992	2001	0.1830	0.0084
1517	1540	2.9727	0.1937	2001	2009	0.2090	0.0095
1540	1561	1.1760	0.0250	2009	2017	0.1811	0.0088
1561	1583	0.8772	0.0127	2017	2026	0.1878	0.0098
1583	1604	0.7713	0.0102	2026	2034	0.1699	0.0095
1604	1625	0.5888	0.0084	2034	2043	0.1678	0.0098
1625	1639	0.4501	0.0096	2043	2051	0.1697	0.0101
1639	1653	0.3612	0.0075	2051	2059	0.1809	0.0107
1653	1666	0.2997	0.0072	2059	2067	0.1777	0.0107
1666	1680	0.3003	0.0071	2067	2076	0.1439	0.0098
1680	1694	0.3446	0.0078	2076	2084	0.1593	0.0107
1694	1707	0.3821	0.0084	2084	2092	0.1564	0.0106
1707	1720	0.3985	0.0085	2092	2100	0.1575	0.0114
1720	1733	0.4116	0.0087	2100	2108	0.1441	0.0103
1733	1746	0.4125	0.0088	2108	2116	0.1549	0.0098
1746	1759	0.4184	0.0091	2116	2124	0.1550	0.0117
1759	1772	0.3901	0.0087	2124	2132	0.1563	0.0108
1772	1785	0.3627	0.0087	2132	2138	0.1551	0.0139
1785	1798	0.3796	0.0089	2138	2143	0.1424	0.0144
1798	1810	0.3804	0.0091	2143	2148	0.1641	0.0137
1810	1823	0.3608	0.0088	2148	2153	0.1461	0.0135
1823	1835	0.3428	0.0088	2153	2159	0.1622	0.0144
1835	1848	0.3614	0.0089	2159	2164	0.1140	0.0129
1848	1860	0.3508	0.0090	2164	2169	0.1477	0.0144
1860	1872	0.3462	0.0099	2169	2174	0.1566	0.0153
1872	1884	0.3170	0.0097	2174	2179	0.1688	0.0144
1884	1896	0.3084	0.0096	2179	2184	0.1681	0.0146
1896	1905	0.2647	0.0104	2184	2190	0.1395	0.0145
1905	1914	0.2579	0.0087	2190	2195	0.1622	0.0157
1914	1923	0.2643	0.0091	2195	2200	0.1396	0.0136
1923	1931	0.2402	0.0089	2200	2205	0.1703	0.0150
1931	1940	0.2571	0.0099	2205	2210	0.1492	0.0146
1940	1949	0.2305	0.0090	2210	2215	0.1415	0.0141
1949	1958	0.2433	0.0090	2215	2220	0.1549	0.0153
1958	1966	0.2413	0.0090	2220	2225	0.1709	0.0156
1966	1975	0.2441	0.0092	2225	2230	0.1710	0.0164
1975	1984	0.2053	0.0086	2230	2235	0.1245	0.0135

A. Appendix

Hydrogen target:  $\cos(\theta_{CMS}) = [0.3, 0.4]$

W / MeV		$d\sigma/d\Omega$ / mb/sr	
lower bound	upper bound	value	stat. error
2235	2241	0.1347	0.0147
2241	2246	0.1412	0.0146
2246	2251	0.1199	0.0140
2251	2256	0.1267	0.0139
2256	2261	0.1251	0.0149
2261	2266	0.1510	0.0155
2266	2270	0.1424	0.0161
2270	2275	0.1363	0.0157
2275	2280	0.1244	0.0148
2280	2285	0.1192	0.0142
2285	2290	0.1278	0.0153
2290	2295	0.1451	0.0162
2295	2300	0.1313	0.0158
2300	2305	0.1016	0.0136
2305	2310	0.1297	0.0160
2310	2315	0.1124	0.0147
2315	2320	0.1356	0.0166
2320	2324	0.1112	0.0145
2324	2329	0.1374	0.0173
2329	2334	0.1167	0.0155
2334	2339	0.1019	0.0147
2339	2344	0.1292	0.0158
2344	2349	0.1258	0.0168
2349	2353	0.1220	0.0162
2353	2358	0.1163	0.0160
2358	2363	0.1061	0.0155
2363	2368	0.1297	0.0173
2368	2372	0.1008	0.0163
2372	2377	0.0804	0.0147
2377	2382	0.0882	0.0141
2382	2387	0.0940	0.0151
2387	2391	0.1192	0.0172

A. Appendix

Hydrogen target:  $\cos(\theta_{CMS}) = [0.4, 0.5]$

W / MeV		$d\sigma/d\Omega$ / mb/sr		W / MeV		$d\sigma/d\Omega$ / mb/sr	
lower bound	upper bound	value	stat. error	lower bound	upper bound	value	stat. error
1472	1495	0.0000	0.0000	1984	1992	0.2279	0.0108
1495	1517	33.6919	5.7273	1992	2001	0.2335	0.0108
1517	1540	3.0482	0.2533	2001	2009	0.2121	0.0108
1540	1561	1.1391	0.0279	2009	2017	0.1814	0.0099
1561	1583	0.8457	0.0128	2017	2026	0.1964	0.0113
1583	1604	0.7412	0.0101	2026	2034	0.1860	0.0113
1604	1625	0.5537	0.0082	2034	2043	0.2280	0.0130
1625	1639	0.4451	0.0095	2043	2051	0.2118	0.0128
1639	1653	0.3563	0.0075	2051	2059	0.1673	0.0116
1653	1666	0.3156	0.0075	2059	2067	0.1962	0.0128
1666	1680	0.3105	0.0074	2067	2076	0.1753	0.0124
1680	1694	0.3364	0.0079	2076	2084	0.1842	0.0132
1694	1707	0.4004	0.0089	2084	2092	0.1557	0.0121
1707	1720	0.4381	0.0094	2092	2100	0.1837	0.0143
1720	1733	0.4474	0.0096	2100	2108	0.1852	0.0136
1733	1746	0.4444	0.0097	2108	2116	0.1617	0.0117
1746	1759	0.4056	0.0095	2116	2124	0.1885	0.0150
1759	1772	0.3989	0.0094	2124	2132	0.1670	0.0132
1772	1785	0.4095	0.0099	2132	2138	0.1894	0.0183
1785	1798	0.3929	0.0098	2138	2143	0.2252	0.0218
1798	1810	0.3760	0.0096	2143	2148	0.2093	0.0185
1810	1823	0.3801	0.0097	2148	2153	0.1393	0.0158
1823	1835	0.3582	0.0096	2153	2159	0.1882	0.0187
1835	1848	0.3482	0.0094	2159	2164	0.1699	0.0192
1848	1860	0.3653	0.0100	2164	2169	0.1736	0.0191
1860	1872	0.3604	0.0110	2169	2174	0.2865	0.0257
1872	1884	0.3269	0.0106	2174	2179	0.1426	0.0165
1884	1896	0.3054	0.0104	2179	2184	0.1665	0.0180
1896	1905	0.2590	0.0113	2184	2190	0.1687	0.0201
1905	1914	0.2744	0.0100	2190	2195	0.1811	0.0208
1914	1923	0.2511	0.0097	2195	2200	0.1805	0.0195
1923	1931	0.2467	0.0099	2200	2205	0.1751	0.0194
1931	1940	0.2667	0.0112	2205	2210	0.1616	0.0194
1940	1949	0.2691	0.0108	2210	2215	0.1232	0.0169
1949	1958	0.2691	0.0107	2215	2220	0.1968	0.0221
1958	1966	0.2524	0.0103	2220	2225	0.1422	0.0185
1966	1975	0.2326	0.0100	2225	2230	0.1583	0.0205
1975	1984	0.2458	0.0106	2230	2235	0.2067	0.0229



A. Appendix

Hydrogen target:  $\cos(\theta_{CMS}) = [0.4, 0.5]$

W / MeV		$d\sigma/d\Omega$ / mb/sr	
lower bound	upper bound	value	stat. error
2235	2241	0.1856	0.0225
2241	2246	0.1774	0.0215
2246	2251	0.1636	0.0218
2251	2256	0.1348	0.0189
2256	2261	0.1696	0.0232
2261	2266	0.1796	0.0230
2266	2270	0.1674	0.0236
2270	2275	0.1590	0.0227
2275	2280	0.1027	0.0183
2280	2285	0.1566	0.0219
2285	2290	0.1217	0.0204
2290	2295	0.1432	0.0219
2295	2300	0.1452	0.0230
2300	2305	0.1586	0.0233
2305	2310	0.1034	0.0195
2310	2315	0.1294	0.0214
2315	2320	0.1205	0.0213
2320	2324	0.1383	0.0224
2324	2329	0.1085	0.0213
2329	2334	0.1015	0.0204
2334	2339	0.0998	0.0205
2339	2344	0.1229	0.0219
2344	2349	0.0936	0.0205
2349	2353	0.1046	0.0215
2353	2358	0.1152	0.0237
2358	2363	0.0847	0.0204
2363	2368	0.1060	0.0233
2368	2372	0.0682	0.0199
2372	2377	0.0528	0.0180
2377	2382	0.0989	0.0228
2382	2387	0.1247	0.0268
2387	2391	0.1366	0.0292

A. Appendix

Hydrogen target:  $\cos(\theta_{CMS}) = [0.5, 0.6]$

W / MeV		$d\sigma/d\Omega$ / mb/sr		W / MeV		$d\sigma/d\Omega$ / mb/sr	
lower bound	upper bound	value	stat. error	lower bound	upper bound	value	stat. error
1472	1495	0.0000	0.0000	1984	1992	0.2583	0.0139
1495	1517	42.3443	8.1372	1992	2001	0.2113	0.0123
1517	1540	3.1161	0.3268	2001	2009	0.2150	0.0134
1540	1561	1.0316	0.0311	2009	2017	0.2011	0.0130
1561	1583	0.8020	0.0131	2017	2026	0.2520	0.0160
1583	1604	0.7099	0.0101	2026	2034	0.2098	0.0152
1604	1625	0.5435	0.0083	2034	2043	0.1868	0.0150
1625	1639	0.4196	0.0096	2043	2051	0.2025	0.0161
1639	1653	0.3248	0.0075	2051	2059	0.1873	0.0160
1653	1666	0.2975	0.0077	2059	2067	0.1872	0.0164
1666	1680	0.2980	0.0077	2067	2076	0.2294	0.0187
1680	1694	0.3262	0.0084	2076	2084	0.2022	0.0185
1694	1707	0.4194	0.0098	2084	2092	0.2111	0.0191
1707	1720	0.4344	0.0100	2092	2100	0.1916	0.0198
1720	1733	0.4638	0.0106	2100	2108	0.2029	0.0195
1733	1746	0.4618	0.0108	2108	2116	0.1841	0.0171
1746	1759	0.4596	0.0110	2116	2124	0.1541	0.0187
1759	1772	0.4355	0.0107	2124	2132	0.2354	0.0219
1772	1785	0.4070	0.0108	2132	2138	0.2018	0.0268
1785	1798	0.4106	0.0109	2138	2143	0.2507	0.0324
1798	1810	0.3795	0.0107	2143	2148	0.1376	0.0216
1810	1823	0.3658	0.0106	2148	2153	0.2094	0.0279
1823	1835	0.3729	0.0110	2153	2159	0.2173	0.0293
1835	1848	0.3596	0.0108	2159	2164	0.2408	0.0335
1848	1860	0.3610	0.0113	2164	2169	0.2226	0.0321
1860	1872	0.3511	0.0124	2169	2174	0.1751	0.0296
1872	1884	0.3284	0.0122	2174	2179	0.1893	0.0286
1884	1896	0.3150	0.0121	2179	2184	0.1409	0.0252
1896	1905	0.2712	0.0133	2184	2190	0.1886	0.0325
1905	1914	0.2651	0.0113	2190	2195	0.1779	0.0327
1914	1923	0.2870	0.0121	2195	2200	0.0772	0.0198
1923	1931	0.2647	0.0120	2200	2205	0.1468	0.0288
1931	1940	0.2757	0.0133	2205	2210	0.1964	0.0349
1940	1949	0.2817	0.0130	2210	2215	0.1137	0.0270
1949	1958	0.2806	0.0127	2215	2220	0.1714	0.0354
1958	1966	0.2584	0.0123	2220	2225	0.1730	0.0348
1966	1975	0.2361	0.0120	2225	2230	0.1596	0.0361
1975	1984	0.2613	0.0131	2230	2235	0.1674	0.0363

A. Appendix

Hydrogen target:  $\cos(\theta_{CMS}) = [0.5, 0.6]$

W / MeV		$d\sigma/d\Omega$ / mb/sr	
lower bound	upper bound	value	stat. error
2235	2241	0.1574	0.0379
2241	2246	0.1560	0.0377
2246	2251	0.1218	0.0355
2251	2256	0.1322	0.0363
2256	2261	0.0856	0.0334
2261	2266	0.1660	0.0450
2266	2270	0.1011	0.0391
2270	2275	0.1077	0.0413
2275	2280	0.0923	0.0390
2280	2285	0.1006	0.0424
2285	2290	0.0723	0.0392
2290	2295	0.0503	0.0336
2295	2300	0.0959	0.0515
2300	2305	0.0393	0.0356
2305	2310	0.1269	0.0666
2310	2315	0.0000	0.0000
2315	2320	0.1314	0.0824
2320	2324	0.2061	0.1076
2324	2329	0.0000	0.0003
2329	2334	0.1356	0.1093
2334	2339	0.1815	0.1382
2339	2344	0.4274	0.2243
2344	2349	0.3071	0.2218
2349	2353	0.0000	0.0016
2353	2358	0.5930	0.3772
2358	2363	0.0000	0.0005
2363	2368	0.0000	0.0024
2368	2372	8.0761	2.2380
2372	2377	5.3784	1.8028
2377	2382	1.8724	0.9827
2382	2387	9.2582	2.8065
2387	2391	4.1988	1.6034

A. Appendix

Hydrogen target:  $\cos(\theta_{CMS}) = [0.6, 0.7]$

W / MeV		$d\sigma/d\Omega$ / mb/sr		W / MeV		$d\sigma/d\Omega$ / mb/sr	
lower bound	upper bound	value	stat. error	lower bound	upper bound	value	stat. err
1472	1495	0.0000	0.0000	1975	1984	0.2976	0.0196
1495	1517	30.4931	5.8243	1984	1992	0.2626	0.0198
1517	1540	3.4533	0.4583	1992	2001	0.2599	0.0198
1540	1561	0.8491	0.0357	2001	2009	0.2361	0.0209
1561	1583	0.7167	0.0135	2009	2017	0.2697	0.0227
1583	1604	0.6923	0.0106	2017	2026	0.2345	0.0238
1604	1625	0.5260	0.0089	2026	2034	0.2473	0.0261
1625	1639	0.4092	0.0105	2034	2043	0.2559	0.0279
1639	1653	0.3112	0.0081	2043	2051	0.2017	0.0266
1653	1666	0.2784	0.0082	2051	2059	0.1797	0.0268
1666	1680	0.2782	0.0083	2059	2067	0.2238	0.0316
1680	1694	0.3197	0.0091	2067	2076	0.1855	0.0311
1694	1707	0.3842	0.0104	2076	2084	0.2133	0.0360
1707	1720	0.4064	0.0107	2084	2092	0.2121	0.0385
1720	1733	0.4291	0.0114	2092	2100	0.2389	0.0469
1733	1746	0.4166	0.0114	2100	2108	0.1954	0.0428
1746	1759	0.3979	0.0114	2108	2116	0.1921	0.0427
1759	1772	0.3875	0.0114	2116	2124	0.3073	0.0702
1772	1785	0.3954	0.0122	2124	2132	0.0990	0.0414
1785	1798	0.3797	0.0121	2132	2138	0.0432	0.0391
1798	1810	0.3714	0.0123	2138	2143	0.1233	0.0779
1810	1823	0.3610	0.0122	2143	2148	0.2300	0.1023
1823	1835	0.3984	0.0133	2148	2153	0.2453	0.1205
1835	1848	0.3612	0.0128	2153	2159	0.1956	0.1181
1848	1860	0.3581	0.0133	2159	2164	0.0000	0.0001
1860	1872	0.3514	0.0149	2164	2169	0.0000	0.0001
1872	1884	0.2916	0.0140	2169	2174	0.8968	0.4017
1884	1896	0.3332	0.0154	2174	2179	0.4575	0.2853
1896	1905	0.2860	0.0173	2179	2184	1.0275	0.4946
1905	1914	0.2965	0.0150	2184	2190	3.7996	1.2583
1914	1923	0.2948	0.0158	2190	2195	14.5334	3.2089
1923	1931	0.2975	0.0165	2195	2200	19.0520	4.3413
1931	1940	0.2993	0.0182				
1940	1949	0.2740	0.0172				
1949	1958	0.3056	0.0180				
1958	1966	0.2901	0.0178				
1966	1975	0.3057	0.0190				

A. Appendix

Hydrogen target:  $\cos(\theta_{CMS}) = [0.7, 0.8]$

W / MeV		$d\sigma/d\Omega$ / mb/sr		W / MeV		$d\sigma/d\Omega$ / mb/sr	
lower bound	upper bound	value	stat. error	lower bound	upper bound	value	stat. err
1472	1495	0.0000	0.0000	1958	1966	0.2445	0.0349
1495	1517	20.2128	4.4050	1966	1975	0.3009	0.0437
1517	1540	3.0077	0.5488	1975	1984	0.3281	0.0529
1540	1561	0.4575	0.0369	1984	1992	0.2846	0.0586
1561	1583	0.4991	0.0134	1992	2001	0.2380	0.0593
1583	1604	0.5534	0.0107	2001	2009	0.2923	0.0795
1604	1625	0.4392	0.0094	2009	2017	0.1656	0.0716
1625	1639	0.3153	0.0107	2017	2026	0.2520	0.1166
1639	1653	0.2561	0.0087	2026	2034	0.4652	0.1954
1653	1666	0.2104	0.0085	2034	2043	0.0000	0.0001
1666	1680	0.2199	0.0088	2043	2051	12.3478	2.3066
1680	1694	0.2629	0.0099				
1694	1707	0.3013	0.0109				
1707	1720	0.3370	0.0116				
1720	1733	0.3681	0.0125				
1733	1746	0.3423	0.0123				
1746	1759	0.3245	0.0125				
1759	1772	0.3078	0.0123				
1772	1785	0.3111	0.0132				
1785	1798	0.3098	0.0135				
1798	1810	0.3229	0.0144				
1810	1823	0.3163	0.0146				
1823	1835	0.2891	0.0148				
1835	1848	0.3322	0.0164				
1848	1860	0.3337	0.0175				
1860	1872	0.2895	0.0190				
1872	1884	0.3019	0.0205				
1884	1896	0.2739	0.0207				
1896	1905	0.2552	0.0249				
1905	1914	0.2924	0.0238				
1914	1923	0.2343	0.0228				
1923	1931	0.3165	0.0295				
1931	1940	0.2603	0.0303				
1940	1949	0.2932	0.0330				
1949	1958	0.3180	0.0370				

A. Appendix

Deuterium target:  $\cos(\theta_{CMS}) = [-0.8,-0.7]$

W / MeV		$d\sigma/d\Omega$ / mb/sr		W / MeV		$d\sigma/d\Omega$ / mb/sr	
lower bound	upper bound	value	stat. error	lower bound	upper bound	value	stat. error
1472	1495	0.2233	0.0171	1958	1966	0.1625	0.0278
1495	1517	0.8666	0.0366	1966	1975	0.1551	0.0277
1517	1540	0.9650	0.0304	1975	1984	0.1108	0.0242
1540	1561	0.8565	0.0257	1984	1992	0.1157	0.0262
1561	1583	0.7656	0.0225	1992	2001	0.1263	0.0277
1583	1604	0.6141	0.0191	2001	2009	0.1372	0.0297
1604	1625	0.5876	0.0186	2009	2017	0.1233	0.0281
1625	1639	0.4757	0.0220	2017	2026	0.1908	0.0382
1639	1653	0.4011	0.0176	2026	2034	0.1033	0.0287
1653	1666	0.3830	0.0185	2034	2043	0.0946	0.0292
1666	1680	0.3781	0.0183	2043	2051	0.0882	0.0286
1680	1694	0.3983	0.0191	2051	2059	0.1082	0.0336
1694	1707	0.3222	0.0175	2059	2067	0.1022	0.0328
1707	1720	0.3094	0.0170	2067	2076	0.0635	0.0271
1720	1733	0.3319	0.0178	2076	2084	0.1006	0.0373
1733	1746	0.2922	0.0171	2084	2092	0.1395	0.0436
1746	1759	0.2559	0.0163	2092	2100	0.1258	0.0459
1759	1772	0.2845	0.0174	2100	2108	0.1263	0.0440
1772	1785	0.2291	0.0163	2108	2116	0.0310	0.0209
1785	1798	0.2592	0.0176	2116	2124	0.1564	0.0589
1798	1810	0.2441	0.0174	2124	2132	0.0964	0.0414
1810	1823	0.2538	0.0183	2132	2138	0.0819	0.0495
1823	1835	0.2124	0.0175	2138	2143	0.1502	0.0751
1835	1848	0.2085	0.0176				
1848	1860	0.2241	0.0196				
1860	1872	0.2459	0.0219				
1872	1884	0.2027	0.0209				
1884	1896	0.1626	0.0204				
1896	1905	0.1934	0.0280				
1905	1914	0.1679	0.0227				
1914	1923	0.1610	0.0240				
1923	1931	0.1672	0.0258				
1931	1940	0.1715	0.0265				
1940	1949	0.1345	0.0228				
1949	1958	0.1972	0.0303				

A. Appendix

Deuterium target:  $\cos(\theta_{CMS}) = [-0.7,-0.6]$

W / MeV		$d\sigma/d\Omega$ / mb/sr		W / MeV		$d\sigma/d\Omega$ / mb/sr	
lower bound	upper bound	value	stat. error	lower bound	upper bound	value	stat. error
1472	1495	0.2388	0.0179	1975	1984	0.1376	0.0142
1495	1517	0.9709	0.0363	1984	1992	0.1430	0.0149
1517	1540	0.9826	0.0261	1992	2001	0.1469	0.0151
1540	1561	0.9544	0.0223	2001	2009	0.1247	0.0144
1561	1583	0.8349	0.0186	2009	2017	0.1302	0.0146
1583	1604	0.7216	0.0160	2017	2026	0.0959	0.0134
1604	1625	0.5646	0.0137	2026	2034	0.1093	0.0149
1625	1639	0.4701	0.0160	2034	2043	0.1305	0.0165
1639	1653	0.4246	0.0133	2043	2051	0.1231	0.0164
1653	1666	0.3584	0.0128	2051	2059	0.1229	0.0169
1666	1680	0.3564	0.0126	2059	2067	0.0961	0.0155
1680	1694	0.3426	0.0123	2067	2076	0.1240	0.0178
1694	1707	0.3426	0.0125	2076	2084	0.1268	0.0188
1707	1720	0.2922	0.0113	2084	2092	0.0787	0.0149
1720	1733	0.2843	0.0112	2092	2100	0.0811	0.0160
1733	1746	0.2825	0.0111	2100	2108	0.0946	0.0173
1746	1759	0.2595	0.0109	2108	2116	0.0775	0.0144
1759	1772	0.2475	0.0104	2116	2124	0.0791	0.0177
1772	1785	0.2449	0.0108	2124	2132	0.1223	0.0207
1785	1798	0.2236	0.0103	2132	2138	0.0739	0.0199
1798	1810	0.2194	0.0104	2138	2143	0.0682	0.0211
1810	1823	0.2290	0.0107	2143	2148	0.0630	0.0192
1823	1835	0.2031	0.0104	2148	2153	0.0846	0.0229
1835	1848	0.2016	0.0104	2153	2159	0.0771	0.0219
1848	1860	0.2239	0.0117	2159	2164	0.0433	0.0174
1860	1872	0.1699	0.0107	2164	2169	0.0298	0.0143
1872	1884	0.1829	0.0114	2169	2174	0.0323	0.0155
1884	1896	0.1744	0.0123	2174	2179	0.0858	0.0248
1896	1905	0.1573	0.0145	2179	2184	0.0601	0.0206
1905	1914	0.1689	0.0129	2184	2190	0.0335	0.0162
1914	1923	0.1432	0.0125				
1923	1931	0.1456	0.0131				
1931	1940	0.1592	0.0140				
1940	1949	0.1338	0.0126				
1949	1958	0.1272	0.0130				
1958	1966	0.1467	0.0141				
1966	1975	0.1312	0.0135				

A. Appendix

Deuterium target:  $\cos(\theta_{CMS}) = [-0.7,-0.6]$

W / MeV		$d\sigma/d\Omega$ / mb/sr	
lower bound	upper bound	value	stat. error
2190	2195	0.0731	0.0240
2195	2200	0.0567	0.0208
2200	2205	0.0535	0.0210
2205	2210	0.0516	0.0210
2210	2215	0.0445	0.0197
2215	2220	0.0295	0.0168
2220	2225	0.0728	0.0252
2225	2230	0.0536	0.0232
2230	2235	0.0609	0.0243
2235	2241	0.0571	0.0245
2241	2246	0.0840	0.0292
2246	2251	0.0392	0.0211



A. Appendix

Deuterium target:  $\cos(\theta_{CMS}) = [-0.6,-0.5]$

W / MeV		$d\sigma/d\Omega$ / mb/sr		W / MeV		$d\sigma/d\Omega$ / mb/sr	
lower bound	upper bound	value	stat. error	lower bound	upper bound	value	stat. error
1472	1495	0.2519	0.0194	1984	1992	0.1304	0.0099
1495	1517	1.0195	0.0373	1992	2001	0.1161	0.0093
1517	1540	1.0673	0.0255	2001	2009	0.1174	0.0096
1540	1561	1.0407	0.0209	2009	2017	0.1290	0.0098
1561	1583	0.8963	0.0169	2017	2026	0.1319	0.0106
1583	1604	0.7345	0.0137	2026	2034	0.1103	0.0100
1604	1625	0.6044	0.0119	2034	2043	0.1518	0.0119
1625	1639	0.4749	0.0134	2043	2051	0.1164	0.0107
1639	1653	0.4308	0.0110	2051	2059	0.1106	0.0107
1653	1666	0.3655	0.0105	2059	2067	0.1067	0.0105
1666	1680	0.3416	0.0100	2067	2076	0.1126	0.0111
1680	1694	0.3074	0.0094	2076	2084	0.1252	0.0121
1694	1707	0.2962	0.0093	2084	2092	0.1099	0.0114
1707	1720	0.3065	0.0092	2092	2100	0.0878	0.0108
1720	1733	0.2873	0.0088	2100	2108	0.1120	0.0120
1733	1746	0.2617	0.0084	2108	2116	0.0883	0.0097
1746	1759	0.2452	0.0082	2116	2124	0.0890	0.0119
1759	1772	0.2542	0.0082	2124	2132	0.0796	0.0103
1772	1785	0.2382	0.0082	2132	2138	0.0814	0.0132
1785	1798	0.2434	0.0083	2138	2143	0.0611	0.0126
1798	1810	0.2386	0.0083	2143	2148	0.0891	0.0140
1810	1823	0.2356	0.0082	2148	2153	0.0745	0.0133
1823	1835	0.2068	0.0079	2153	2159	0.0478	0.0105
1835	1848	0.1892	0.0076	2159	2164	0.0795	0.0142
1848	1860	0.1858	0.0079	2164	2169	0.0653	0.0128
1860	1872	0.1722	0.0080	2169	2174	0.0655	0.0130
1872	1884	0.1717	0.0081	2174	2179	0.0907	0.0152
1884	1896	0.1707	0.0089	2179	2184	0.0591	0.0121
1896	1905	0.1603	0.0106	2184	2190	0.0748	0.0144
1905	1914	0.1525	0.0089	2190	2195	0.0523	0.0121
1914	1923	0.1640	0.0097	2195	2200	0.0716	0.0140
1923	1931	0.1259	0.0087	2200	2205	0.0370	0.0099
1931	1940	0.1595	0.0100	2205	2210	0.0741	0.0147
1940	1949	0.1406	0.0092	2210	2215	0.0398	0.0107
1949	1958	0.1406	0.0099	2215	2220	0.0440	0.0115
1958	1966	0.1208	0.0090	2220	2225	0.0688	0.0141
1966	1975	0.1475	0.0100	2225	2230	0.0818	0.0163
1975	1984	0.1295	0.0095	2230	2235	0.0329	0.0101

A. Appendix

Deuterium target:  $\cos(\theta_{CMS}) = [-0.6,-0.5]$

W / MeV		$d\sigma/d\Omega$ / mb/sr	
lower bound	upper bound	value	stat. error
2235	2241	0.0454	0.0123
2241	2246	0.0265	0.0091
2246	2251	0.0516	0.0135
2251	2256	0.0321	0.0103
2256	2261	0.0584	0.0147
2261	2266	0.0457	0.0126
2266	2270	0.0671	0.0159
2270	2275	0.0432	0.0128
2275	2280	0.0289	0.0105
2280	2285	0.0407	0.0122
2285	2290	0.0390	0.0125
2290	2295	0.0524	0.0145
2295	2300	0.0698	0.0172
2300	2305	0.0622	0.0157
2305	2310	0.0395	0.0132
2310	2315	0.0455	0.0137
2315	2320	0.0533	0.0155
2320	2324	0.0505	0.0149
2324	2329	0.0401	0.0139
2329	2334	0.0412	0.0137
2334	2339	0.0337	0.0127
2339	2344	0.0366	0.0124
2344	2349	0.0393	0.0142
2349	2353	0.0310	0.0121
2353	2358	0.0215	0.0104
2358	2363	0.0397	0.0144
2363	2368	0.0279	0.0121
2368	2372	0.0353	0.0140
2372	2377	0.0346	0.0140
2377	2382	0.0401	0.0145
2382	2387	0.0189	0.0103
2387	2391	0.0254	0.0123

A. Appendix

Deuterium target:  $\cos(\theta_{CMS}) = [-0.5,-0.4]$

W / MeV		$d\sigma/d\Omega$ / mb/sr		W / MeV		$d\sigma/d\Omega$ / mb/sr	
lower bound	upper bound	value	stat. error	lower bound	upper bound	value	stat. error
1472	1495	0.2787	0.0225	1984	1992	0.1244	0.0081
1495	1517	1.0329	0.0397	1992	2001	0.1183	0.0079
1517	1540	1.2274	0.0276	2001	2009	0.0237	0.0036
1540	1561	1.1143	0.0209	2009	2017	0.1243	0.0081
1561	1583	1.0426	0.0173	2017	2026	0.1414	0.0092
1583	1604	0.8070	0.0136	2026	2034	0.1222	0.0087
1604	1625	0.6475	0.0114	2034	2043	0.1203	0.0088
1625	1639	0.5254	0.0130	2043	2051	0.1006	0.0081
1639	1653	0.4439	0.0102	2051	2059	0.1012	0.0084
1653	1666	0.3998	0.0101	2059	2067	0.1081	0.0087
1666	1680	0.3602	0.0093	2067	2076	0.0849	0.0078
1680	1694	0.3240	0.0087	2076	2084	0.1095	0.0092
1694	1707	0.3304	0.0088	2084	2092	0.1116	0.0092
1707	1720	0.3045	0.0083	2092	2100	0.1062	0.0095
1720	1733	0.3192	0.0084	2100	2108	0.0995	0.0090
1733	1746	0.3041	0.0081	2108	2116	0.0918	0.0080
1746	1759	0.2886	0.0080	2116	2124	0.0823	0.0091
1759	1772	0.2636	0.0074	2124	2132	0.1095	0.0097
1772	1785	0.2626	0.0077	2132	2138	0.0765	0.0101
1785	1798	0.2419	0.0073	2138	2143	0.0565	0.0094
1798	1810	0.2338	0.0071	2143	2148	0.0830	0.0106
1810	1823	0.2338	0.0072	2148	2153	0.0814	0.0109
1823	1835	0.2311	0.0073	2153	2159	0.0673	0.0098
1835	1848	0.2089	0.0069	2159	2164	0.0781	0.0111
1848	1860	0.2036	0.0072	2164	2169	0.0719	0.0104
1860	1872	0.2012	0.0075	2169	2174	0.0790	0.0112
1872	1884	0.1956	0.0075	2174	2179	0.0615	0.0096
1884	1896	0.1630	0.0075	2179	2184	0.0800	0.0109
1896	1905	0.1710	0.0094	2184	2190	0.0815	0.0116
1905	1914	0.1702	0.0080	2190	2195	0.0732	0.0110
1914	1923	0.1447	0.0077	2195	2200	0.0757	0.0110
1923	1931	0.1566	0.0083	2200	2205	0.0619	0.0099
1931	1940	0.1678	0.0088	2205	2210	0.0688	0.0108
1940	1949	0.1451	0.0080	2210	2215	0.0788	0.0116
1949	1958	0.1592	0.0089	2215	2220	0.0553	0.0099
1958	1966	0.1446	0.0083	2220	2225	0.0592	0.0099
1966	1975	0.1318	0.0080	2225	2230	0.0515	0.0097
1975	1984	0.1430	0.0085	2230	2235	0.0597	0.0101

A. Appendix

Deuterium target:  $\cos(\theta_{CMS}) = [-0.5,-0.4]$

W / MeV		$d\sigma/d\Omega$ / mb/sr	
lower bound	upper bound	value	stat. error
2235	2241	0.0495	0.0097
2241	2246	0.0435	0.0088
2246	2251	0.0428	0.0091
2251	2256	0.0495	0.0095
2256	2261	0.0477	0.0099
2261	2266	0.0596	0.0106
2266	2270	0.0553	0.0108
2270	2275	0.0452	0.0096
2275	2280	0.0431	0.0094
2280	2285	0.0603	0.0108
2285	2290	0.0443	0.0097
2290	2295	0.0403	0.0091
2295	2300	0.0476	0.0102
2300	2305	0.0502	0.0102
2305	2310	0.0453	0.0101
2310	2315	0.0442	0.0098
2315	2320	0.0240	0.0074
2320	2324	0.0291	0.0079
2324	2329	0.0532	0.0114
2329	2334	0.0595	0.0116
2334	2339	0.0294	0.0083
2339	2344	0.0469	0.0099
2344	2349	0.0455	0.0105
2349	2353	0.0347	0.0090
2353	2358	0.0479	0.0108
2358	2363	0.0444	0.0104
2363	2368	0.0437	0.0104
2368	2372	0.0351	0.0097
2372	2377	0.0313	0.0092
2377	2382	0.0351	0.0093
2382	2387	0.0285	0.0086
2387	2391	0.0413	0.0104

A. Appendix

Deuterium target:  $\cos(\theta_{CMS}) = [-0.4,-0.3]$

W / MeV		$d\sigma/d\Omega$ / mb/sr		W / MeV		$d\sigma/d\Omega$ / mb/sr	
lower bound	upper bound	value	stat. error	lower bound	upper bound	value	stat. error
1472	1495	0.2646	0.0237	1984	1992	0.1485	0.0079
1495	1517	1.0954	0.0435	1992	2001	0.1460	0.0078
1517	1540	1.1772	0.0275	2001	2009	0.1425	0.0078
1540	1561	1.1515	0.0209	2009	2017	0.1188	0.0069
1561	1583	1.0571	0.0168	2017	2026	0.1313	0.0078
1583	1604	0.8857	0.0136	2026	2034	0.1140	0.0074
1604	1625	0.6692	0.0110	2034	2043	0.1143	0.0075
1625	1639	0.5397	0.0124	2043	2051	0.1201	0.0079
1639	1653	0.4607	0.0098	2051	2059	0.1104	0.0077
1653	1666	0.4108	0.0096	2059	2067	0.1074	0.0077
1666	1680	0.3501	0.0085	2067	2076	0.1045	0.0077
1680	1694	0.3428	0.0084	2076	2084	0.1126	0.0082
1694	1707	0.3306	0.0082	2084	2092	0.1163	0.0083
1707	1720	0.3212	0.0078	2092	2100	0.0886	0.0076
1720	1733	0.3172	0.0077	2100	2108	0.0890	0.0075
1733	1746	0.2995	0.0074	2108	2116	0.0839	0.0067
1746	1759	0.2943	0.0074	2116	2124	0.0849	0.0080
1759	1772	0.2772	0.0070	2124	2132	0.0784	0.0071
1772	1785	0.2815	0.0073	2132	2138	0.0942	0.0098
1785	1798	0.2627	0.0069	2138	2143	0.0948	0.0105
1798	1810	0.2405	0.0067	2143	2148	0.0720	0.0086
1810	1823	0.2422	0.0067	2148	2153	0.0992	0.0104
1823	1835	0.2205	0.0065	2153	2159	0.0792	0.0091
1835	1848	0.2170	0.0064	2159	2164	0.0591	0.0082
1848	1860	0.2138	0.0067	2164	2169	0.0730	0.0090
1860	1872	0.1895	0.0066	2169	2174	0.0762	0.0095
1872	1884	0.1821	0.0065	2174	2179	0.0835	0.0096
1884	1896	0.1830	0.0071	2179	2184	0.0785	0.0092
1896	1905	0.1733	0.0086	2184	2190	0.0899	0.0104
1905	1914	0.1695	0.0072	2190	2195	0.0905	0.0103
1914	1923	0.1628	0.0074	2195	2200	0.0610	0.0084
1923	1931	0.1610	0.0076	2200	2205	0.0690	0.0089
1931	1940	0.1563	0.0076	2205	2210	0.0681	0.0091
1940	1949	0.1629	0.0076	2210	2215	0.0740	0.0094
1949	1958	0.1422	0.0075	2215	2220	0.0590	0.0085
1958	1966	0.1480	0.0075	2220	2225	0.0579	0.0083
1966	1975	0.1388	0.0073	2225	2230	0.0641	0.0090
1975	1984	0.1439	0.0075	2230	2235	0.0732	0.0095

A. Appendix

Deuterium target:  $\cos(\theta_{CMS}) = [-0.4,-0.3]$

W / MeV		$d\sigma/d\Omega$ / mb/sr	
lower bound	upper bound	value	stat. error
2235	2241	0.0726	0.0098
2241	2246	0.0566	0.0083
2246	2251	0.0591	0.0089
2251	2256	0.0564	0.0084
2256	2261	0.0462	0.0081
2261	2266	0.0602	0.0089
2266	2270	0.0667	0.0098
2270	2275	0.0806	0.0105
2275	2280	0.0643	0.0095
2280	2285	0.0473	0.0079
2285	2290	0.0469	0.0082
2290	2295	0.0623	0.0095
2295	2300	0.0606	0.0094
2300	2305	0.0709	0.0099
2305	2310	0.0479	0.0085
2310	2315	0.0605	0.0093
2315	2320	0.0508	0.0086
2320	2324	0.0489	0.0083
2324	2329	0.0513	0.0091
2329	2334	0.0374	0.0074
2334	2339	0.0525	0.0091
2339	2344	0.0424	0.0077
2344	2349	0.0558	0.0093
2349	2353	0.0400	0.0077
2353	2358	0.0447	0.0083
2358	2363	0.0443	0.0083
2363	2368	0.0639	0.0100
2368	2372	0.0416	0.0084
2372	2377	0.0323	0.0073
2377	2382	0.0347	0.0073
2382	2387	0.0359	0.0075
2387	2391	0.0458	0.0089

A. Appendix

Deuterium target:  $\cos(\theta_{CMS}) = [-0.3,-0.2]$

W / MeV		$d\sigma/d\Omega$ / mb/sr		W / MeV		$d\sigma/d\Omega$ / mb/sr	
lower bound	upper bound	value	stat. error	lower bound	upper bound	value	stat. error
1472	1495	0.2618	0.0260	1984	1992	0.1363	0.0071
1495	1517	1.1306	0.0478	1992	2001	0.1280	0.0068
1517	1540	1.2692	0.0300	2001	2009	0.1362	0.0071
1540	1561	1.2233	0.0217	2009	2017	0.1282	0.0067
1561	1583	1.1314	0.0172	2017	2026	0.1280	0.0072
1583	1604	0.8949	0.0133	2026	2034	0.1299	0.0073
1604	1625	0.6727	0.0106	2034	2043	0.1069	0.0067
1625	1639	0.5484	0.0121	2043	2051	0.1299	0.0075
1639	1653	0.4513	0.0092	2051	2059	0.1003	0.0067
1653	1666	0.4162	0.0092	2059	2067	0.1141	0.0073
1666	1680	0.3617	0.0083	2067	2076	0.1060	0.0071
1680	1694	0.3419	0.0080	2076	2084	0.1082	0.0074
1694	1707	0.3488	0.0081	2084	2092	0.1093	0.0074
1707	1720	0.3339	0.0077	2092	2100	0.1028	0.0075
1720	1733	0.3199	0.0074	2100	2108	0.1020	0.0073
1733	1746	0.3145	0.0073	2108	2116	0.0813	0.0060
1746	1759	0.3030	0.0072	2116	2124	0.0828	0.0073
1759	1772	0.3167	0.0071	2124	2132	0.0978	0.0072
1772	1785	0.2897	0.0070	2132	2138	0.0970	0.0090
1785	1798	0.2738	0.0067	2138	2143	0.0858	0.0092
1798	1810	0.2686	0.0067	2143	2148	0.0948	0.0089
1810	1823	0.2460	0.0064	2148	2153	0.0834	0.0086
1823	1835	0.2470	0.0065	2153	2159	0.1051	0.0096
1835	1848	0.2367	0.0063	2159	2164	0.0838	0.0089
1848	1860	0.2193	0.0064	2164	2169	0.0773	0.0084
1860	1872	0.2192	0.0067	2169	2174	0.0626	0.0077
1872	1884	0.1886	0.0062	2174	2179	0.1009	0.0095
1884	1896	0.1976	0.0070	2179	2184	0.0669	0.0077
1896	1905	0.1818	0.0082	2184	2190	0.0803	0.0089
1905	1914	0.1843	0.0071	2190	2195	0.0778	0.0087
1914	1923	0.1848	0.0074	2195	2200	0.0863	0.0090
1923	1931	0.1593	0.0070	2200	2205	0.0768	0.0085
1931	1940	0.1607	0.0072	2205	2210	0.0701	0.0083
1940	1949	0.1633	0.0071	2210	2215	0.0709	0.0083
1949	1958	0.1339	0.0068	2215	2220	0.0805	0.0090
1958	1966	0.1299	0.0066	2220	2225	0.0846	0.0090
1966	1975	0.1455	0.0070	2225	2230	0.0583	0.0078
1975	1984	0.1505	0.0072	2230	2235	0.0706	0.0085

A. Appendix

Deuterium target:  $\cos(\theta_{CMS}) = [-0.3,-0.2]$

W / MeV		$d\sigma/d\Omega$ / mb/sr	
lower bound	upper bound	value	stat. error
2235	2241	0.0695	0.0087
2241	2246	0.0784	0.0088
2246	2251	0.0590	0.0080
2251	2256	0.0687	0.0083
2256	2261	0.0901	0.0102
2261	2266	0.0489	0.0072
2266	2270	0.0576	0.0081
2270	2275	0.0658	0.0086
2275	2280	0.0553	0.0079
2280	2285	0.0629	0.0082
2285	2290	0.0639	0.0085
2290	2295	0.0574	0.0081
2295	2300	0.0504	0.0077
2300	2305	0.0566	0.0079
2305	2310	0.0625	0.0086
2310	2315	0.0526	0.0077
2315	2320	0.0339	0.0063
2320	2324	0.0382	0.0065
2324	2329	0.0656	0.0090
2329	2334	0.0475	0.0074
2334	2339	0.0582	0.0083
2339	2344	0.0524	0.0074
2344	2349	0.0489	0.0077
2349	2353	0.0456	0.0073
2353	2358	0.0484	0.0077
2358	2363	0.0497	0.0076
2363	2368	0.0533	0.0081
2368	2372	0.0371	0.0069
2372	2377	0.0337	0.0065
2377	2382	0.0422	0.0071
2382	2387	0.0463	0.0075
2387	2391	0.0371	0.0069



A. Appendix

Deuterium target:  $\cos(\theta_{CMS}) = [-0.2,-0.1]$

W / MeV		$d\sigma/d\Omega$ / mb/sr		W / MeV		$d\sigma/d\Omega$ / mb/sr	
lower bound	upper bound	value	stat. error	lower bound	upper bound	value	stat. error
1472	1495	0.2538	0.0276	1984	1992	0.1398	0.0068
1495	1517	1.1561	0.0514	1992	2001	0.1484	0.0069
1517	1540	1.3589	0.0327	2001	2009	0.1386	0.0068
1540	1561	1.2801	0.0226	2009	2017	0.1472	0.0069
1561	1583	1.1411	0.0173	2017	2026	0.1509	0.0074
1583	1604	0.9139	0.0132	2026	2034	0.1286	0.0069
1604	1625	0.7105	0.0107	2034	2043	0.1386	0.0073
1625	1639	0.5607	0.0119	2043	2051	0.1201	0.0069
1639	1653	0.4928	0.0095	2051	2059	0.1190	0.0070
1653	1666	0.4076	0.0089	2059	2067	0.1172	0.0070
1666	1680	0.3432	0.0078	2067	2076	0.1042	0.0067
1680	1694	0.3709	0.0081	2076	2084	0.1078	0.0070
1694	1707	0.3455	0.0078	2084	2092	0.1223	0.0074
1707	1720	0.3342	0.0074	2092	2100	0.1200	0.0077
1720	1733	0.3434	0.0074	2100	2108	0.0938	0.0067
1733	1746	0.3447	0.0074	2108	2116	0.0800	0.0056
1746	1759	0.3126	0.0071	2116	2124	0.0821	0.0068
1759	1772	0.3149	0.0069	2124	2132	0.0999	0.0069
1772	1785	0.3073	0.0070	2132	2138	0.0871	0.0081
1785	1798	0.2878	0.0067	2138	2143	0.0897	0.0089
1798	1810	0.2864	0.0067	2143	2148	0.0943	0.0085
1810	1823	0.2714	0.0065	2148	2153	0.0846	0.0082
1823	1835	0.2554	0.0064	2153	2159	0.0899	0.0084
1835	1848	0.2591	0.0064	2159	2164	0.1023	0.0093
1848	1860	0.2323	0.0063	2164	2169	0.0846	0.0083
1860	1872	0.2220	0.0065	2169	2174	0.0804	0.0083
1872	1884	0.2054	0.0063	2174	2179	0.0935	0.0087
1884	1896	0.2103	0.0069	2179	2184	0.0858	0.0083
1896	1905	0.1778	0.0077	2184	2190	0.0821	0.0084
1905	1914	0.1819	0.0067	2190	2195	0.0718	0.0078
1914	1923	0.1882	0.0072	2195	2200	0.0703	0.0076
1923	1931	0.1655	0.0069	2200	2205	0.0737	0.0079
1931	1940	0.1673	0.0070	2205	2210	0.0754	0.0081
1940	1949	0.1717	0.0069	2210	2215	0.0856	0.0085
1949	1958	0.1635	0.0072	2215	2220	0.0805	0.0085
1958	1966	0.1649	0.0071	2220	2225	0.0677	0.0075
1966	1975	0.1470	0.0067	2225	2230	0.0878	0.0089
1975	1984	0.1485	0.0068	2230	2235	0.0690	0.0078

A. Appendix

Deuterium target:  $\cos(\theta_{CMS}) = [-0.2,-0.1]$

W / MeV		$d\sigma/d\Omega$ / mb/sr	
lower bound	upper bound	value	stat. error
2235	2241	0.0690	0.0079
2241	2246	0.0781	0.0082
2246	2251	0.0795	0.0087
2251	2256	0.0730	0.0080
2256	2261	0.0745	0.0086
2261	2266	0.0632	0.0074
2266	2270	0.0395	0.0062
2270	2275	0.0650	0.0078
2275	2280	0.0770	0.0085
2280	2285	0.0648	0.0076
2285	2290	0.0678	0.0081
2290	2295	0.0518	0.0070
2295	2300	0.0536	0.0073
2300	2305	0.0619	0.0076
2305	2310	0.0520	0.0072
2310	2315	0.0555	0.0072
2315	2320	0.0559	0.0074
2320	2324	0.0523	0.0070
2324	2329	0.0521	0.0074
2329	2334	0.0535	0.0072
2334	2339	0.0479	0.0070
2339	2344	0.0423	0.0062
2344	2349	0.0569	0.0076
2349	2353	0.0620	0.0078
2353	2358	0.0568	0.0076
2358	2363	0.0467	0.0068
2363	2368	0.0648	0.0080
2368	2372	0.0418	0.0066
2372	2377	0.0286	0.0055
2377	2382	0.0408	0.0063
2382	2387	0.0491	0.0070
2387	2391	0.0489	0.0072

A. Appendix

Deuterium target:  $\cos(\theta_{CMS}) = [-0.1, 0]$

W / MeV		$d\sigma/d\Omega$ / mb/sr		W / MeV		$d\sigma/d\Omega$ / mb/sr	
lower bound	upper bound	value	stat. error	lower bound	upper bound	value	stat. error
1472	1495	0.3069	0.0331	1984	1992	0.1478	0.0069
1495	1517	1.1829	0.0556	1992	2001	0.1573	0.0070
1517	1540	1.4000	0.0350	2001	2009	0.1595	0.0072
1540	1561	1.3339	0.0238	2009	2017	0.1329	0.0063
1561	1583	1.1578	0.0174	2017	2026	0.1355	0.0068
1583	1604	0.9030	0.0130	2026	2034	0.1482	0.0073
1604	1625	0.6997	0.0104	2034	2043	0.1232	0.0067
1625	1639	0.5506	0.0116	2043	2051	0.1258	0.0069
1639	1653	0.4630	0.0090	2051	2059	0.1344	0.0072
1653	1666	0.3996	0.0086	2059	2067	0.1184	0.0068
1666	1680	0.3614	0.0079	2067	2076	0.1410	0.0075
1680	1694	0.3599	0.0078	2076	2084	0.1105	0.0068
1694	1707	0.3541	0.0078	2084	2092	0.1125	0.0068
1707	1720	0.3608	0.0076	2092	2100	0.1140	0.0073
1720	1733	0.3379	0.0072	2100	2108	0.1015	0.0067
1733	1746	0.3629	0.0074	2108	2116	0.1042	0.0062
1746	1759	0.3222	0.0070	2116	2124	0.0805	0.0065
1759	1772	0.3189	0.0068	2124	2132	0.0909	0.0064
1772	1785	0.3216	0.0070	2132	2138	0.1040	0.0085
1785	1798	0.2998	0.0067	2138	2143	0.1141	0.0097
1798	1810	0.2923	0.0066	2143	2148	0.1050	0.0085
1810	1823	0.2961	0.0066	2148	2153	0.1036	0.0088
1823	1835	0.2555	0.0062	2153	2159	0.1226	0.0094
1835	1848	0.2638	0.0063	2159	2164	0.0932	0.0086
1848	1860	0.2617	0.0066	2164	2169	0.1067	0.0089
1860	1872	0.2360	0.0065	2169	2174	0.0877	0.0084
1872	1884	0.2274	0.0065	2174	2179	0.0906	0.0082
1884	1896	0.1991	0.0066	2179	2184	0.0958	0.0083
1896	1905	0.1930	0.0079	2184	2190	0.0807	0.0081
1905	1914	0.1900	0.0067	2190	2195	0.0986	0.0088
1914	1923	0.1927	0.0071	2195	2200	0.1025	0.0089
1923	1931	0.1863	0.0072	2200	2205	0.0897	0.0082
1931	1940	0.1857	0.0073	2205	2210	0.0953	0.0087
1940	1949	0.1812	0.0069	2210	2215	0.0956	0.0086
1949	1958	0.1653	0.0071	2215	2220	0.0856	0.0084
1958	1966	0.1656	0.0069	2220	2225	0.0844	0.0081
1966	1975	0.1570	0.0068	2225	2230	0.0917	0.0088
1975	1984	0.1578	0.0068	2230	2235	0.0759	0.0078

A. Appendix

Deuterium target:  $\cos(\theta_{CMS}) = [-0.1,0]$

W / MeV		$d\sigma/d\Omega$ / mb/sr	
lower bound	upper bound	value	stat. error
2235	2241	0.0767	0.0081
2241	2246	0.0799	0.0080
2246	2251	0.0730	0.0080
2251	2256	0.0750	0.0078
2256	2261	0.0841	0.0087
2261	2266	0.0661	0.0074
2266	2270	0.0783	0.0084
2270	2275	0.0707	0.0079
2275	2280	0.0652	0.0076
2280	2285	0.0512	0.0066
2285	2290	0.0598	0.0073
2290	2295	0.0830	0.0086
2295	2300	0.0675	0.0079
2300	2305	0.0642	0.0075
2305	2310	0.0659	0.0078
2310	2315	0.0753	0.0081
2315	2320	0.0485	0.0067
2320	2324	0.0705	0.0079
2324	2329	0.0687	0.0081
2329	2334	0.0655	0.0077
2334	2339	0.0596	0.0074
2339	2344	0.0732	0.0078
2344	2349	0.0612	0.0075
2349	2353	0.0396	0.0060
2353	2358	0.0529	0.0070
2358	2363	0.0541	0.0071
2363	2368	0.0666	0.0079
2368	2372	0.0586	0.0076
2372	2377	0.0576	0.0075
2377	2382	0.0611	0.0074
2382	2387	0.0469	0.0066
2387	2391	0.0520	0.0071

A. Appendix

Deuterium target:  $\cos(\theta_{CMS}) = [0,0.1]$

W / MeV		$d\sigma/d\Omega$ / mb/sr		W / MeV		$d\sigma/d\Omega$ / mb/sr	
lower bound	upper bound	value	stat. error	lower bound	upper bound	value	stat. error
1472	1495	0.2553	0.0328	1984	1992	0.1651	0.0072
1495	1517	1.2155	0.0602	1992	2001	0.1753	0.0074
1517	1540	1.3860	0.0370	2001	2009	0.1540	0.0070
1540	1561	1.3766	0.0253	2009	2017	0.1679	0.0071
1561	1583	1.1836	0.0181	2017	2026	0.1561	0.0073
1583	1604	0.9745	0.0137	2026	2034	0.1427	0.0071
1604	1625	0.7125	0.0106	2034	2043	0.1401	0.0071
1625	1639	0.5628	0.0118	2043	2051	0.1358	0.0071
1639	1653	0.4764	0.0091	2051	2059	0.1330	0.0072
1653	1666	0.4144	0.0088	2059	2067	0.1393	0.0074
1666	1680	0.3994	0.0084	2067	2076	0.1344	0.0073
1680	1694	0.3838	0.0081	2076	2084	0.1121	0.0069
1694	1707	0.3590	0.0078	2084	2092	0.1249	0.0072
1707	1720	0.3779	0.0078	2092	2100	0.1243	0.0076
1720	1733	0.3739	0.0076	2100	2108	0.1023	0.0068
1733	1746	0.3897	0.0077	2108	2116	0.1139	0.0065
1746	1759	0.3559	0.0074	2116	2124	0.1156	0.0078
1759	1772	0.3397	0.0070	2124	2132	0.1063	0.0069
1772	1785	0.3424	0.0073	2132	2138	0.1106	0.0088
1785	1798	0.3147	0.0069	2138	2143	0.1163	0.0098
1798	1810	0.3157	0.0069	2143	2148	0.1137	0.0089
1810	1823	0.3041	0.0068	2148	2153	0.1135	0.0092
1823	1835	0.3092	0.0070	2153	2159	0.0984	0.0085
1835	1848	0.2826	0.0066	2159	2164	0.0957	0.0087
1848	1860	0.2869	0.0070	2164	2169	0.0924	0.0085
1860	1872	0.2693	0.0070	2169	2174	0.1150	0.0096
1872	1884	0.2551	0.0069	2174	2179	0.1261	0.0098
1884	1896	0.2302	0.0071	2179	2184	0.0977	0.0085
1896	1905	0.2513	0.0091	2184	2190	0.1034	0.0092
1905	1914	0.2171	0.0072	2190	2195	0.0880	0.0083
1914	1923	0.2075	0.0074	2195	2200	0.1186	0.0096
1923	1931	0.1837	0.0071	2200	2205	0.1116	0.0093
1931	1940	0.1933	0.0074	2205	2210	0.0975	0.0088
1940	1949	0.1915	0.0072	2210	2215	0.1092	0.0093
1949	1958	0.1900	0.0076	2215	2220	0.0954	0.0089
1958	1966	0.1821	0.0073	2220	2225	0.0875	0.0083
1966	1975	0.1895	0.0075	2225	2230	0.1019	0.0093
1975	1984	0.1689	0.0071	2230	2235	0.1033	0.0092

A. Appendix

Deuterium target:  $\cos(\theta_{CMS}) = [0,0.1]$

W / MeV		$d\sigma/d\Omega$ / mb/sr	
lower bound	upper bound	value	stat. error
2235	2241	0.0765	0.0082
2241	2246	0.1090	0.0094
2246	2251	0.0899	0.0089
2251	2256	0.0899	0.0086
2256	2261	0.0996	0.0095
2261	2266	0.0781	0.0080
2266	2270	0.1024	0.0096
2270	2275	0.0826	0.0087
2275	2280	0.0776	0.0083
2280	2285	0.0865	0.0086
2285	2290	0.0714	0.0080
2290	2295	0.0841	0.0086
2295	2300	0.0713	0.0081
2300	2305	0.0765	0.0080
2305	2310	0.0614	0.0076
2310	2315	0.0861	0.0087
2315	2320	0.0675	0.0079
2320	2324	0.0628	0.0074
2324	2329	0.0655	0.0079
2329	2334	0.0752	0.0082
2334	2339	0.0727	0.0083
2339	2344	0.0805	0.0081
2344	2349	0.0597	0.0075
2349	2353	0.0636	0.0075
2353	2358	0.0565	0.0072
2358	2363	0.0633	0.0076
2363	2368	0.0626	0.0076
2368	2372	0.0571	0.0074
2372	2377	0.0601	0.0076
2377	2382	0.0615	0.0074
2382	2387	0.0583	0.0073
2387	2391	0.0545	0.0072

A. Appendix

Deuterium target:  $\cos(\theta_{CMS}) = [0.1, 0.2]$

W / MeV		$d\sigma/d\Omega$ / mb/sr		W / MeV		$d\sigma/d\Omega$ / mb/sr	
lower bound	upper bound	value	stat. error	lower bound	upper bound	value	stat. error
1472	1495	0.2377	0.0342	1984	1992	0.1965	0.0080
1495	1517	1.1507	0.0628	1992	2001	0.1733	0.0074
1517	1540	1.4459	0.0400	2001	2009	0.1762	0.0076
1540	1561	1.3995	0.0267	2009	2017	0.1634	0.0071
1561	1583	1.2155	0.0187	2017	2026	0.1705	0.0078
1583	1604	0.9720	0.0138	2026	2034	0.1535	0.0075
1604	1625	0.7076	0.0105	2034	2043	0.1700	0.0081
1625	1639	0.5532	0.0115	2043	2051	0.1476	0.0075
1639	1653	0.4670	0.0089	2051	2059	0.1519	0.0078
1653	1666	0.4239	0.0088	2059	2067	0.1405	0.0076
1666	1680	0.3836	0.0081	2067	2076	0.1568	0.0081
1680	1694	0.3635	0.0078	2076	2084	0.1411	0.0079
1694	1707	0.3776	0.0080	2084	2092	0.1533	0.0082
1707	1720	0.3880	0.0079	2092	2100	0.1256	0.0078
1720	1733	0.3724	0.0076	2100	2108	0.1347	0.0079
1733	1746	0.4035	0.0079	2108	2116	0.1344	0.0072
1746	1759	0.3826	0.0077	2116	2124	0.1297	0.0085
1759	1772	0.3510	0.0071	2124	2132	0.1312	0.0078
1772	1785	0.3540	0.0074	2132	2138	0.1195	0.0093
1785	1798	0.3470	0.0072	2138	2143	0.1217	0.0101
1798	1810	0.3301	0.0071	2143	2148	0.1093	0.0088
1810	1823	0.3384	0.0071	2148	2153	0.1482	0.0107
1823	1835	0.3176	0.0071	2153	2159	0.1104	0.0091
1835	1848	0.3265	0.0072	2159	2164	0.1354	0.0105
1848	1860	0.2964	0.0071	2164	2169	0.1249	0.0099
1860	1872	0.2881	0.0073	2169	2174	0.1182	0.0099
1872	1884	0.2695	0.0071	2174	2179	0.1190	0.0096
1884	1896	0.2435	0.0073	2179	2184	0.1044	0.0089
1896	1905	0.2460	0.0090	2184	2190	0.1390	0.0108
1905	1914	0.2346	0.0075	2190	2195	0.1344	0.0105
1914	1923	0.2177	0.0076	2195	2200	0.1104	0.0094
1923	1931	0.2193	0.0078	2200	2205	0.1045	0.0090
1931	1940	0.2118	0.0078	2205	2210	0.1267	0.0102
1940	1949	0.1963	0.0073	2210	2215	0.1082	0.0094
1949	1958	0.1996	0.0078	2215	2220	0.1232	0.0102
1958	1966	0.2070	0.0078	2220	2225	0.1116	0.0094
1966	1975	0.1850	0.0074	2225	2230	0.1228	0.0104
1975	1984	0.1782	0.0074	2230	2235	0.1096	0.0095

A. Appendix

Deuterium target:  $\cos(\theta_{CMS}) = [0.1, 0.2]$

W / MeV		$d\sigma/d\Omega$ / mb/sr	
lower bound	upper bound	value	stat. error
2235	2241	0.1245	0.0105
2241	2246	0.1139	0.0097
2246	2251	0.0841	0.0087
2251	2256	0.0928	0.0088
2256	2261	0.0941	0.0094
2261	2266	0.1060	0.0096
2266	2270	0.1156	0.0104
2270	2275	0.0949	0.0092
2275	2280	0.0858	0.0088
2280	2285	0.1013	0.0094
2285	2290	0.0819	0.0087
2290	2295	0.1020	0.0096
2295	2300	0.0915	0.0093
2300	2305	0.0840	0.0086
2305	2310	0.1062	0.0102
2310	2315	0.0966	0.0094
2315	2320	0.0971	0.0097
2320	2324	0.0706	0.0080
2324	2329	0.0794	0.0089
2329	2334	0.0776	0.0086
2334	2339	0.0767	0.0086
2339	2344	0.0567	0.0069
2344	2349	0.0887	0.0094
2349	2353	0.0939	0.0094
2353	2358	0.0670	0.0081
2358	2363	0.0633	0.0077
2363	2368	0.0874	0.0092
2368	2372	0.0705	0.0085
2372	2377	0.0794	0.0090
2377	2382	0.0662	0.0078
2382	2387	0.0845	0.0090
2387	2391	0.0799	0.0090



A. Appendix

Deuterium target:  $\cos(\theta_{CMS}) = [0.2, 0.3]$

W / MeV		$d\sigma/d\Omega$ / mb/sr		W / MeV		$d\sigma/d\Omega$ / mb/sr	
lower bound	upper bound	value	stat. error	lower bound	upper bound	value	stat. error
1472	1495	0.3656	0.0481	1984	1992	0.2217	0.0090
1495	1517	1.2562	0.0715	1992	2001	0.2176	0.0088
1517	1540	1.5138	0.0441	2001	2009	0.2001	0.0086
1540	1561	1.4732	0.0288	2009	2017	0.2087	0.0086
1561	1583	1.2533	0.0198	2017	2026	0.2172	0.0093
1583	1604	1.0303	0.0146	2026	2034	0.1913	0.0089
1604	1625	0.7699	0.0112	2034	2043	0.1743	0.0086
1625	1639	0.5744	0.0120	2043	2051	0.1888	0.0091
1639	1653	0.5050	0.0095	2051	2059	0.1712	0.0088
1653	1666	0.4214	0.0089	2059	2067	0.1625	0.0086
1666	1680	0.4004	0.0084	2067	2076	0.1944	0.0096
1680	1694	0.4008	0.0084	2076	2084	0.1680	0.0091
1694	1707	0.3804	0.0082	2084	2092	0.1563	0.0088
1707	1720	0.4251	0.0084	2092	2100	0.1586	0.0093
1720	1733	0.4153	0.0083	2100	2108	0.1513	0.0089
1733	1746	0.4052	0.0081	2108	2116	0.1639	0.0085
1746	1759	0.3998	0.0081	2116	2124	0.1665	0.0103
1759	1772	0.3994	0.0079	2124	2132	0.1489	0.0089
1772	1785	0.3973	0.0081	2132	2138	0.1655	0.0118
1785	1798	0.3905	0.0080	2138	2143	0.1502	0.0121
1798	1810	0.3699	0.0078	2143	2148	0.1656	0.0118
1810	1823	0.3713	0.0078	2148	2153	0.1456	0.0114
1823	1835	0.3427	0.0076	2153	2159	0.1758	0.0124
1835	1848	0.3574	0.0078	2159	2164	0.1615	0.0124
1848	1860	0.3390	0.0079	2164	2169	0.1436	0.0114
1860	1872	0.3378	0.0082	2169	2174	0.1522	0.0121
1872	1884	0.3217	0.0082	2174	2179	0.1325	0.0109
1884	1896	0.2734	0.0082	2179	2184	0.1510	0.0115
1896	1905	0.2852	0.0103	2184	2190	0.1469	0.0120
1905	1914	0.2733	0.0086	2190	2195	0.1656	0.0127
1914	1923	0.2613	0.0088	2195	2200	0.1348	0.0112
1923	1931	0.2415	0.0087	2200	2205	0.1514	0.0119
1931	1940	0.2467	0.0089	2205	2210	0.1403	0.0117
1940	1949	0.2409	0.0086	2210	2215	0.1509	0.0121
1949	1958	0.2514	0.0093	2215	2220	0.1537	0.0125
1958	1966	0.2298	0.0088	2220	2225	0.1482	0.0120
1966	1975	0.2478	0.0092	2225	2230	0.1420	0.0121
1975	1984	0.2311	0.0089	2230	2235	0.1352	0.0116

A. Appendix

Deuterium target:  $\cos(\theta_{CMS}) = [0.2, 0.3]$

W / MeV		$d\sigma/d\Omega$ / mb/sr	
lower bound	upper bound	value	stat. error
2235	2241	0.1285	0.0117
2241	2246	0.1388	0.0117
2246	2251	0.1545	0.0129
2251	2256	0.1370	0.0119
2256	2261	0.1387	0.0127
2261	2266	0.1150	0.0109
2266	2270	0.1417	0.0128
2270	2275	0.1507	0.0128
2275	2280	0.1379	0.0124
2280	2285	0.1157	0.0111
2285	2290	0.1259	0.0119
2290	2295	0.1093	0.0110
2295	2300	0.0962	0.0105
2300	2305	0.1431	0.0125
2305	2310	0.1275	0.0123
2310	2315	0.0882	0.0099
2315	2320	0.1078	0.0112
2320	2324	0.1442	0.0126
2324	2329	0.0900	0.0104
2329	2334	0.0943	0.0103
2334	2339	0.1057	0.0111
2339	2344	0.1146	0.0109
2344	2349	0.0871	0.0101
2349	2353	0.0918	0.0102
2353	2358	0.1215	0.0120
2358	2363	0.0849	0.0099
2363	2368	0.0993	0.0107
2368	2372	0.0871	0.0104
2372	2377	0.0963	0.0109
2377	2382	0.0885	0.0099
2382	2387	0.1031	0.0110
2387	2391	0.0721	0.0094

A. Appendix

Deuterium target:  $\cos(\theta_{CMS}) = [0.3, 0.4]$

W / MeV		$d\sigma/d\Omega$ / mb/sr		W / MeV		$d\sigma/d\Omega$ / mb/sr	
lower bound	upper bound	value	stat. error	lower bound	upper bound	value	stat. error
1472	1495	0.3750	0.0551	1984	1992	0.2217	0.0097
1495	1517	1.0682	0.0698	1992	2001	0.2442	0.0102
1517	1540	1.4552	0.0454	2001	2009	0.2293	0.0100
1540	1561	1.4462	0.0301	2009	2017	0.2246	0.0097
1561	1583	1.3231	0.0214	2017	2026	0.2362	0.0106
1583	1604	1.0887	0.0157	2026	2034	0.2273	0.0106
1604	1625	0.8128	0.0119	2034	2043	0.2168	0.0106
1625	1639	0.6032	0.0125	2043	2051	0.2334	0.0111
1639	1653	0.4866	0.0095	2051	2059	0.1999	0.0105
1653	1666	0.4159	0.0091	2059	2067	0.1977	0.0105
1666	1680	0.4066	0.0087	2067	2076	0.2031	0.0108
1680	1694	0.4089	0.0087	2076	2084	0.2128	0.0114
1694	1707	0.4190	0.0088	2084	2092	0.1914	0.0108
1707	1720	0.4161	0.0086	2092	2100	0.1918	0.0114
1720	1733	0.4374	0.0087	2100	2108	0.1787	0.0109
1733	1746	0.4402	0.0087	2108	2116	0.1913	0.0102
1746	1759	0.4386	0.0088	2116	2124	0.1720	0.0117
1759	1772	0.4247	0.0084	2124	2132	0.1772	0.0108
1772	1785	0.4085	0.0086	2132	2138	0.1904	0.0142
1785	1798	0.4019	0.0084	2138	2143	0.1811	0.0147
1798	1810	0.4024	0.0085	2143	2148	0.1859	0.0139
1810	1823	0.4032	0.0085	2148	2153	0.2212	0.0155
1823	1835	0.3902	0.0086	2153	2159	0.1769	0.0138
1835	1848	0.3851	0.0086	2159	2164	0.2517	0.0171
1848	1860	0.3715	0.0088	2164	2169	0.1751	0.0142
1860	1872	0.3347	0.0087	2169	2174	0.1833	0.0148
1872	1884	0.3422	0.0090	2174	2179	0.1980	0.0150
1884	1896	0.3269	0.0096	2179	2184	0.1738	0.0139
1896	1905	0.3211	0.0117	2184	2190	0.1986	0.0156
1905	1914	0.3000	0.0096	2190	2195	0.1816	0.0148
1914	1923	0.2925	0.0099	2195	2200	0.1691	0.0141
1923	1931	0.2930	0.0103	2200	2205	0.1826	0.0147
1931	1940	0.2927	0.0104	2205	2210	0.1818	0.0150
1940	1949	0.2554	0.0095	2210	2215	0.1847	0.0150
1949	1958	0.2728	0.0105	2215	2220	0.1675	0.0146
1958	1966	0.2698	0.0102	2220	2225	0.1496	0.0134
1966	1975	0.2537	0.0100	2225	2230	0.1632	0.0148
1975	1984	0.2282	0.0096	2230	2235	0.1767	0.0149

A. Appendix

Deuterium target:  $\cos(\theta_{CMS}) = [0.3, 0.4]$

W / MeV		$d\sigma/d\Omega$ / mb/sr	
lower bound	upper bound	value	stat. error
2235	2241	0.1545	0.0143
2241	2246	0.1544	0.0141
2246	2251	0.1260	0.0132
2251	2256	0.1786	0.0152
2256	2261	0.1633	0.0155
2261	2266	0.1804	0.0157
2266	2270	0.1433	0.0146
2270	2275	0.1196	0.0131
2275	2280	0.1546	0.0149
2280	2285	0.1305	0.0135
2285	2290	0.1453	0.0149
2290	2295	0.1381	0.0143
2295	2300	0.1495	0.0153
2300	2305	0.1527	0.0150
2305	2310	0.1507	0.0156
2310	2315	0.1304	0.0141
2315	2320	0.1219	0.0140
2320	2324	0.1083	0.0128
2324	2329	0.1462	0.0159
2329	2334	0.1607	0.0161
2334	2339	0.1456	0.0158
2339	2344	0.0938	0.0120
2344	2349	0.1200	0.0146
2349	2353	0.1267	0.0145
2353	2358	0.1371	0.0156
2358	2363	0.1071	0.0137
2363	2368	0.1159	0.0146
2368	2372	0.1176	0.0151
2372	2377	0.0936	0.0134
2377	2382	0.1025	0.0135
2382	2387	0.1167	0.0146
2387	2391	0.1388	0.0167

A. Appendix

Deuterium target:  $\cos(\theta_{CMS}) = [0.4, 0.5]$

W / MeV		$d\sigma/d\Omega$ / mb/sr		W / MeV		$d\sigma/d\Omega$ / mb/sr	
lower bound	upper bound	value	stat. error	lower bound	upper bound	value	stat. error
1472	1495	0.3691	0.0630	1984	1992	0.2932	0.0126
1495	1517	1.1486	0.0797	1992	2001	0.2654	0.0119
1517	1540	1.3654	0.0478	2001	2009	0.2628	0.0121
1540	1561	1.4565	0.0322	2009	2017	0.2634	0.0118
1561	1583	1.3039	0.0223	2017	2026	0.2235	0.0116
1583	1604	1.0733	0.0163	2026	2034	0.2598	0.0128
1604	1625	0.7898	0.0122	2034	2043	0.2346	0.0125
1625	1639	0.5789	0.0127	2043	2051	0.2511	0.0131
1639	1653	0.4941	0.0099	2051	2059	0.2649	0.0137
1653	1666	0.4192	0.0093	2059	2067	0.2045	0.0121
1666	1680	0.3943	0.0088	2067	2076	0.2368	0.0133
1680	1694	0.3868	0.0087	2076	2084	0.2338	0.0137
1694	1707	0.4077	0.0089	2084	2092	0.2307	0.0136
1707	1720	0.4444	0.0091	2092	2100	0.2189	0.0140
1720	1733	0.4366	0.0090	2100	2108	0.2125	0.0136
1733	1746	0.4384	0.0090	2108	2116	0.2149	0.0126
1746	1759	0.4483	0.0093	2116	2124	0.2211	0.0153
1759	1772	0.4396	0.0090	2124	2132	0.1935	0.0133
1772	1785	0.4477	0.0095	2132	2138	0.2215	0.0182
1785	1798	0.4168	0.0091	2138	2143	0.2279	0.0198
1798	1810	0.4121	0.0092	2143	2148	0.2164	0.0180
1810	1823	0.4131	0.0092	2148	2153	0.2065	0.0180
1823	1835	0.4024	0.0094	2153	2159	0.2430	0.0196
1835	1848	0.3984	0.0093	2159	2164	0.2022	0.0188
1848	1860	0.3846	0.0096	2164	2169	0.2033	0.0185
1860	1872	0.3735	0.0099	2169	2174	0.2301	0.0204
1872	1884	0.3584	0.0099	2174	2179	0.2196	0.0196
1884	1896	0.3491	0.0107	2179	2184	0.2439	0.0203
1896	1905	0.3539	0.0133	2184	2190	0.2470	0.0217
1905	1914	0.3240	0.0109	2190	2195	0.2246	0.0205
1914	1923	0.3101	0.0112	2195	2200	0.2279	0.0207
1923	1931	0.3268	0.0120	2200	2205	0.2309	0.0209
1931	1940	0.3096	0.0118	2205	2210	0.2014	0.0202
1940	1949	0.2989	0.0114	2210	2215	0.2330	0.0218
1949	1958	0.3096	0.0123	2215	2220	0.1899	0.0203
1958	1966	0.3039	0.0121	2220	2225	0.2248	0.0215
1966	1975	0.2956	0.0120	2225	2230	0.2090	0.0216
1975	1984	0.2616	0.0115	2230	2235	0.2465	0.0231

A. Appendix

Deuterium target:  $\cos(\theta_{CMS}) = [0.4, 0.5]$

W / MeV		$d\sigma/d\Omega$ / mb/sr	
lower bound	upper bound	value	stat. error
2235	2241	0.2202	0.0228
2241	2246	0.2216	0.0221
2246	2251	0.2052	0.0226
2251	2256	0.2061	0.0218
2256	2261	0.1844	0.0223
2261	2266	0.1745	0.0207
2266	2270	0.2197	0.0243
2270	2275	0.1812	0.0219
2275	2280	0.1555	0.0204
2280	2285	0.1926	0.0222
2285	2290	0.1759	0.0220
2290	2295	0.1801	0.0226
2295	2300	0.1875	0.0233
2300	2305	0.1501	0.0203
2305	2310	0.1552	0.0218
2310	2315	0.1146	0.0182
2315	2320	0.1345	0.0205
2320	2324	0.1557	0.0215
2324	2329	0.1633	0.0235
2329	2334	0.1697	0.0235
2334	2339	0.1852	0.0253
2339	2344	0.1615	0.0224
2344	2349	0.1299	0.0214
2349	2353	0.1142	0.0197
2353	2358	0.1163	0.0211
2358	2363	0.1504	0.0239
2363	2368	0.0831	0.0180
2368	2372	0.0965	0.0201
2372	2377	0.0929	0.0203
2377	2382	0.1270	0.0227
2382	2387	0.0793	0.0187
2387	2391	0.0934	0.0209

A. Appendix

Deuterium target:  $\cos(\theta_{CMS}) = [0.5, 0.6]$

W / MeV		$d\sigma/d\Omega$ / mb/sr		W / MeV		$d\sigma/d\Omega$ / mb/sr	
lower bound	upper bound	value	stat. error	lower bound	upper bound	value	stat. error
1472	1495	0.4958	0.0895	1984	1992	0.3281	0.0159
1495	1517	1.3155	0.0994	1992	2001	0.3182	0.0156
1517	1540	1.3472	0.0518	2001	2009	0.2911	0.0153
1540	1561	1.3612	0.0332	2009	2017	0.2855	0.0150
1561	1583	1.2665	0.0236	2017	2026	0.2337	0.0147
1583	1604	1.0948	0.0177	2026	2034	0.2697	0.0162
1604	1625	0.7923	0.0130	2034	2043	0.2654	0.0166
1625	1639	0.5830	0.0135	2043	2051	0.2453	0.0164
1639	1653	0.4719	0.0102	2051	2059	0.2868	0.0184
1653	1666	0.4194	0.0099	2059	2067	0.2856	0.0186
1666	1680	0.3835	0.0091	2067	2076	0.2884	0.0194
1680	1694	0.3832	0.0091	2076	2084	0.2422	0.0185
1694	1707	0.4012	0.0094	2084	2092	0.2938	0.0207
1707	1720	0.4254	0.0095	2092	2100	0.2422	0.0200
1720	1733	0.4209	0.0095	2100	2108	0.2594	0.0204
1733	1746	0.4336	0.0097	2108	2116	0.2731	0.0196
1746	1759	0.4253	0.0098	2116	2124	0.2960	0.0246
1759	1772	0.4249	0.0096	2124	2132	0.2872	0.0226
1772	1785	0.4415	0.0102	2132	2138	0.2360	0.0263
1785	1798	0.4265	0.0100	2138	2143	0.2729	0.0308
1798	1810	0.4028	0.0099	2143	2148	0.2665	0.0284
1810	1823	0.4131	0.0101	2148	2153	0.2902	0.0307
1823	1835	0.4267	0.0107	2153	2159	0.2318	0.0282
1835	1848	0.3967	0.0104	2159	2164	0.2281	0.0289
1848	1860	0.3837	0.0108	2164	2169	0.1770	0.0257
1860	1872	0.3882	0.0115	2169	2174	0.2613	0.0323
1872	1884	0.3833	0.0116	2174	2179	0.2651	0.0324
1884	1896	0.3657	0.0125	2179	2184	0.2100	0.0281
1896	1905	0.3563	0.0152	2184	2190	0.2389	0.0329
1905	1914	0.3701	0.0135	2190	2195	0.2590	0.0345
1914	1923	0.3620	0.0139	2195	2200	0.2091	0.0312
1923	1931	0.3319	0.0138	2200	2205	0.1878	0.0304
1931	1940	0.3318	0.0142	2205	2210	0.2464	0.0355
1940	1949	0.3385	0.0140	2210	2215	0.1948	0.0320
1949	1958	0.3034	0.0143	2215	2220	0.1877	0.0335
1958	1966	0.3301	0.0147	2220	2225	0.1691	0.0313
1966	1975	0.2888	0.0140	2225	2230	0.2579	0.0424
1975	1984	0.3141	0.0148	2230	2235	0.1481	0.0310

A. Appendix

Deuterium target:  $\cos(\theta_{CMS}) = [0.5, 0.6]$

W / MeV		$d\sigma/d\Omega$ / mb/sr	
lower bound	upper bound	value	stat. error
2235	2241	0.2083	0.0398
2241	2246	0.1772	0.0356
2246	2251	0.1934	0.0404
2251	2256	0.1908	0.0401
2256	2261	0.1559	0.0402
2261	2266	0.1408	0.0379
2266	2270	0.1520	0.0421
2270	2275	0.1100	0.0372
2275	2280	0.1299	0.0409
2280	2285	0.1062	0.0387
2285	2290	0.1652	0.0527
2290	2295	0.1684	0.0547
2295	2300	0.0788	0.0391
2300	2305	0.1180	0.0512
2305	2310	0.1661	0.0672
2310	2315	0.1044	0.0573
2315	2320	0.0793	0.0548
2320	2324	0.1439	0.0804
2324	2329	0.0000	0.0000
2329	2334	0.0584	0.0571
2334	2339	0.0000	0.0002
2339	2344	0.1525	0.1034
2344	2349	0.1075	0.1043
2349	2353	0.2286	0.1598
2353	2358	0.0000	0.0000
2358	2363	0.0000	0.0001
2363	2368	0.2358	0.2130
2368	2372	0.2600	0.2386
2372	2377	0.0000	0.0005
2377	2382	0.0000	0.0001
2382	2387	0.0000	0.0010
2387	2391	0.0000	0.0000



A. Appendix

Deuterium target:  $\cos(\theta_{CMS}) = [0.6, 0.7]$

W / MeV		$d\sigma/d\Omega$ / mb/sr		W / MeV		$d\sigma/d\Omega$ / mb/sr	
lower bound	upper bound	value	stat. error	lower bound	upper bound	value	stat. error
1472	1495	0.4247	0.1067	1966	1975	0.3777	0.0220
1495	1517	1.4087	0.1287	1975	1984	0.3493	0.0222
1517	1540	1.4511	0.0658	1984	1992	0.3142	0.0222
1540	1561	1.3689	0.0389	1992	2001	0.3415	0.0234
1561	1583	1.2708	0.0271	2001	2009	0.3657	0.0255
1583	1604	1.0753	0.0198	2009	2017	0.3144	0.0238
1604	1625	0.8044	0.0149	2017	2026	0.3078	0.0261
1625	1639	0.5582	0.0149	2026	2034	0.3218	0.0283
1639	1653	0.4520	0.0112	2034	2043	0.3383	0.0304
1653	1666	0.4027	0.0109	2043	2051	0.3012	0.0301
1666	1680	0.3445	0.0097	2051	2059	0.3342	0.0334
1680	1694	0.3637	0.0099	2059	2067	0.3104	0.0342
1694	1707	0.4077	0.0107	2067	2076	0.3550	0.0387
1707	1720	0.4133	0.0106	2076	2084	0.2915	0.0374
1720	1733	0.4264	0.0108	2084	2092	0.2335	0.0353
1733	1746	0.4491	0.0112	2092	2100	0.2896	0.0446
1746	1759	0.4330	0.0112	2100	2108	0.3444	0.0521
1759	1772	0.4294	0.0111	2108	2116	0.2630	0.0431
1772	1785	0.4028	0.0112	2116	2124	0.3052	0.0613
1785	1798	0.4167	0.0115	2124	2132	0.3011	0.0628
1798	1810	0.4092	0.0116	2132	2138	0.3338	0.0902
1810	1823	0.3847	0.0114	2138	2143	0.0770	0.0500
1823	1835	0.4230	0.0125	2143	2148	0.2242	0.0848
1835	1848	0.3927	0.0124	2148	2153	0.3602	0.1200
1848	1860	0.3996	0.0131	2153	2159	0.1426	0.0836
1860	1872	0.3856	0.0138	2159	2164	0.2772	0.1314
1872	1884	0.3700	0.0140	2164	2169	0.0000	0.0001
1884	1896	0.3615	0.0154	2169	2174	0.0988	0.0963
1896	1905	0.3710	0.0195	2174	2179	0.1804	0.1314
1905	1914	0.3624	0.0169	2179	2184	2.8970	0.6938
1914	1923	0.3527	0.0177	2184	2190	0.0000	0.0000
1923	1931	0.3614	0.0189	2190	2195	0.7583	0.3833
1931	1940	0.3699	0.0198	2195	2200	1.4278	0.6060
1940	1949	0.3403	0.0189				
1949	1958	0.3426	0.0206				
1958	1966	0.3675	0.0216				

A. Appendix

Deuterium target:  $\cos(\theta_{CMS}) = [0.7, 0.8]$

W / MeV		$d\sigma/d\Omega$ / mb/sr		W / MeV		$d\sigma/d\Omega$ / mb/sr	
lower bound	upper bound	value	stat. error	lower bound	upper bound	value	stat. error
1472	1495	0.0009	0.0059	1931	1940	0.3753	0.0343
1495	1517	1.6150	0.1777	1940	1949	0.2447	0.0287
1517	1540	1.4280	0.0823	1949	1958	0.3761	0.0407
1540	1561	1.2567	0.0467	1958	1966	0.3619	0.0420
1561	1583	1.1660	0.0316	1966	1975	0.4280	0.0500
1583	1604	1.0335	0.0238	1975	1984	0.3766	0.0529
1604	1625	0.7490	0.0172	1984	1992	0.4026	0.0612
1625	1639	0.5153	0.0172	1992	2001	0.3175	0.0591
1639	1653	0.4240	0.0129	2001	2009	0.2980	0.0653
1653	1666	0.2985	0.0111	2009	2017	0.5302	0.0990
1666	1680	0.2945	0.0106	2017	2026	0.3336	0.0955
1680	1694	0.2963	0.0106	2026	2034	0.2356	0.0968
1694	1707	0.3041	0.0109	2034	2043	0.4766	0.1577
1707	1720	0.3322	0.0113	2043	2051	0.9859	0.2851
1720	1733	0.3089	0.0109				
1733	1746	0.3337	0.0116				
1746	1759	0.3061	0.0113				
1759	1772	0.3553	0.0122				
1772	1785	0.3251	0.0123				
1785	1798	0.3231	0.0125				
1798	1810	0.3324	0.0132				
1810	1823	0.3428	0.0139				
1823	1835	0.3422	0.0147				
1835	1848	0.3322	0.0150				
1848	1860	0.3386	0.0164				
1860	1872	0.3234	0.0175				
1872	1884	0.3355	0.0192				
1884	1896	0.3085	0.0210				
1896	1905	0.3411	0.0283				
1905	1914	0.3304	0.0252				
1914	1923	0.2827	0.0252				
1923	1931	0.3476	0.0301				